UNIVERSIDADE DO ALGARVE

Steady-state and lifetime fluorescence studies of pyrene probes in model membranes: trailblazing analysis of two-dimensional quenching kinetics with nitroxide probes and excimer formation

Miguel Alexandre da Silva Manuel

Dissertação de Doutoramento em Ciências Biológicas

(Especialidade de Bioquímica)

Trabalho efectuado sob orientação de:

Professor Doutor Jorge Martins

Co-orientação: Professor Doutor Eurico Melo

2013

Steady-state and lifetime fluorescence studies of pyrene probes in model membranes: trailblazing analysis of two-dimensional quenching kinetics with nitroxide probes and excimer formation

<u>Declaração de autoria de trabalho</u>

Declaro ser o autor deste trabalho, que é original e inédito.

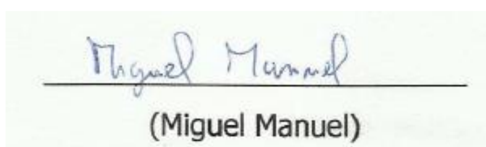

Miguel Alexandre da Silva Manuel recebeu financiamento (bolsa de doutoramento SFRH/BD/40671/2007) da Fundação para a Ciência e a Tecnologia (FCT), de Janeiro de 2008 a Dezembro de 2011.

FCT Fundação para a Ciência e a Tecnologia
MINISTÉRIO DA EDUCAÇÃO E CIÊNCIA

Este trabalho foi realizado no IBB-CBME (Instituto de Biotecnologia e Bioengenharia – Centro de Biomedicina Molecular e Estrutural), Universidade do Algarve.

IBB

CBME
Centro de Biomedicina Molecular e Estrutural

Agradecimentos

Ao Professor Doutor Jorge Martins, pela sua orientação e ensinamentos, e pela sua energia contagiante que sempre nos tenta transmitir cada vez que entra no laboratório. Pela ajuda inestimável na elaboração desta tese e na realização do trabalho. E acima de tudo por toda a amizade, paciência e compreensão ao longo destes 8 anos em que tive o prazer de trabalhar consigo.

Ao Professor Doutor Eurico Melo, meu co-orientador, pelas valiosas discussões e conselhos que permitiram levar este trabalho a bom termo.

A todos os meus amigos e colegas de laboratório ao longo destes anos, desde o início do estágio, Dalila companheira das aventuras fosfolipídicas desde o princípio, Susana, Teresa, Sandra, Ana Margarida, Dorinda que mesmo estando longe a tua amizade esteve sempre perto, Pedro pelas nossas conversas, cafés e idas ao sushi, André, Ana Catarina, Margarida, Catarina, Mónica e Ricardo que tive o prazer de ajudar na passagem pelo nosso laboratório, e Joana cuja boa disposição e alegria ajudaram bastante no stresse dos últimos dias de escrita. Um agradecimento especial ao Professor Doutor Manuel Aureliano Alves pela sua amizade e preocupação.

Aos meus avós Belmira e João, pelo seu amor e carinho. Á minha avó Lídia, pelo seu afecto e amor incondicionais, por me alegrar o dia com o seu sorriso. Aos meus pais Rosa e João, por tudo o sacrificaram por mim, por me ensinarem a pensar por mim próprio, pela força que sempre me dão, pelo apoio inesgotável e pelo amor sempre presente entre nós.

À Carina, por seres a minha namorada, companheira e melhor amiga, por seres o meu “ombro” nos piores momentos e partilhares e seres a causa dos melhores momentos, por todo o encorajamento e compreensão em especial durante a escrita deste trabalho. Por todo o teu amor, tudo o que quero é continuar o nosso caminho por esta vida contigo. Esta tese é te dedicada. Amo-te.

Resumo

O principal objectivo era demonstrar que o uso de um modelo cinético dirigido a meios confinados a duas dimensões (2D) para a análise de reacções bimoleculares em bicamadas fosfolipídicas, é de facto apropriado e de importância crucial para interpretar correctamente resultados experimentais, mantendo presente a complexa natureza das membranas lipídicas.

As membranas biológicas desempenham um papel essencial à vida, pois para além de serem a delimitação natural das células, são o local onde acontecem uma grande variedade de processos bioquímicos fundamentais. Algumas das proteínas mais importantes da célula estão associadas às membranas biológicas, juntamente com os lípidos membranares, que formam a bicamada fosfolipídica. Tanto as proteínas como os lípidos difundem com diferentes graus de liberdade ao longo do plano da membrana. São conhecidas muitas reacções que dependem desta difusão para ocorrerem, como é o caso de cadeia respiratória mitocondrial, do sistema fotossintético de transporte de electrões em cloroplastos e de processos sensoriais e regulatórios na interface da membrana plasmática.

A modelização de reacções em membranas biológicas é normalmente realizada em membranas modelo, chamadas lipossomas, com composição lipídica definida. Estas bicamadas fosfolipídicas artificiais permitem o estudo de reacções com controlo total de parâmetros.

A difusão lateral em membranas tem sido exaustivamente estudada mas é notória a necessidade da utilização do formalismo teórico adequado a reacções em 2D. O formalismo cinético introduzido por Razi Naqvi em 1974, uma abordagem hidrodinâmica a reacções controladas por difusão, é dos que produz melhores aproximações à prática, permitindo o estudo sem demasiadas complicações a nível matemático. Considerando uma aplicação ao estado estacionário, entretanto introduzida, utilizamos a extinção de fluorescência de várias sondas de pireno, uma técnica frequentemente utilizada no estudo de bicamadas lipídicas, como reacção modelo para analisar com este formalismo.

No 2º Capítulo estudamos a extinção de fluorescência de lípidos funcionalizados com sondas pirenilo, por sondas de *spin* também ligadas covalentemente a fosfolípidos, em vesiculas multilamelares (MLV) de 1-palmitoil-2-oleoil-sn-glicero-3-fosfotidilcolina (POPC). Utilizando fluorescência resolvida no tempo, determinou-se o tempo de vida de fluorescência das sondas 1-palmitoil-2-(1-pirenodecanoílo)-*sn*-glicero-3-fosfotidilcolina (py10-PC) e 1-palmitoil-2-(1-

pirenohexanoílo)-sn-glicero-3-fosfotidilcolina (py6-PC). Com estes tempos de vida e com todos os outros parâmetros previamente definidos, analisamos a extinção de fluorescência destas sondas por 1-palmitoíl-2-esteroíl-(10-DOXYL)-*sn*-glicero-3-fosfotidilcolina (10-DOXYL-PC) e 1-palmitoíl-2-esteroíl-(5-DOXYL)-*sn*-glicero-3-fosfotidilcolina, respectivamente, através de fluorescência de estado estacionário. Verificamos que a extinção de fluorescência de py10-PC por 10-DOXYL-PC foi, dentro do erro experimental, em completa concordância com a previsão teórica entre 1 e 8% de proporção da sonda de *spin* na bicamada. No entanto, o sistema envolvendo py6-PC e 5-DOXYL-PC revelou largos desvios em relação ao esperado, com um aparente aumento da eficiência da extinção de fluorescência, mas o aumento da distância colisional no modelo teórico permitiu uma muito boa aproximação aos valores experimentais. Discutiram-se várias possíveis influências que podem explicar esta situação.

No 3º Capítulo, estudamos a extinção de fluorescência através da formação de excímero das sondas py10-PC e py6-PC, em MLV de POPC, através de fluorescência de estado estacionário. Utilizando fluorescência resolvida no tempo, determinou-se o tempo de vida de fluorescência dos excímeros usando para isso as sondas 1,2-bis-(1-pirenodecanoíl)-*sn*-glicero-3-fosfotidilcolina (Bis-py10-PC) e 1,2-bis-(1-pirenobutanoíl)-sn-glicero-3-fosfotidilcolina (Bis-py4-PC), tempos de vida necessários ao formalismo cinético. Mostrou-se que a auto-extinção de fluorescência de py10-PC e de py6-PC está de acordo com a previsão teórica até a proporção molar de sonda fluorescente de 2 e 4%, respectivamente. Acima destas proporções, os resultados demonstraram uma eficiência de extinção inferior ao teoricamente esperado, para uma análise considerando que os coeficientes de difusão lateral não se alteram a uma temperatura fixa. No entanto, se se considerar que estes coeficientes são mais baixos para maiores concentrações de sonda, então obtém-se um acordo preciso com a teoria. Simulações de dinâmica molecular mostraram que aumenta a ordenação e existe maior empacotamento das cadeias acilo nas proximidades destas sondas e que existe também interdigitação do grupo de pireno para a monocamada adjacente. Isto explica a diminuição da difusão de ambas as sondas, com a sonda py10-PC a causar obviamente maior fricção entre as monocamada adjacentes.

No 4º Capítulo estudamos a extinção de fluorescência de pireno e de pirenosulfonato (PSA) por 5-DOXYL-PC, em MLV de POPC, através de fluorescência de estado estacionário. Utilizando fluorescência resolvida no tempo, determinou-se o tempo de vida de fluorescência das sondas de pireno e de PSA, para completar os parâmetros necessários ao formalismo cinético. Ao analisar a extinção de fluorescência do pireno, verificou-se um caso semelhante ao observado no capitulo 2 com e extinção de fluorescência de py6-PC pelo mesmo 5-DOXYL-PC, com uma análise consistente a necessitar do aumento da distância colisional para maior do que o raio de van der Waals. Para a sonda PSA, observou-se que a eficiência da extinção de fluorescência experimental foi consistentemente bastante mais baixa do que o esperado. Para interpretar este resultado, tem de se chegar à conclusão que a sonda PSA deve estar bem fora da influência do grupo de extinção, quando comparado com as experiências de pireno.

No 5º Capítulo estudamos a extinção de fluorescência com a formação de excímero das sondas py10-PC e py6-PC, em MLV de mistura de POPC com colesterol, através de fluorescência de estado estacionário. Utilizando fluorescência resolvida no tempo, determinou-se o tempo de vida de fluorescência dos monómeros de py10-PC e py6-PC e dos excímeros de Bis-py10-PC e de Bis-py4-PC na presença de colesterol, tempos de vida necessários ao formalismo cinético. Observou-se que um alto conteúdo de colesterol reduz significativamente a dinâmica difusional de ambas as sondas, apesar de estes desvios parecem menores com o aumento da temperatura. Este decréscimo na difusão lateral resulta da organização introduzida pela presença do colesterol. Os resultados gerais apresentados nesta tese são a prova de que é possível ganhar conhecimento valioso sobre a membrana lipídica estudando a cinética de reacção em 2D com o formalismo adequado, usando principalmente fluorescência de estado estacionário. Os resultados também demonstram que as características e propriedades das sondas utilizadas, a definição precisa das distâncias colisionais e a acessibilidade das sondas de extinção aos fluoróforos são complicações que devem ser tidas em consideração quando se estuda processos de extinção de fluorescência na secção mais ordenada e hidratada das bicamadas fosfolipídicas.

Palavras Chave: Bicamadas Lipídicas; Reacções controladas por difusão; Cinética a duas dimensões; Sondas de Pireno; Extinção de Fluorescência; Formação de Excímero.

Abstract

Many fundamental biochemical processes occur in biological membranes, a great number of which depend on lateral diffusion, such as the mitochondrial respiratory chain, the photosynthetic electron transport system and sensory and regulatory processes. Lateral diffusion in membranes has been exhaustedly studied but seldom has a theoretical formalism adequate to 2D reactions been used. In his work, the kinetic formalism introduced by Razi Naqvi in 1974 was used to analyze fluorescence quenching and excimer of several pyrene probes.

We found that the fluorescence quenching of py10-PC by the spin probe 10-DOXYL-PC is, within the experimental error, in complete accordance with the theoretical prediction. However, for the system involving py6-PC quenched by 5-DOXYL-PC, large deviations are perceived, with the quenching efficiency appearing to be higher than the theoretical prediction, but increasing the collisional distance allows for a very good approximation with the experimental values. We discuss several possible influences that may explain this situation, which analogously occurred in the quenching of free pyrene by the same spin-probe.

We show that the excimer formation of py10-PC and py6-PC is in complete accordance with the theoretical prediction, until probe molar proportion of 2 and 4 mol %, respectively. Above these proportions, the experiments display a quenching efficiency lower than expected. Molecular dynamics have shown increased ordering and more tight packing in the py10-PC vicinity and interdigitation of pyrene group into the apposed leaflet, accounting for the diminishing diffusion of both probes. We also found that high cholesterol content severely hinders the diffusion dynamics of both probes, this decrease seems to result from the organization introduced by the cholesterol presence.

The results overall presented are proof that it is possible to gain valuable knowledge of the lipid membrane by studying the kinetics of reactions in 2D with the adequate formalism, while mainly using steady-state fluorescence.

Keywords: Lipid Bilayers; Diffusion-Controlled Reactions; Two-dimensional Kinetics; Pyrene Probes; Fluorescence Quenching; Excimer Formation

Abbreviations, Conventions and Symbols

Bis-py4-PC	1,2-bis-(1-pyrenebutanoyl)-*sn*-glycero-3-phosphocholine
Bis-py10-PC	1,2-bis-(1-pyrenedecanoyl)-*sn*-glycero-3-phosphocholine
$\boldsymbol{c}$	Concentration of particles
Chol	Cholesterol
Complex I	NADH-ubiquinone oxidoreductase
Complex II	Succinate-ubiquinone oxidoreductase
Complex III	Ubiquinone-cytochome c oxidoreductase
Complex IV	Cytochrome c-O_2 oxidoreductase
$\boldsymbol{D}$	Molecular diffusion coefficient
2D	Two-dimensional
3D	Three-dimensional
$\boldsymbol{D}_{\mathbf{m}}$	Mutual diffusion coefficient
DMPC	1,2-dimyristoyl-sn-glycero-3-phosphocholine
DOPC	1,2-dioleoyl-sn-glycero-3-phosphocholine
5-DOXYL-PC	1-palmitoyl-2-stearoyl-(5-DOXYL)-*sn*-glycero-3-phosphocholine
10-DOXYL-PC	1-palmitoyl-2-stearoyl-(10-DOXYL)-*sn*-glycero-3-phosphocholine
DPH	Diphenylhexatriene
ESR	Electron spin resonance
FCS	Fluorescence correlation spectroscopy
FRAP	Fluorescence recovery after photobleaching
FRET	Förster resonance energy transfer
GPCR	G-protein-coupled receptors
GUV	Giant unilamellar vesicles
$\mathbf{I_0}$	Fluorescence intensity in the absence of a quencher
I	Fluorescence intensity in the presence of a quencher
$\mathbf{I_E}$	Fluorescence intensity of the excimer
$\mathbf{I_M}$	Fluorescence intensity of the monomer
$\boldsymbol{k_3(t)}$	Rate coefficient of a diffusion controlled process in 3D geometry
$\boldsymbol{k_2(t)}$	Rate coefficient of a diffusion controlled process in 2D geometry

k_{FE}	Pyrene excimer radiative rate constant
k_{FM}	Pyrene monomer radiative rate constant
K_n	Modified Bessel functions of order n
L_α	Liquid-crystalline phase
$L_{\beta'}$	Gel tilted phase
L_c	Crystal phase
LUV	Large unilamellar vesicles
MD	Molecular dynamics
MLV	Multilamellar vesicles
N	Avogadro constant
NADH	Nicotinamide adenine dinucleotide, reduced form
$NADP^+$	Nicotinamide adenine dinucleotide, phosphate, oxidized form
NMR	Nuclear magnetic resonance
$P_{\beta'}$	Rippled-gel phase
PC	phosphatidylcholine
pK_a	Acid dissociation constant
POPC	1-palmitoyl-2-oleoyl-sn-glycero-3-phosphocholine
PSI	Photosystem I
PSII	Photosystem II
PSA	1-pyrenesulfonate
py6-PC	1-palmitoyl-2-(1-pyrenehexanoyl)-*sn*-glycero-3-phosphocholine
py10-PC	1-palmitoyl-2-(1-pyrenedecanoyl)-*sn*-glycero-3-phosphocholine
pyr	Pyrene
$[Q]_2$	2D Quencher molecular concentration
R	Distance between the geometrical centers of two diffusing molecules
R_C	Collisional distance between the geometrical centers of two reacting molecules
SPT	Single particle tracking
SUV	Small unilamellar vesicles
t	Time
T_m	Main phase transition temperature of a phospholipid bilayer

$\boldsymbol{\tau}$	Unquenched fluorescence lifetime
$\boldsymbol{\tau}_{\mathbf{E}}$	Excimer fluorescence lifetime
$\boldsymbol{\tau}_{\mathbf{M}}$	Monomer fluorescence lifetime
UV	Ultraviolet range of the electromagnetic spectrum

Contents

Chapter 1

General Introduction

1.1 Biological Membranes

Biological membranes are essential to life, they are the natural delimitation of all cells and its several intracellular compartments, controlling the communication between the inside and the outside of the living cellular units. However, biological evolution provided that the most vital aspect of biological membranes is that it serves as a “scenario” for a large variety of a fundamental biochemical processes [Gennis, 1989].

1.1.1 Biomembrane Structure

The major constituents of biological membranes are lipids and proteins. Protein-to-lipid ratios in membranes vary considerably with membrane function, although most membranes are at least one-half protein in weight. Biomembranes are supramolecular assemblies, where membrane proteins carry out the dynamic processes associated with membranes, while lipids form the phospholipid bilayers, the base structure of biological bilayers (Figure 1.1). Lipids are elongated methilenic molecules of amphiphilic characteristics, which, in aqueous media, spontaneously self-organize so that their hydrophilic headgroups are exposed to water and their hydrophobic ‘tails’ are hidden from it. The hydrophobic effect ensures that above a certain concentration of amphiphiles in aqueous media, they always form amphiphilic structures, such as lipid bilayers. Membrane proteins come in many forms, integral or intrinsic proteins are tightly bound to membranes by hydrophobic forces, whereas peripheral or extrinsic proteins are bound to the membrane interface. Many lipids and proteins carry oligosaccharide groups that project into the surrounding external aqueous medium. The two sides are almost always asymmetrical and have distinct lipid and protein composition [Gennis, 1989; Voet & Voet, 2011].

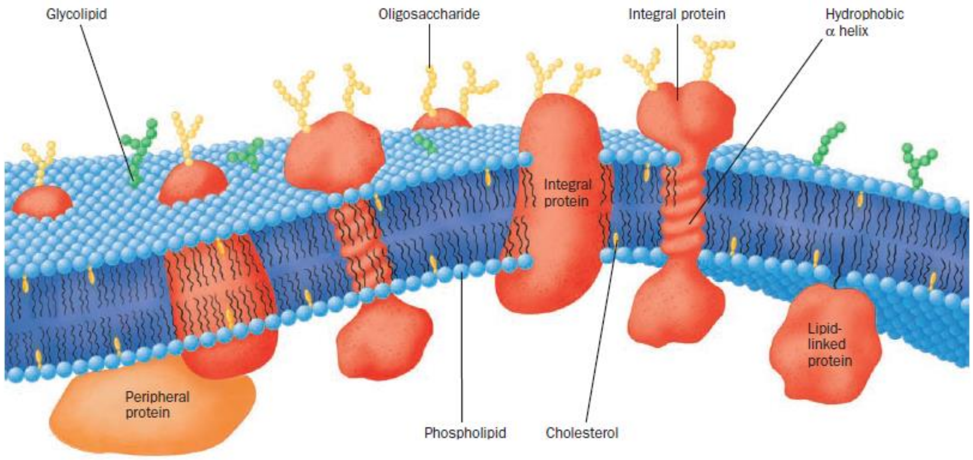

Figure 1.1 – Diagram of a plasma membrane. Integral proteins are embedded in a bilayer composed of phospholipids and cholesterol. The carbohydrate components of glycoproteins and glycolipids occur only on the external face of the membrane. Most biological membranes have a higher proportion of protein than is drawn here. From Voet & Voet (2011).

In 1972, Singer and Nicolson proposed the Fluid Mosaic Model, defining the membrane as a two-dimensional (2D) fluid, in which proteins and lipids diffuse freely in the plane of the membrane. Currently there is a general consensus and a conviction that in some biological membranes, namely in the plasma membrane, there are micro-disperse lipid domains due to lipid lateral phase separation [Edidin, 2003; Simons & Vaz, 2004; Meder *et al.*, 2006]. The hydrophobic interior of natural membranes generally has a low viscosity and a fluid-like, rather than gel-like, consistency. Maintenance of this bilayer fluidity appears to be essential for normal cell growth and reproduction. All cell membranes contain a mixture of different fatty acyl chains and are fluid at the temperature at which the cell is grown. Animal and bacterial cells adapt to a decrease in growth temperature by increasing the proportion of unsaturated to saturated fatty acids in the membrane, which tends to maintain a fluid bilayer at the reduced temperature. Membrane cholesterol is another major determinant of bilayer fluidity. Cholesterol tends to immobilize their fatty acyl chains and restrict the random movement of the fatty acyl chains, which are closest to the outer surfaces of the leaflets, but it separates and disperses their tails, causing the inner regions of the bilayer to become slightly more fluid. The net effect of cholesterol on membrane fluidity varies, depending on the lipid composition [Lodish *et al.*, 2000].

1.1.2 Lateral Diffusion

In biological systems, diffusion is one of the most intriguing processes that arise from the dynamics of biological molecules. Membrane lipids and proteins are generally free to move laterally within membranes if they are not restricted by certain interactions. Lateral diffusion is a fairly quick and spontaneous process. It might be expect that Nature would work in a manner that is orderly and deterministic but plenty of evidence exists that diffusion in living systems is often governed by this simple principle of randomness. Random diffusion is a non-specific process that over time may provide for essential reaction pathways in living matter, although it is too disordered and disorganized to be relied on in delicate life processes. Therefore, in order to take advantage of the ubiquity and toughness of random diffusion, life has over evolutionary time scales developed strategies to compartmentalize and structure living matter on scales from nanometers to the size of whole cells and organisms. Within these structures, macromolecules, macromolecular assemblies, as well as sub-cellular entities perform random as well as directed diffusion. The compartmentalization and structure are provided by biomembranes, as well as a host of fibers and scaffolding structures. [Vattulainen & Mouritsen, 2005].

The lipid lateral diffusion coefficient, D, is usually studied in homogeneous lipid fluid phases because of the complexity of native membranes. It can be derived from free volume theory and its extension to free-area theory for 2D systems. Originally, Cohen and Turnbull derived the free-volume theory to describe three-dimensional (3D) diffusion of hard spheres [Cohen & Turnbull, 1959; Turnbull & Cohen, 1970], but later it has been applied to a number of systems including for diffusion in 2D systems [Clegg & Vaz, 1985; Almeida *et al.*, 1992]. This was shown to quantitatively describe diffusion in lipid bilayers in the liquid-crystalline phase [Vaz *et al.*, 1985]. According to free-volume theory, diffusion of a particle of comparable size of the molecules that constitute the fluid, takes place only when a free volume greater than a certain critical size exists next to the particle. Free volumes smaller than this critical size, do not contribute to diffusion, and the problem is reduced to determining the statistical distribution of free volume throughout the whole system [Almeida & Vaz, 1995].

The methods to measure lateral diffusion coefficients of lipids most frequently applied both in synthetic and natural membranes to model membrane systems are: fluorescence quenching [Fato *et al.*, 1985; Martins & Melo, 2001], neutron scattering [Pfeiffer *et al.*, 1988; Tabony & Perly, 1990]; ESR [Traüble & Sackmann, 1972; Freed, 1994], FRAP [Axelrod *et al.*, 1976; Jovin & Vaz, 1989], NMR [Lindblom & Orädd, 1994; Bloom & Thewalt, 1994]; and SPT [Saxton & Jacobson, 1997]. The results of these measurements clearly demonstrate that the lateral motion of lipids depends on many factors such as chemical structures, degree of hydration, phase state and temperature, along with the presence of cholesterol and proteins. The values of diffusion coefficient in the lamellar phase, for a large variety of probe molecules and matrix bilayer systems, typically fall on the $10^{-8}\mathrm{cm}^2\,\mathrm{s}^{-1}$ range for fluorescence quenching, FRAP and NMR determinations [Martins *et al.*, 1996], and in the $10^{-7}\mathrm{cm}^2.\mathrm{s}^{-1}$ range when ESR is used [Tocanne *et al.*, 1994].

1.1.3 Reactions in Biological Membranes

Biological membranes are not passive molecular structures whose sole purpose is the compartementalization of cells. Is has been well established that most of the fundamental cellular functions involve membranes at some point. Such processes as DNA replication, biosynthesis of both proteins of lipids and signal transduction are examples of the most important reactions occurring in cell membranes, and many essential enzymes are membrane associated [Gennis, 1989]. These enzymes may catalyze transmembrane reactions that entail reactants in both sides of the membrane, they can participate in active transport and be required in sequential reactions occurring in the plane of the membrane, while others may have membrane-bound substrates or be affect biosynthesis of the membrane and its maintenance. The Human Genome Project has found that roughly between one third and half of genes are coding for membrane-associated proteins. Nevertheless, the kinetics of bimolecular reactions that occur under the constraints imposed by a biological membrane has not received due attention, particularly from the experimental point of view [Melo & Martins, 2006].

It is widely known that lateral diffusion is crucial to a wide range of cellular processes occurring in the plane of the membrane [Axelrod, 1983; McCloskey & Poo, 1984]. Some enzymes have been found to have kinetic parameters that could be interpreted to involve diffusion-controlled limited reactions in homogeneous solution [Fersht, 1999], and there are likely some membrane processes that are also thought to depend on diffusion-controlled kinetics at some point [Tocanne *et al.*, 1994; Almeida & Vaz, 1995]. Among those are the following examples of membrane enzymology and chemoreception: electron transport chains; enzymes that utilize membrane-bound substrates; enzymes that shuttle between the cytosol and the membrane and whose activities are modulated by membrane binding; and sensory and regulatory processes at the membrane interface [Melo & Martins, 2006].

One such example is the mitochondrial electron transport system (Figure 1.2) was originally conceived as being fixed in the inner membrane [Winkstöm & Saraste, 1984], but its components are known to move freely and interact by random collisions since the early 1980s [Hackenbrock *et al.*, 1986]. There is strong evidence that the overall kinetics of this electron transfer chain is largely diffusion-controlled in vivo, occurring between randomly distributed components of the electron transport chain [Winkstöm & Saraste, 1984].

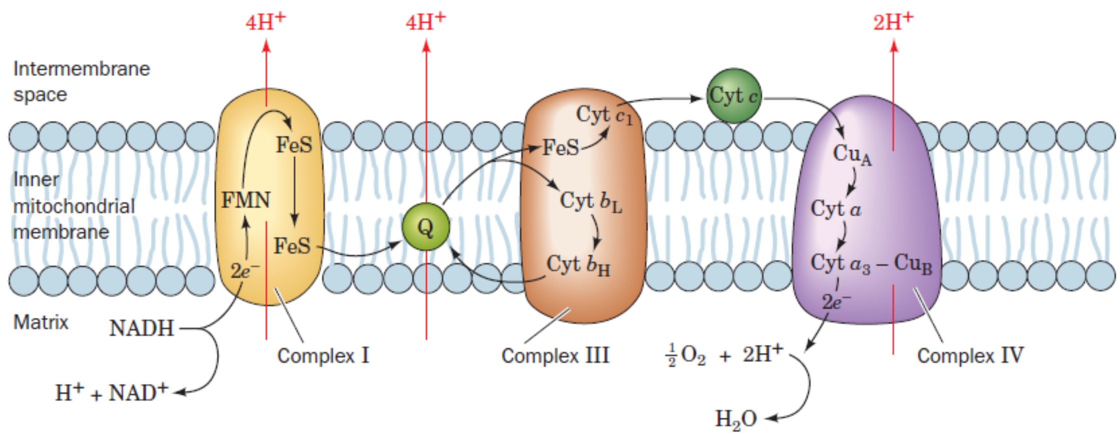

Figure 1.2 – The mitochondrial electron-transport chain. The pathways of electron transfer and proton pumping are indicated. Electrons are transferred between Complexes I and III by membrane-soluble CoQ (Q) and between Complexes III and IV by the peripheral membrane protein cytochrome c (Cyt c). Complex II (not shown) transfers electrons from succinate to CoQ. From Voet & Voet (2011).

The mechanism of absorption of light and its conversion into chemical energy in eukaryotic plants involving photosystem I (PSI) and photosystem II (PSII) is mediated by the transfer of reducing equivalents between these two complexes. This transfer is accomplished by water-soluble plastocyanin and membrane-associated plastoquinone. The two photosystems are linked kinetically by an electron transport chain that conducts reducing equivalents extracted from water by PSII to PSI, and delivers electrons to $NADP^+$ at the end of the pathway [Melo &

Martins, 2006]. It is now well established that diffusion in the thylakoid membrane is highly restricted. Theories considering domain-limited reactivity [Melo *et al.*, 1992; Saxton, 2002; Vaz, 1994] and/or anomalous lateral diffusion [Dewey, 1997] are required because of the heterogeneous distribution of the involved components and the crowding of the medium.

Precise control of physiological phenomena is performed by various kinds of receptor-mediated signaling. The vast majority of receptors belong to a superfamily of G-protein-coupled receptors (GPCR), are implicated in a wide range of extracellular chemical messengers including neurotransmitters, hormones, lipids, photons, odorants, taste ligands, nucleotides and calcium ions [Hur & Kim, 2002]. The classical view of GPCR signaling is based on random collisions between proteins that diffuse freely in the plasma membrane [Rimon *et al.*, 1978; Hanski *et al.*, 1979]. However, recent evidence suggests that receptors, G proteins and effectors are less mobile than previously appreciated [Cherry *et al.*, 1998]. Moreover, the specificity of signaling in intact cells appears to be significantly greater than in reconstituted systems. Thus, a more organized system, rather than a pure freely diffusible arrangement, has been suggested to enable both rapid and specific propagation of extracellular stimuli to intracellular signaling molecules [Neubig, 1994].

1.2 Model Systems

The inherent complexity of native membranes makes it quite difficult to interpret experimental results quantitatively. The most commonly used tools to model to study reactions in biological membranes are synthetic membranes, with the reactants and the membrane chemically well defined, allowing a reaction with homogeneous distribution of reactants. More specifically, artificial phospholipid bilayers are an experimental model where the parameters can be controlled and questions can be asked in answered in a more exact way.

Fluorescence quenching is an experimental technique that has many applications in the study of phospholipid bilayers [Lakowicz, 2006]. It has long been employed to investigate lateral diffusion in lipid vesicles [Fato *et al.*, 1985; Martins & Melo, 2001]. In the present study, we make use of pyrene and several derivatives through either self-quenching with excimer formation or quenching by DOXYL-labeled phospholipid spin probes.

1.2.1 Model Membranes

Liposomes are concentrically enclosed multilamellar structures with layers of aqueous solution entrapped. They are vesicles formed spontaneously when a dry film of phospholipids is hydrated in excess water at a temperature above the main phase transition temperature (T_m) [Bangham *et al.*, 1965]. These onion-like liposomes are called MLV (multilamellar vesicles), are usually very easy to produce and are heterogeneous in size and shape [New, 1990].
Unilamellar vesicles may also be produced to model membranes. These can be obtained with several average diameters: SUV (small unilamellar vesicles) typically are between 20 to 50 nm average diameter [Huang, 1969]; LUV (large unilamellar vesicles) have an average diameter from 100 nm to 500 nm [Hope *et al.*, 1985]; and GUV (giant unilamellar vesicles) are normally bigger than 1000 nm [Crommelin & Schreir, 1994].
The majority of the lipids that constitute membranes are amphipathic molecules composed of hydrophilic and hydrophobic moieties. These amphipathic lipids are customarily divided into three large groups: glycerophospholipids (commonly referred simply as phospholipids), sphingolipids and sterols. Although convened this way from a chemical point of view, each of these groups compromise a wide range of different species, while sharing some common basic chemical structure [Dowhan, 1997].
The more abundant lipids in eukaryotic cells are the glycerophospholipids, and in particularly, phosphatidylcholines (PC). In this work we used 1-palmitoyl-2-oleoyl-sn-glycero-3-phosphocholine (POPC), a PC with a C16:0 fatty acid sterified in *sn*-1 and a C18:1Δ^9 in *sn*-2 (Figure 1.3). The pK_a of the phosphate group is around 1.3 therefore the headgroup of PC at physiological pH is zwitterionic,.

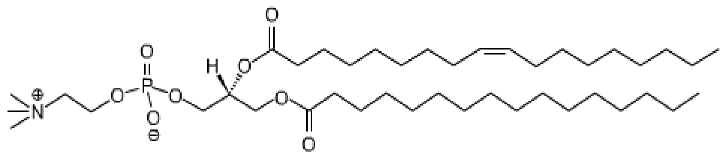

Figure 1.3 – Chemical structure of POPC.

In the fifth chapter of this work we studied mixtures of POPC with cholesterol (Chol). Cholesterol is a major component of animal plasma membranes (the most abundant steroid in animals), where it is typically present at 30 to 40 mol %, and occurs in lesser amounts in the membranes of their subcellular organelles. It is a modified sterol consisting of four linked hydrocarbon rings forming the bulky steroid structure (Figure 1.4). There is a hydrocarbon tail linked to one end of the steroid and a hydroxyl group linked to the other end. The hydroxyl group is able to form hydrogen bonds with nearby carbonyl oxygen of phospholipid and sphingolipid head groups.

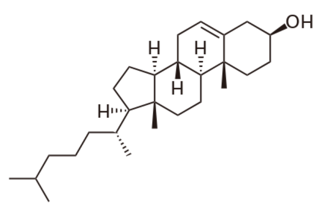

Figure 1.4 – Chemical structure of Cholesterol.

The phospholipid bilayer has different levels of organization called phases. The predominance of a phase depends on such parameters as: molar lipid fraction, temperature, pressure, ionic strength and pH of the aqueous phase [Gennis, 1989]. When water is in excess, single-component PC bilayers display several transition temperatures between lamellar organizations (Figure 1.5), denoted as crystal (L_c), gel tilted ($L_{\beta'}$), rippled-gel ($P_{\beta'}$), and liquid-crystalline (L_α) [Small, 1986].

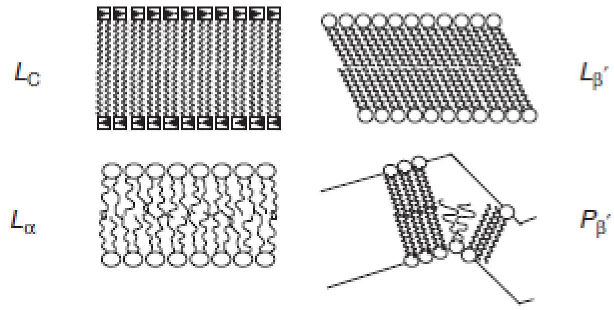

Figure 1.5 – Diagrams of the layer structures of the several phases of phospholipid bilayers discussed. Adapted from Vaz (2008).

The acyl chains in the L_c state are well ordered, essentially in all-*trans* conformation, with the molecules very tightly packed. The gel phases are slightly less ordered in the hydrocarbon region than the L_c phase, characterized by the direction of chain tilt to the bilayer interface.

When raising the temperature above a characteristic temperature, T_m, which depends on the type of lipid that constitutes the bilayer, the ordered or gel phase is converted into a so-called "liquid-crystalline" "fluid," or L_α phase in which the acyl chain configuration is characterized by a low *trans*/*gauche* configurational ratio and the chains are still packed in a more or less hexagonal lattice but with a low coherence length and a lattice spacing of about 0.45 nm. Lipid bilayers in the fluid phase have low conformational, rotational, and translational order. The chain-melting transition at T_m is observed in all lipid bilayers regardless of the chemical identity of the lipid that constitutes the bilayer. The different transitions in the gel phase do not occur in all lipid bilayers, in which transitions depend on the lipid species of which the bilayer is constituted [Vaz, 2008]. This liquid-crystalline phase is the most usual phase in which biological membranes are encountered, although ordering depends heavily on sterol content.

In L_α phase phosphatidylcholine bilayers, the choline head group has a probability distribution function that places it very close to the probability distribution function for the phosphate group (the choline head group lies roughly parallel to the bilayer plane and only slightly above the level of the phosphate group). The glycerol backbone of the lipid is oriented almost perpendicular to the membrane plane and the *sn*-1 acyl chain proceeds vertically into the bilayer, whereas the *sn*-2 acyl chain is kinked at the second carbon. This structure makes the effective length of the *sn*-2 chain slightly (about 1.5 methylene groups) shorter than the *sn*-1 acyl chain [Nagle & Tristram-Nagle, 2000; Vaz, 2008].

The $L_{\beta'}$ and the L_{α} of PC phospholipid bilayers have been the most extensively studied by X-ray diffraction methods. These results indicate that in the $L_{\beta'}$ phase the acyl chains are highly ordered, with a tilt orientation relative to the axis perpendicular to the bilayer surface. The first complete picture of the structure of a fluid membrane was obtained by liquid-crystallography, in which X-ray and neutron diffraction are combined trough joint-refinement procedures [Wiener & White, 1992]. The $1/e$ – half-width of the Gaussian distributions are taken as measure of the precision in the location of the group, and since the narrowest thermal distribution is that of the glycerol region, this indicates that the glycerol backbone is the most rigid portion in a fluid phospholipid bilayer (Figure 1.6).

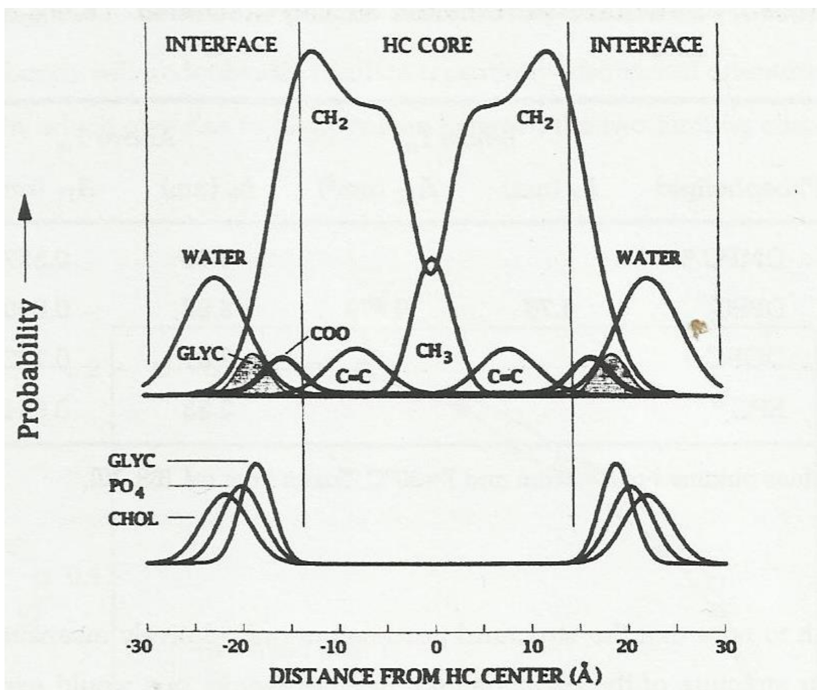

Figure 1.6 – Quasimolecular model and multi-Gaussian representation of a 1,2-dioleoyl-*sn*-glycero-3-phosphocholine (DOPC) fluid bilayer. The structure consists of the time-averaged distributions of the principal structural groups of the lipid projected onto an axis normal to the bilayers plane. The distributions are Gaussians whose areas equal the number of structural groups represented by them; the distributions therefore represent the probability of finding a structural group at a particular location. It is of note that the interfaces of the bilayer, each about 1,5 nm thick, account for about half of the bilayer thickness. Adapted from Wiener & White (1996).

The order parameters profile of pure POPC bilayers, determined by NMR methods and also by molecular dynamics (MD) simulations, have been published very recently (Figure 1.7) [Ferreira *et al.*, 2013]. POPC acyl chains display a higher order parameter at the upper carbons while showing greater disorder at the end of the chain. This initial segment near the interface is associated with tethering of the acyl chain to the interface, while below this region the segments are substantially more disordered [Brown, 1996]. Profiles of similar order parameters are usually obtained for various lipids such as phosphatidylserine (POPS) and sphingomyelin [Gennis, 1989]. Ferreira *et al.* (2013) also show that with increasing cholesterol concentration the acyl chains of POPC gradually adopt a more extended conformation while the orientation and dynamics of the polar groups are rather unaffected.

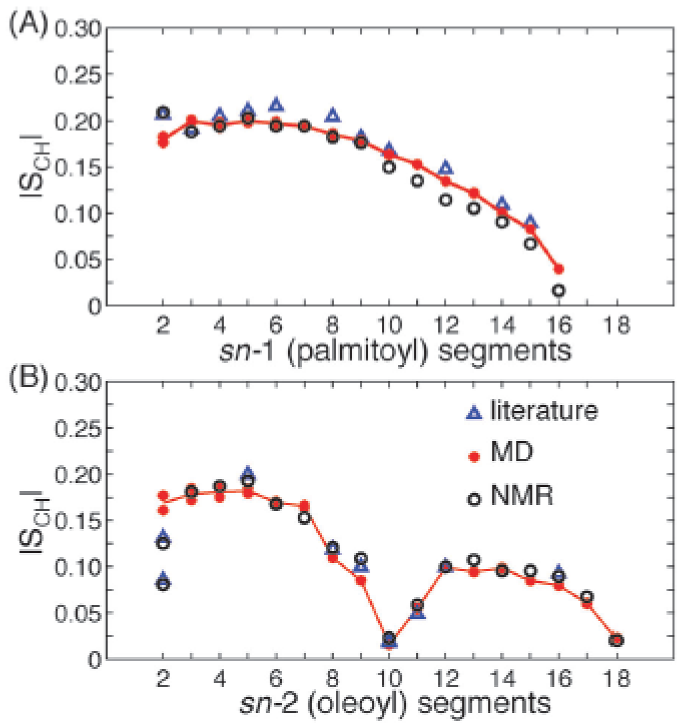

Figure 1.7 – Order parameter magnitude $|S_{CH}|$ vs. carbon segment number for the *sn*-1 and *sn*-2 acyl chains of POPC (A and B respectively). Data from fully hydrated POPC at 300 K obtained with $^{1}H–^{13}C$ solid-state NMR (hollow dots) and MD simulations (full dots), as well as literature data (triangles) from ^{2}H NMR (*sn*-1 and *sn*-2 at 300 K). Adapted from Ferreira *et al.* (2013).

1.2.2 Pyrene Probes

Pyrene probes and its derivatives have a long history in the study of membrane properties [Brocklehurst *et al.*, 1970; Vaughan & Weber, 1970]. This is mainly due to their particular photophysical properties, i.e. their ability to form excimers depending on their local concentration. At low concentrations pyrene displays a highly structured emission. At higher concentrations the previously invisible UV emission of pyrene becomes visible at 470 nm. This long-wavelength emission is due to excimer formation. The term "excimer" is an abbreviation for an excited state dimer [Lakowicz, 2006].

The structures of the four fluorescent probes we used in this work are displayed in Figure 1.8.

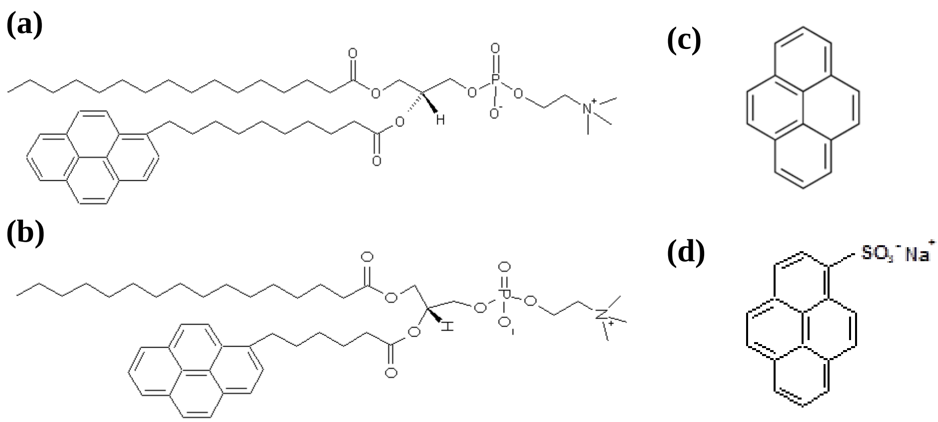

Figure 1.8 – Structures of **(a)** py10-PC, **(b)** py6-PC, **(c)** pyrene and **(d)** PSA.

Pyrene-labeled lipids like 1-palmitoyl-2-(1-pyrenedecanoyl)-*sn*-glycero-3-phosphocholine (py10-PC) and 1-palmitoyl-2-(1-pyrenehexanoyl)-*sn*-glycero-3-phosphocholine (py6-PC) have found numerous applications in membrane biophysics, biochemistry and cell biology. They have some advantages over non-lipid probes as “system probes”, for instance, the depth and orientation of the fluorophore in the bilayer is often better defined than is the case with a free fluorophore. The average location of the pyrene group and dynamics of py10-PC have been studied by molecular dynamics [Repákova *et al.*, 2006]. Another important advantage of pyrene lipids is that the pyrene moiety is hydrophobic and thus does not strongly modify the hydrophobic character of a linked acyl chain. The other advantage is that the system should be sterically less perturbed when the probe is an integral part of a system component, e.g. a lipid molecule. However, it is clear that some perturbation of the system is unavoidable, independent of the chemical structure of the fluorophore [Somerharju, 2002]. Florescence lifetimes of py10-PC has been determined in fluid DMPC bilayers [Martins & Melo, 2001], and been found to be around 200 ns in degassing conditions at 25ºC.

Free pyrene is notable for its spectroscopic properties and is known as a probe of hydrophobic regions [Valeur, 2002]. The complete partition of pyrene into bilayers is guaranteed by the following considerations: pyrene is essentially insoluble in water (solubility of about 6.5×10^{-7} M, at 25ºC [Pearlman *et al.*, 1984]) but fairly soluble in aliphatic hydrocarbons (e.g. solubility in dodecane 7.4×10^{-2} M, at room temperature [Almgren *et al.*, 1979]), one can estimate a very high value of about 10^5 for the partition constant into the hydrophobic interior of bilayers. The localization of free pyrene inside lipid bilayers has been established by direct methods such as NMR [Podo & Blasie, 1977; Hoff *et al.*, 2005] and molecular dynamics simulations [Hoff *et al.*, 2005; Čurdova *et al.*, 2007; Loura *et al.*, 2013]. It displays a lifetime near 400 ns in degassed organic solvents, but lower lifetimes have been found in lipid bilayers [Martins & Melo, 2001], furthermore its sensitivity to polarity has been shown to be very useful [Arrais & Martins, 2007].

Pyrenesulfonate is a water soluble amphiphile. The partition coefficient of PSA to model membranes from an aqueous solution has been determined previously. With $K_p = 6.9\times10^3$ at 25ºC [Manuel & Martins, 2008] there is no doubts about its complete partition into fluid bilayers in the experimental conditions of this work. Additionally, Kachel *et al.*, 1998 have estimated the localization of PSA to be about 17 Å from the center of a fluid DOPC (1,2-dioleoyl- *sn*-glycero-3-phosphocholine), e.g. at the level of carbonyls and below the phosphocholine group. PSA is also a strong acid, with a pK_a close to 1 [Weast, 1983], and therefore has a formal negative charge at neutral pH. It's lifetime in water is around 65 ns [Bohne *et al.*, 1990].

All of the four pyrene probes utilized have excitations maximums below 350 nm, with fluorescence emission coming in between 350 and 450 nm. It is of note that pyrene has a much more complex emission, while its derivatives a couple of well-defined peaks (Figure 1.9)

(a)

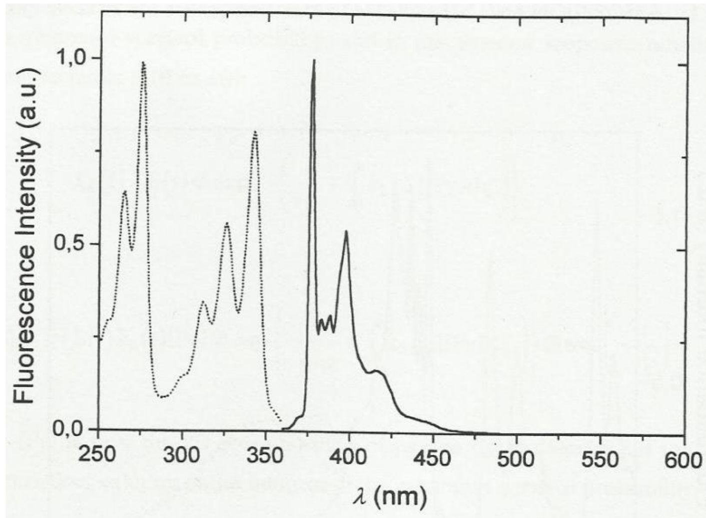

(b)

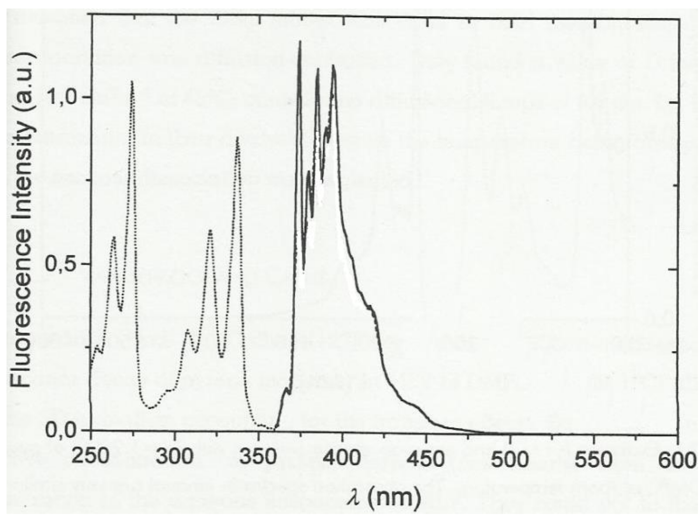

(c)

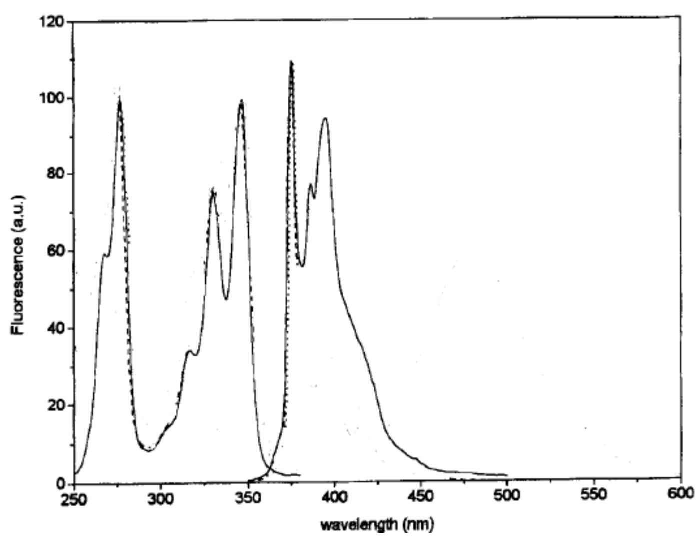

Figure 1.9 – Excitation and emission spectra of: **(a)** py10-PC in DMPC MLV, from Martins, 2000; **(b)** Pyrene in DMPC MLV, adapted from Martins, 2000; **(c)** PSA in DMF, adapted from Uznanski *et al.*, 1998.

1.3 Diffusion Controlled 2D Kinetics

Several approaches to the theory of diffusion-influenced reactions in a (3D) space have a counterpart in the studies in 2D media. Fluorescence quenching, due to its theoretical and experimental simplicity and good mimesis of the diffusion-controlled reactions, has been widely used as a model reaction for the bilayer resident reactants. In the present experimental approach, the majority of works follow the hydrodynamic theory for diffusion-controlled reactions [Melo & Martins, 2006].

1.3.1 Hydrodynamic Theory

The hydrodynamic approach to diffusion controlled bimolecular reactions makes use of the integration of the Fick's law of diffusion, Equation 1.1, as originally proposed by Smoluchowski (1916 & 1917) to model the kinetics of colloid coagulation:

$$\frac{\partial c(R,t)}{\partial t} = D\nabla^2 c(R,t) \quad (\mathbf{Eq.\,1.1})$$

where D is the diffusion coefficient of the moving particles, and the concentration of particles, c, is a function of distance, R, and time, t. For the integration, Smoluchowski used the initial condition of uniform concentration, $c(R_\mathrm{C},0) = c_0$, and the boundary conditions of infinite reservoir, $c(\infty,t) = c_0$, and immediate reaction at R_C, the collisional distance, $c(R_\mathrm{C},t) = 0$. Under these constraints the time-dependent rate coefficient is given by Equation 1.2 where D_m is the mutual diffusion coefficient (sum of the diffusion coefficients of the particle and trap) and N the Avogadro constant.

$$k_3(t) = 4\pi N D_\mathrm{eff} R_\mathrm{C}\left(1 + \frac{R_\mathrm{C}}{\sqrt{\pi D_\mathrm{m}}}\right) \quad (\mathbf{Eq.\,1.2})$$

As previously commented, for large t values $k_3(t)$; $4\pi N D_{\mathrm{m}} R_{\mathrm{C}}$ is practically time independent, and the reaction velocity proportional to the reagent concentrations.

In 1974, Razi Naqvi presented an analytical solution for the time-dependent rate coefficient of diffusion-controlled quenching of excited molecules in 2D, Equation 1.3:

$$k_2(t) = \frac{8D_{\mathrm{m}}N}{\pi}\int_0^{\infty} \exp(-\alpha u^2)\frac{du}{u[J_0^2(u) + Y_0^2(u)]} \quad (\mathbf{Eq. 1.3})$$

In the equation, α is a function of D_{m} and R_{C}, $\alpha = D_{\mathrm{m}}/R_{\mathrm{C}}^2$, $J_0^2(u)$ and $Y_0^2(u)$ are the zero-order Bessel functions of the first and second kind, and u a dummy integration variable. Eq. 1.3 was obtained from the integration of Fick's law of diffusion with the Smoluchowski's initial and boundary conditions, and is the equivalent in two dimensions to the Smoluchowski–Sveshnikoff formalism for 3D fluorescence quenching. Shortly after this publication, Owen (1975) published the same equation for the same physical situation, pure 2D diffusion-controlled quenching.

The previous Equations 1.2 and 1.3, based on the Smoluchowski's initial and boundary conditions, are only valid for diffusion-controlled reactions. In the case of diffusion influenced reactions, where not all collisions are effective, Collins and Kimball (1949) radiation boundary condition should be used instead.

Razi Naqvi and Owen both introduced approximate mathematical expressions to Eq. 1.3, based on estimations valid for some ranges of the parameters and time. Besides them, several other authors have proposed simplified formulas to use in the analysis of time-resolved and steady-state diffusion-controlled reactions in 2D [Szabo *et al.*, 1987; Caruso *et al.*, 1991; Baros *et al.*, 1991; Medhage & Almgren, 1992; Razi Naqvi *et al.*, 2000]. Some of these simplified formalisms recognize that, within certain time limits, depending on D_{m} and R_{C}, the time decay of the excited species concentration, $I_2(t)$, may be approximated by a square root law formally identical to that of 3D but in which A_2, coefficient of t, and B_2, of $\sqrt{t}$, are adapted to the 2D condition as shown in Equation 1.4, in which $[Q]_2$ is the 2D molecular concentration [Owen, 1975; Caruso *et al.*, 1991; Baros *et al.*, 1991].

$$I_2(t) \cong I_2(0)\exp\left[-\left(A_2 t + B_2\sqrt{t}\right)\right] \quad (\mathbf{Eq. 1.4})$$

$$A_2 = \frac{1}{\tau_{\mathrm{E}}} + a[\mathrm{Q}]_2 D_{\mathrm{m}}$$

$$B_2 = bR_{\mathrm{C}}[\mathrm{Q}]_2\sqrt{D_{\mathrm{m}}}$$

Different authors give non-identical values for the best fitting parameters *a* and *b*, those proposed in 1991 by Caruso *et al.* and in 2000 by Razi Naqvi *et al.* giving the best approximations.
The objective of these simplifications was enunciated as being a help to those that wanted to make such studies without the hassle of the mathematic delicacies involved in the calculation of the original equation. The formulas presented are, indeed, very convenient and, within the applicability range, sufficient for most practical cases. However, not many researchers in the field took advantage of those recipes except the authors themselves [Melo & Martins, 2006].

1.3.2 Steady-state Fluorescence Approximation

The methodology was pointed out by Szabo (1989) who termed it the mean-field approach, and yields results which are essentially indistinguishable from those calculated by using the exact formalism. This alternative approach can in fact be traced all the way back to Waite (1957) who was among the first to apply a many-body treatment to the kinetics of diffusion-controlled reactions. It was pointed out that Waite's formalism leads to a steady-state rate constant that depends on the concentration of the quencher [Peak *et al.*, 1976]. Based on the underlying reasoning for this, described in detail by Razi Naqvi (1994), the implicit equation which must be solved for finding k_2 is equation 1.5:

$$k_2([\mathrm{Q}]_2) = 2.\pi.D_m.q.R_{\mathrm{C}}.\frac{K_1(q.R)}{K_0(q.R)} \quad (\mathbf{Eq. 1.5})$$

where $K_n(x)$ denotes modified Bessel function of the second kind and order *n*, and $q^2 = (1/\tau + k_2.[\mathrm{Q}]_2)/D_{\mathrm{m}}$.

Equation 1.5 is easy to solve numerically and can be handled even by a commercially available spreadsheet program, if one begins an iterative process by writing Equation 1.7:

$$y^{(n+1)} \equiv \frac{k_2^{(n+1)}([\mathrm{Q}]_2)}{2\pi.D\mathrm{m}} = \frac{\left(\sqrt{2\varphi_2.y^{(n)}+\mathrm{C}}\right).K_1\left(\sqrt{2\varphi_2.y^{(n)}+\mathrm{C}}\right)}{K_0\left(\sqrt{2\varphi_2.y^{(n)}+\mathrm{C}}\right)} \qquad (\mathbf{Eq.\,1.7})$$

where $\varphi_{2=}\pi.R^2.[\mathrm{Q}]_2$ and $\mathrm{C} = {R_\mathrm{C}}^2/\tau.D_m$. Carrying the iteration out by a computer, a convenient initial guess for the process is $y^{(0)} = 1$, which usually takes about 10 steps if performed manually.

Moreover Razi Naqvi *et al.*, 2000 verified that pyrene excimer formation studied through steady-state data can be successfully analyzed and the values agree with that calculated from the relation which emerges from the steady-state analysis, Equation 1.8.

$$\frac{\mathrm{I_E}}{\mathrm{I_M}} = \frac{k_{FE}}{k_{FM}}.k_2.[\mathrm{Q}]_2.\tau_\mathrm{E} \qquad (\mathbf{Eq.\,1.8})$$

$\mathrm{I_E}$ and $\mathrm{I_M}$ are the fluorescence intensities of the excimer and monomer, respectively, k_{FE} and k_{FM} are the rate constants for the excimer and monomer fluorescence and τ_E is the fluorescence lifetime. However, only a very limited range of self-quenching concentration range was tested (probe to lipid ratio varying from 0.5 to 1.33 mol%) [Martins *et al.*, 1996].

To our knowledge, besides the introductory presentation of the methodology and its application to published data by Razi Naqvi and colaborators [2000], there has only been one work applying this approximation using steady-state fluorescence. Medevdeva *et al.* (2005) did it while studying quenching of a cascade reaction involving erythrosin B and 4-dimethylamino-4’-aminostilbene, with nitroxide radical 5-DOXYL stearic acid. Their approach is rather enigmatic and difficult to fully decipher. In the present work, we executed and make available a clear cut and simple description of how to apply the necessary and sufficient Razi Naqvi formalism to analyze simple model systems of 2D diffusion-controlled reactions through steady-state fluorescence approach.

1.4 References

Almeida, P.F.F., Vaz, W.L.C., Thompson, T.E., Lateral diffusion in the liquid phases of dimyristoylphosphatidylcholine/cholesterol lipid bilayers: A free volume analysis, Biochemistry 31, 6739–6747 (1992).

Almeida, P.F.F., Vaz, W.L.C., Lateral diffusion in membranes, in: R. Lipowsky, E. Sackmann (Eds.), Handbook of Biological Physics, Elsevier, Amsterdam, 1995.

Almgren, M., Grieser, F., Thomas, J.K., Dynamic and static aspects of solubilization of neutral arenes in ionic micellar solutions, J. Am. Chem.Soc. 101, 279–291 (1979).

Arrais, D., Martins, J., Bilayer polarity and its thermal dependency in the ℓ_o and ℓ_d phases of binary phosphatidylcholine/cholesterol mixtures, Biochim. Biophys. Acta 1768, 2914–2922 (2007).

Axelrod, D., Koppel, D.E., Schlessinger, J., Elson E., Webb, W.W., Mobility measurements by analysis of fluorescence photobleaching recovery kinetics, Biophys. J. 16, 1055–1069 (1976).

Axelrod, D., Lateral motion of membrane proteins and biological fuction, J. Memb. Biol. 75, 1-10 (1983).

Bangham, A.D., Standish, M.M., Watkins, J.D., Diffusion of univalent ions across the lamellae of swollen phospholipids. J. Mol. Biol.., 13, 238-251 (1965).

Baros, F., Naoumi, A., Viriot, M.-L., Andre, J.C., Lateral diffusion in synthetic membranes: models and experiments of protein influence, J. Chem. Soc., Faraday Trans. 87, 2039–2046 (1991).

Bohne, C., Abuin, E.B., Scaiano, J.C., Characterization of the triplet-triplet annihilation process of pyrene and several derivatives under laser excitation, J. Am. Chem. Soc. 112, 4226-4231 (1990).

Bloom, M., Thewalt, J.L., Spectroscopic determination of lipid dynamics in membranes. Chem. Phys. Lipids 73, 27-38 (1994).

Brocklehurst, J.R., Freedman, R.B., Hancock, D.J., Radda, G.K., Membrane studies with polarity-dependent and excimer-forming fluorescent probes. Biochem. J. 116, 721-731 (1970).

Brown, M. F., Membrane Structure and Dynamics Studied with NMR Spectroscopy, in Membrane Structure and Dynamics (Merz, K. M., and Roux, B., Eds.), Birkhäuser, Boston, pp. 175-252, (1996).

Caruso, F., Grieser, F., Murphy, A., Thistlethwaite, P., Urquhart, R., Almgren, M., Wistus, E., Determination of lateral diffusion coefficients in air–water monolayers by fluorescence quenching measurements, J. Am. Chem. Soc. 113, 4838–4843 (1991).

Cherry, R.J., Smith, P.R., Morrison, I.E.G., Fernandez, N., Mobility of cell surface receptors: a re-evaluation, FEBS Lett. 430, 88–91 (1998).

Clegg, R.M., Vaz, W.L.C., Translational diffusion of proteins and lipids in artificial lipid bilayer membranes. A comparison of experiment with theory, in: Progress in Protein–Lipid Interactions, Vol. 1, eds A. Watts and J.J.H.H.M. De Pont, Elsevier, Amsterdam, 1985.

Cohen, M.H., Turnbull, D., Molecular transport in liquids and glasses, J. Chem. Phys. 31, 1164–1169 (1959).

Collins, F.C., Kimball, G.E., Diffusion-controlled reaction rates, J. Colloid Sci. 4, 425–437 (1949).

Crommelin, D.J.A., Schreir, H., Liposomes. In Colloidal Drug Delivery Systems. J. Kreuter, editor. Marcel Dekker, New York, 1994.

Čurdova, J., Čapková, P., Plášek, J., Repáková, J., Vattulainen, I., Free pyrene probes in gel and fluid membranes: perspective through atomistic simulations, J. Phys. Chem. B 111, 3640–3650 (2007).

Dewey, T.G., Fractals in Molecular Biophysics, Oxford University Press, New York, 1997.

Dowhan, W., Molecular basis for membrane phospholipid diversity: why are there so many lipids? Annu. Rev. Biochem. 66, 199-232 (1997).

Edidin, M., The state of lipid rafts: from model membranes to cells, Annu. Rev. Biophys. Biomol. Struct. 32, 257–283 (2003).

Fato, R., Battino, M., Castelli, G.P., Lenaz, G., Measurements of the lateral diffusion coefficients of ubiquinones in lipid vesicles by fluorescence quenching of 12-(9-anthroyl)stearate, FEBS Lett. 179, 238–242 (1985).

Ferreira, T.M., Coreta-Gomes, F., Ollila, O.H., Moreno, M.J., Vaz, W.L.C., Topgaard, D., Cholesterol and POPC segmental order parameters in lipid membranes: solid state ^{1}H–^{13}C NMR and MD simulation studies, Phys. Chem. Chem. Phys. 15, 1976- 1989 (2013).

Fersht, A., Structure and Mechanism in Protein Science: A Guide to Enzyme Catalysis and Protein Folding, W. H. Freeman, New York, 1999.

Freed, J.H., Field gradient ESR and molecular diffusion in model membranes, Annu. Rev. Biophys. Biomol. Struct. 23, 1–25 (1994).

Gennis, R.B., Biomembranes, Molecular Structure and Function, Springer-Verlag, New York, 1989.

Hackenbrock, C.R., Chazotte, B., Gupte, S.S., The random collision model and a critical assessment of diffusion and collision in mitochondrial electron transport, J. Bioenerg. Biomembranes 18, 331–368 (1986).

Hanski, E., Rimon, G., Levitzki, A., Adenylate cyclase activation by the β-adrenergic receptors as a diffusion-controlled process, Biochemistry 18, 846–853 (1979).

Hoff, B., Strandberg, E., Ulrich, A.S., Tieleman, D.P., Posten, C., ^{2}H-NMR study and molecular dynamics simulation of the location, alignment,and mobility of pyrene in POPC bilayers, Biophys. J. 88, 1818–1827 (2005).

Hope, M.J., Bally, M.B., Webb, G., Cullis, P.R., Production of large unilamellar vesicles by rapid extrusion procedure. Characterization of size distribution, trapped volume and ability to maintain a membrane potential. Biochim. Biophys Acta 812, 55-63 (1985).

Huang, C.-h., Studies on phosphatidylcholine vesicles. Formation and physical charecteristics, Biochemistry 8, 344-352 (1969).

Hur, E.-M., Kim, K.-T., G protein-coupled receptor signalling and cross-talk. Achieving rapidity and specificity, Cell. Signal. 14, 397–405 (2002).

Jovin, T.M., Vaz, W.L.C., Rotational and translational diffusion in membranes measured by fluorescence and phosphorescence methods, Methods Enzymol. 172, 471–513 (1989).

Kachel, K., Asuncion-Punzalan,E., London, E., The location of fluorescence probes with charged groups in model membranes, Biochim. Biophys. Acta 1374, 63-76 (1998).

Lakowicz, J.R, Principles of Fluorescence Spectrocopy 3rd Ed., Springer Science, 2006.

Lindblom, G., Orädd, G., NMR studies of translational diffusion in lyotropic liquid crystals. Prog Nucl. Magm. Reson. Spectrosc. 26, 483-515 (1994).

Lodish, H., Berk, A., Zipursky. S.L., Matsudaira, P., Baltimore, D., Darnell, J., Molecular Cell Biology, 4th edition, W. H. Freeman, New York, 2000.

Loura, L.M.S., Martins do Canto, A.M.T., Martins, J., Sensing hydration and behavior of pyrene in POPC and POPC/cholesterol bilayers: A molecular dynamics study, Biochim. Biophys. Acta 1828, 1094–1101 (2013).

Manuel, M., Martins, J., Partitioning of 1-pyrenesulfonate into zwitterionic and mixed zwitterionic/anionic fluid phospholipid bilayers, Chem. Phys. Lipids 154, 79-86 (2008).

Martins, J., Vaz, W.L.C., Melo, E., Long-range diffusion coefficients in two-dimensional fluid media measured by the pyrene excimer reaction, J. Phys. Chem. 100, 1889-1895 (1996).

Martins, J., On Modeling Reactions in Biological Membranes: Diffusion-Controlled Kinetics in Homogeneous Phospholipid Bilayers, Ph.D. Thesis, Oeiras, 2000.

Martins, J., Melo, E., Molecular mechanism of lateral diffusion of py_{10}-PC and free pyrene in fluid DMPC bilayers, Biophys. J. 80, 832-840 (2001).

McCloskey, M., Poo, M.-m., Protein diffusion in cell membranes: some biological implications, Int. Rev. Cytol. 87, 19-81 (1984).

Meder, D., Moreno, M.J., Verkade, P., Vaz, W.L.C., Simons, K., Phase coexistence and connectivity in the apical membrane of polarized epithelial cells, Proc. Natl. Acad. Sci. USA 103, 329–334 (2006).

Medhage, B., Almgren, M., Diffusion-influenced fluorescence quenching dynamics in one to three dimensions, J. Fluoresc. 2, 2–21 (1992).

Medvedeva, N., Papperb, V., Likhtenshtein, G.I., Study of rare encounters in a membrane using quenching of cascade reaction between triplet and photochrome probes with nitroxide radicals, Phys. Chem. Chem. Phys. 7, 3368–3374 (2005).

Melo, E.C.C., Lourtie, I.M.G., Sankaram, M.B., Thompson, T.E., Vaz, W.L.C., Effects of domain connection and disconnection on the yields of in-plane bimolecular reactions in membranes, Biophys. J. 63, 1506–1512 (1992).

Melo, E., Martins, J., Kinetics of bimolecular reactions in model bilayers and biological membranes. A critical review, Biophys. Chem. 123, 77–94 (2006).

Nagle, J.F., Tristram-Nagle, S., Structure of lipid bilayers, Biochim Biophys Acta. 1469 (3), 159-195 (2000).

Neubig, R.R., Membrane organization in G-protein mechanism, FASEB J. 8, 939–946 (1994).

New, R.R.C, Preparation of liposomes. In Liposomes: A Practical Approach. IRL Press, Oxford, 1990.

Owen, C.S., Two dimensional diffusion theory: cylindrical diffusion model applied to fluorescence quenching, J. Chem. Phys. 62, 3204-3207 (1975).

Peak, D., Pearlman, K., Wantuck, P.J., Competitive effects on the rate of the diffusion-controlled reaction A+B→C, J. Chem. Phys. 65, 5538 (1976).

Pearlman, R.S., Yalkowsky, S.H., Banerjee, S., Water solubilities of polynuclear aromatic and heteroaromatic compounds, J. Phys. Chem. Ref. Data 13, 555–562 (1984).

Pfeiffer, W., Schlosssbauer, G., Knoll, W., Farago, B., Steyer A., Sackmann, E., Ultracold neutron scattering study of local lipid mobility in bilayer membranes, J. Phys. (France) 49, 1077–1082 (1988).

Podo, F., Blasie, J.K., Nuclear magnetic resonance studies of lecithin bimolecular leaflets with incorporated fluorescent probes, Proc. Natl.Acad. Sci. USA 74, 1032–1036 (1977).

Razi Naqvi, K., Diffusion-controlled reactions in two-dimensional fluids: discussion of measurements of lateral diffusion of lipids in biological membranes, Chem. Phys. Lett. 28 280–284 (1974).

Razi Naqvi, K., In Condensed Matter Theories, Nova Science Publishers: New York, Vol. 9, p 233, 1994.

Razi Naqvi, K., Martins, J., Melo, E., Recipes for analyzing diffusion-controlled reactions in two dimensions: time-resolved and steady-state measurements, J. Phys. Chem. B, 104, 12035-12038 (2000).

Repáková, J., Holopainen, J.M., Karttunen, M., Vattulainen, I., Influence of pyrene-labeling on fluid lipid membranes, J. Phys. Chem. B 110, 15403-15410 (2006).

Rimon, G., Hanski, E., Braun, S., Levitzki, A., Mode of coupling between hormone receptors and adenylate cyclase elucidated by modulation of membrane fluidity, Nature 276, 394–396 (1978).

Saxton, M.J., Jacobson, K., Single-particle tracking: applications to membrane dynamics. Annu. Rev. Biophys. Biomol. Struct. 26, 373-399 (1997).

Saxton, M.J., Chemically limited reactions on a percolation cluster, J. Chem. Phys. 116, 203–208 (2002).

Simons, K., Vaz, W.L.C., Model systems, lipid rafts, and cell membranes, Annu. Rev. Biophys. Biomol. Struct. 33, 269–295 (2004).

Singer, S.J., Nicolson, G.L., The fluid mosaic model of the structure of cell membranes, Science 175 (4023), 720-731 (1972).

Small, D.M., Phospholipids. In The Physical Chemistry of Lipids: From Alkanes to Phospholipids. Handbook of Lipid Research, Vol 3. D.J. Hanahan, editor. Plenum Press, New York, 1986.

Smoluchowski, M.V., Drei vorträge über diffusion, brownsche molekularbewegung und koagulation von kolloidteilchen, Phys. Z. 17, 557–571 and 587–599 (1916).

Smoluchowski, M.V., Versuch einer mathematischen theorie der koagulationskinetic kolloider lösungen, Z. Phys. Chem. 92, 129–168 (1917).

Somerharju, P., Pyrene-labeled lipids as tools in membrane biophysics and cell biology, Chem. Phys. Lipids 116, 57–74 (2002).

Szabo, A., Cope, D.K., Tallman, D.E., Kovach, P.M., Wightman, R.M., Chronoamperometric current at hemicylinder and band microelectrodes: theory and experiment, J. Electroanal. Chem. 217, 417–423 (1987).

Szabo, A., Theory of diffusion-influenced fluorescence quenching, J. Phys. Chem. 93, 6929-6939 (1989).

Tabony, J., Perly, B., Quasielastic neutron scattering study of fast local translational diffusion of lipid molecules in phospholipid bilayers, Biochim. Biophys. Acta 1063, 67–72 (1990).

Tocanne, J.-F., Dupou-Cézanne, L., Lopez, A., Lateral diffusion of lipids in model and natural membranes, Prog. Lipid Res. 33, 203–237 (1994).

Traüble, H., Sackmann, E., Studies of the crystalline-liquid crystalline phase transition of lipid model membranes, III. Structure of a steroid-lecithin system below and above the lipid phase transition, J. Am. Chem. Soc. 94, 4499–4510 (1972).

Turnbull, D., Cohen, M.H., On the free volume model of the liquid-glass transition, J. Chem. Phys. 52, 3038–3041 (1970).

Uznanski, P., Pecherz, J., Wolszczak, M., Kryszewski, M., Photophysical studies of funcionalised polyionene complexes in solutions and in the solid state, J. Photochem. Photobiol. A: Chemistry 115, 129-136 (1998).

Valeur, B., Molecular Fluorescence: Principles and Applications, Wiley-VCH, 2002.

Vattulainen, I., Mouritsen, O.G., Diffusion in condensed matter: Methods, materials, models, 2nd Edition, pp. 471–509, Springer-Verlag, Berlin, 2005.

Vaughan, W.M., Weber, G., Oxygen quenching of pyrenebutyric acid in water. A dynamic probe of the microenviroment, Biochemistry 9, 466-473 (1970).

Vaz, W.L.C., Clegg, R.M., Hallmann, D., Translational diffusion of lipids in liquid crystalline phase phosphatidylcholine multibilayers. A comparison of experiment with theory, Biochemistry 24, 781–786 (1985).

Vaz, W.L.C., Diffusion and chemical reactions in phase-separated membranes, Biophys. Chem. 50, 139–145 (1994).

Vaz, W.L.C., Lipid Bilayers: Properties. Wiley Encyclopedia of Chemical Biology. 1–15 (2008).

Voet, D., Voet, J.G., Biochemistry 4th Ed., John Wiley & Sons Inc., (1995).

Waite, T.R., Diffusion-limited annealing of radiation damage in germanium, Phys. Rev. 107, 471–478 (1957).

Weast, R.C., Handbook of Chemistry and Physics, 6th Ed., CRC Press, 1983.

Wikström, M., Saraste, M., The mitochondrial respiratory chain, in: L. Ernster (Ed.), Bioenergetics, Elsevier, Amsterdam, 1984.

Chapter 2

Quenching of Lipid-bound 1-Pyrenyl Fluorescent Probes by DOXYL-labeled Phospholipid Spin Probes

2.1 Introduction

Biological membranes are dynamic supramolecular structures by nature, and the frequency and extent of motion are important in considering biological functions [Axelrod, 1983; Almeida & Vaz, 1995]. For example, some enzymatic or lipoperoxidation radical reactions require the reactants (membrane components) to be freely diffusing within the plane of the bilayer [Melo & Martins, 2006], whereas other processes clearly rely on constraints imposed on the mobility of membrane components [Kalay *et al.*, 2012; Saxton, 2012]. An increasing literature is being developed about quantitative and qualitative aspects of the dynamics and kinetics of membrane reacting components [Melo & Martins, 2006; Kalay, 2012]. From all this has emerged a useful physical description of membranes which encompasses the ways in which proteins and lipids move and how they mutually interact inserted and/or associated in biological membranes. Translational motion of lipids and proteins is modeled as a two-dimensional (2D) diffusion problem [Clegg & Vaz, 1985]. The measurement of lateral diffusion coefficients utilizes sophisticated applications of optical and magnetic resonance spectroscopies [Almeida & Vaz, 1995], while other advanced approaches (such as fluorescence recovery after photobleaching (FRAP), fluorescence correlation (FCS) and single molecule (SPT) spectroscopies, and derived technical improvements) have been developed to address specifically questions pertinent to membranes dynamics, where barriers somehow hinders free lateral diffusion of molecules [Elson, 2011; Chen *et al.*, 2006; Wieser & Schütz, 2008]. However, despite the existence of substantial fraction of work about the lateral diffusion of membrane components [Saxton, 1999], studies about the specificities of kinetics concerning reactions and processes occurring in biomembranes have received much less attention [Melo & Martins, 2006; Kalay, 2012]. The kinetics of bimolecular diffusion-controlled reactions in model bilayers has been reviewed by Melo and Martins (2006), being implicit that the development of proper analysis of 2D kinetics is persistently hampered due to the exceedingly mathematics embodied in the kinetic formalisms [Medhage & Almgren, 1992]. As shown, Smoluchowski's formalism yields, in the case of 2D systems [Razi Naqvi, 1974], unwieldy expressions for the time-dependent rate-coefficient (used to solve the differential equations inherent to kinetic schemes), and for the corresponding concentration-dependent rate constant (which determines the rate of a diffusion-controlled reaction under stationary conditions) [Razi Naqvi *et al.*, 2000]. A consistent analysis of pyrene excimer formation in fluid homogeneous bilayers used the 2D variant of the Smoluchowski formalism for diffusion-controlled reactions [Martins *et al.*, 1996; Martins & Melo, 2001]. Still, most of the efforts were devoted to the analysis of time-resolved fluorescence data, and it must be recognized that the analysis of photostationary results did not reach the level of removing the tedious mathematical difficulties in data analysis [Martins *et al.*, 1996, Martins & Melo, 2001]. Fortunately, Razi Naqvi and coworkers (2000) developed a recipe, based on a mean-field approach presented by Szabo (1989), to analyze photostationary fluorescence quenching experiments, and verified that pyrene excimer formation studied through steady-state data can be successfully analyzed [Razi Naqvi *et al.*, 2000]. Yet, only a very limited range of self-quenching concentration range was tested (probe to lipid ratio varying from 0.5 to 1.33 mol %) [Martins *et al.*, 1996].

In the present study, we focused in developing a reliable and coherent analysis of diffusion-controlled steady-state quenching of fluorescent pyrenyl-labeled phospholipids probes, by spin-labeled phospholipids, in fluid homogeneous POPC (1-palmitoyl-2-oleoyl-*sn*-glycero-3-phosphocholine) bilayers. It is exact for a wider range of quenching species (until the proportion 8 mol% of the spin-labeled phospholipid), and makes use of an intermediate level instrumentation, available in most of the fluorescence laboratories. The first qualitative assessment of this type of fluorescence quenching in lipid bilayers was presented in the mid 70's by Bieri and Wallach (1975). Soon after, London and Feigenson (1981) elaborated about the analysis of quenching for several small fluorophores (diphenylhexatriene – DPH, *p*-terphenyl, pyrene) by a spin-labeled phospholipid, and introduced a non-linear variation for the classical Stern-Volmer plot (the ratio of the fluorescence quantum yield in absence of quencher, divided by the corresponding quantum yield in the presence of quencher, depends linearly on the quencher concentration [Valeur, 2002]), based on a theoretical volumic sphere of action for the fluorescence quenching process (previously developed by Chance *at al.* (1975) in the analysis of 12-(9-anthroyl) stearic acid fluorescence by ubiquinones, in mitochondrial membranes). These early works already called the attention for a non-linear dependence of the experimental data of photostationary fluorescence quenching in membranes. However, due principally to the very high concentrations of quenching species used, to the *a priori* assumption of a static mechanism of quenching, and to the wrong dimensionality of the kinetic formalisms and of concentration units, an unequivocal attribution of the physical-chemical basis of this observation was not attained. The first contribution toward a dependable analysis of steady-state fluorescence quenching studies was undertaken by Blackwell *et al.* (1987), presenting an empirical method (founded in the work of Owen (1975) and applying numerical evaluations and diverse mathematical approximations) for estimating lateral diffusion coefficients from quenching data. A comprehensive survey on the mean-field approach to photostationary diffusion-controlled fluorescence quenching (in homogeneous media, either volumic (3D), or surface (2D)), was presented by Szabo (1989), yielding results indistinguishable from those obtained by using the exact 2D formalism and requiring little mathematical efforts [Razi Naqvi *et al.*, 2000]. We make use of this recipe in the analysis of 2D fluorescence quenching data, showing that it is exact for specific experimental conditions and reveal some deviations of experimental circumstances, from the various requirements embodied in the theoretical framework.

We studied two similar systems, both in POPC multilamellar vesicles (MLV), quenching of two membrane-bound pyrenyl probes by a DOXYL group also attached to a phospolipidic chain at the same respective depths (Structures in Fig 2.1), at several temperatures.

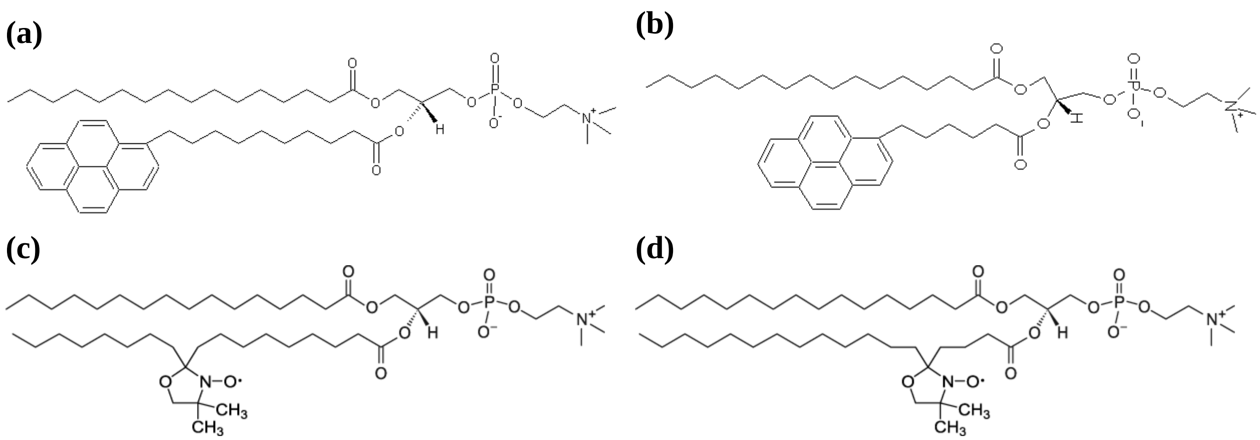

Figure 2.1 – Structures of **(a)** py10-PC, **(b)** py6-PC, **(c)** 10-DOXYL-PC and **(d)** 5-DOXYL-PC.

We found that the fluorescence quenching of py10-PC (1-palmitoyl-2-(1-pyrenedecanoyl)-*sn*-glycero-3-phosphocholine) by the spin probe 10-DOXYL-PC (1-palmitoyl-2-stearoyl-(10-DOXYL)-*sn*-glycero-3-phosphocholine) is, within the experimental error, in complete accordance with the theoretical prediction. All the analysis is based in independent values of lateral diffusion coefficients (for both reactants) previously determined [Martins *et al.*, 1996; Vaz *et al.*, 1985], as well as for the py10-PC experimental fluorescence lifetimes. The collisional distance was calculated from well-established molecular considerations [Edward, 1970; Zhao *et al.*, 2003], and was taken as 6.7 Å (the sum of the van der Waals radius of the pyrenyl and of the DOXYL groups). In this case, the remarkable agreement between experiment and theory is observed for proportions of spin-labeled phospholipid from 1 until 8 mol % (which is within the range of acceptable values for kinetic experiments in model membranes, using either fluorescence or electron spin resonance spectroscopies). However, for the system involving py6-PC (1-palmitoyl-2-(1-pyrenehexanoyl)-*sn*-glycero-3-phosphocholine) quenched by the spin-probe 5-DOXYL-PC (1-palmitoyl-2-stearoyl-(5-DOXYL)-*sn*-glycero-3-phosphocholine), large deviations are perceived (the quenching efficiency appears to be higher than the theoretical prediction), and we attribute these deviancies to several possible influences. Interestingly, increasing the collisional distance (R_C) in the theoretical model from 6.7 Å to 11 Å allows for a very good approximation with the experimental values, and we discuss why this could be a useful attempt to comprehend the results observed.

2.2. Experimental Methods

2.2.1 Chemicals and Solvents

1-Palmitoyl-2-oleoyl-sn-glycero-3-phosphocholine (POPC), purity > 99.9%, 1-Palmitoyl-2-stearoyl-(5-DOXYL)-*sn*-glycero-3-phosphocholine (5-DOXYL-PC) and 1-palmitoyl-2-stearoyl-(10-DOXYL)-*sn*-glycero-3-phosphocholine (10-DOXYL-PC) were purchased from Avanti Polar Lipids (Alabaster, AL, USA). 1-Hexadecanoyl-2-(1-pyrenedecanoyl)-sn-glycero-3-phosphocholine (py10-PC) and 1-Hexadecanoyl-2-(1-pyrenehexanoyl)-sn-glycero-3-phosphocholine (py6-PC) were purchased from Molecular Probes (Eugene, Oregon, USA). MilliQ water was obtained using a Millipore Simplicity 185 system (electrical conductivity and pH are $5.4 \times 10^{-6}\ \mathrm{S}.m^{-1}$ and around 6.6–7, respectively, at room temperature). All organic solvents (highest purity) were from Merck (Darmstadt, Germany).

2.2.2 Stock Solutions

Lipids and probes obtained in the form of powder were diluted in a chloroform:methanol 2:1 (v/v) mixture to the desired concentrations. When acquired as a solution in chloroform instead of powder form, dilutions using the same mixture were made. The stock solutions were then kept at -20ºC.

2.2.3 Aqueous Liposome Suspensions

MLV were prepared according to a modified protocol of a firmly established method [Szoka, Jr. & Papahadjopolous, 1980] as described before [Manuel & Martins, 2008]. Stock solutions of phospholipid, fluorescent probe and spin probe, dissolved in chloroform:methanol 2:1 (v/v), were mixed in settled proportions in a evaporating flask (volume of 20 cm^3) with a conical shape bottom, this increases the homogeneity of the dry lipid film. The organic solvents were then dried at 50ºC using a rotary evaporator Heidolph VV-micro (vacuum pump Büchi V-500, coupled to a Büchi V-800 digital control, isolated from the rotary evaporator by a liquid N_2 trap) with slow rotation, 15 min at 150 mBar until a homogeneous lipid film was formed, followed by 1 h at 5 mBar, to remove traces of organic solvents. The lipidic film was hydrated with MilliQ water during at least 1 h at 50ºC, well above the phase transition temperature (T_M) of POPC (T_M = -2.6ºC) [Marsh, 1990], vortexing regularly, forming multilamellar vesicles (MLV) as the lipid sheets detach during agitation and self-close.

In order to minimize light scattering, fluorescence lifetimes were determined using large unilamellar vesicles (LUV). These were prepared by the extrusion method (MacDonald et al., 1993), using an Avanti Mini-Extruder (Alabaster, AL, USA), forcing the MLV to pass 15 times at room temperature through a pair of Nucleopore polycarbonate filters (Wathman, USA), with pore size of 0.1 μm.

Liposome solutions were kept in the refrigerator and usually used within 24 hours.

2.2.4 Time-resolved Fluorescence

Time-resolved fluorescence measurements in the absence of quenching were made in a Spex Fluoromax-4 spectrofluorimeter (Jobin Yvon–Horiba, France) equipped with a thermostated cell holder with magnetic stirring accessory, coupled to a refrigerated/heated circulator Julabo F12-ED (precision of 0.1 °C). The LUV suspensions were placed in 1 cm quartz cuvettes and were stirred continuously during the measurements. Excitation wavelength was 342 nm while emission wavelength was set to 376 nm, and slit width was 1 nm for both excitation and emission. Collections were made in 1024 channels and measurement range was 800 ns. A collection of the prompt for the lamp (at 342 nm) was made before the each collection of a corresponding sample. Collections were only stopped when counts reached at least around 10^4 at the beginning of the decay. Total lipid concentration of LUV suspensions used was 0.1 mM, with probe molecular percentage set at 0.125% (1 probe per 800 phospholipids). Along with the low concentration and LUV utilization, a cut-off filter of 360 nm (Corion, WG360) was used to try to minimize light scattering. Decays were fitted with the manufacturer's software using two exponentials and no initial constrictions, and fluorescence lifetimes were determined by averaging the best decays obtained with χ^2 below 1.2.

2.2.5 Steady-state Fluorescence

Fluorescence spectra were recorded on a Spex Fluoromax-3 spectrofluorimeter (Jobin Yvon–Horiba, France) equipped with a thermostated cell holder with magnetic stirring accessory, coupled to a refrigerated/heated circulator Julabo F12-ED (precision of 0.1 °C). Emission spectra were corrected for the wavelength dependent response of monochromators, collimating optics and detection using the correction file provided by the manufacturer.

The MLV suspensions, total lipid concentration of 1 mM, were placed in 1 cm quartz cuvettes and were stirred continuously during the measurements. Spectra were acquired between 360 and 600 nm, slit width of 1 nm, and wavelength sampling interval of 0.5 nm, at temperatures of 25, 35 and 45ºC. Before each spectroscopic determination, the samples were always allowed to thermostatize for at least 10 minutes at the desired temperature. Samples with spin probe molecular percentage of 1, 2, 3, 5 and 8% were studied, while fluorescent probe content was kept at 0.1%. Values to quantify quenching were retrieved at the peak of maximum emission at 376 nm, and at least four different experiments were averaged.

2.2.6 Two-dimensional Kinetic Analysis

In fluorescence quenching cases like the py10-PC and py6-PC quenching by 10-DOXYL-PC and 5-DOXYL-PC, respectively, in POPC MLV an adapted 2D Stern-Volmer formalism should be used:

$$\frac{I_0}{I} = 1 + k_2.[Q]_2.\tau \qquad \textbf{(Eq. 2.1)}$$

The mathematical basis for this has been well established by both Szabo (1989) and Razi Naqvi et al. (2000), but requires certain premises to be met: that the fluorescence quenching is being studied in a system that can be modeled as a 2D medium; that the reaction is controlled by diffusion; that the average distance traversed by an excited molecule must be comparable to the average separation (around 3 nm) between the excited molecule and the quencher, which means, since the diffusion coefficient of a lipid molecule lies in the 10^{-8}–10^{-7} cm^2.s^{-1} range; and that the mean lifetime (τ) of the unquenched fluorophore should not be much shorter than 10^{-7}s [Razi Naqvi et al., 2000].

I_0 and I are the fluorescence intensities in absence and presence of the quencher, respectively. The steady-state rate constant for quenching reactions occurring in 2D media is k_2, while the quencher 2D concentration is represented by $[Q]_2$. The steady-state rate constant for quenching reactions occurring in 2D media (like membrane bilayers) is dependent on the quencher 2D concentration and should be calculated by iteratively solving the implicit Equation 2.2 [Razi Naqvi et al., 2000]. In this equation, $K_n(q.\,R_C)$ are modified Bessel functions of order n, D_m is the mutual diffusion coefficient, R is the collisional distance and $q^2 = (1/\tau + k_2.[Q]_2)/D_m$.

$$k_2([Q]_2) = 2.\pi.D_m.q.R_C.\frac{K_1(q.R_C)}{K_0(q.R_C)} \qquad \textbf{(Eq. 2.2)}$$

In order to solve Eq. 2.2 numerically we used a commercially available spreadsheet program, beginning the interactive process by writing Equation 2.3 (Razi Naqvi et al, 2000):

$$y^{(n+1)} \equiv \frac{k_2^{(n+1)}([\mathrm{Q}]_2)}{2\pi.D_\mathrm{m}} = \frac{\left(\sqrt{2\varphi_2.y^{(n)} + \mathrm{C}}\right).K_1\left(\sqrt{2\varphi_2.y^{(n)} + \mathrm{C}}\right)}{K_0\left(\sqrt{2\varphi_2.y^{(n)} + \mathrm{C}}\right)} \qquad (\mathbf{Eq.2.3})$$

where $\varphi_{2=}\pi.R^2.[\mathrm{Q}]_2$ and $\mathrm{C} = R^2/\tau.D_m$. The several terms used here are all reasonably known: 2D concentration can be calculated approximately with the area of POPC, 68,5 Å [Kučerka et al, 2005], R_C was calculated from well-established molecular considerations [Edward, 1970; Zhao et al, 2003], and was taken as 6.7 Å (the sum of the radius of the pyrene and DOXYL groups), while τ was determined experimentally in this work. This diffusions constants of py10-PC in phospholipid bilayers that have been determined previously [Martins & Melo, 2001], we estimated slightly higher coefficients for the py6-PC probe, and for the DOXYL probes an approximation to POPC diffusion was used [Vaz et al, 1985].

The process was started by calculating $[\mathrm{Q}]_2$ for each of the quencher concentrations and with that determining φ_2 for each individual concentration used. After this we calculated each of the terms on the right of Eq. 2.3 with the suggested initial guess of $y^{(0)} = 1$, and solved until $y^{(n)}$ was equal for at least three interactions (for example when $y^{11} = y^{12} = y^{13}$, Figure 2.2).

This usually took between 10-20 iterative steps, and in general took more iterations with increasing temperature. It also required more iterations when increasing concentration of quenching probe but the number of steps was relatively equal for both fluorescent probe – spin probe systems. Because the value of every term is established, from there we can obtain k_2 for every quencher concentration desired and from there use Eq. 2.1 to estimate it's theoretical I_0/I ratio, to be compared to the ratio obtained experimentally.

		$(\sqrt{2\phi_2 y^{(n)} + C})$	$K_1(\sqrt{2\phi_2 y^{(n)} + C})$	$K_0(\sqrt{2\phi_2 y^{(n)} + C})$
$y^{(0)} =$	**1**			
$y^{(1)} =$	**0,899489455541405**	0,503215517870991	1,642902098432860	0,919114532339480
$y^{(2)} =$	**0,894926348726504**	0,499086450733356	1,660319116399620	0,925934045933278
$y^{(3)} =$	**0,894718189581901**	0,498898183091510	1,661120051563800	0,926246705691004
$y^{(4)} =$	**0,894708691723104**	0,498889593031106	1,661156609971310	0,926260974969934
$y^{(5)} =$	**0,894708258351677**	0,498889201081401	1,661158278098350	0,926261626060119
$y^{(6)} =$	**0,894708238577654**	0,498889183197384	1,661158354212290	0,926261655768304
$y^{(7)} =$	**0,894708237675398**	0,498889182381366	1,661158357685240	0,926261657123840
$y^{(8)} =$	**0,894708237634229**	0,498889182344132	1,661158357843710	0,926261657185691
$y^{(9)} =$	**0,894708237632351**	0,498889182342433	1,661158357850940	0,926261657188512
$y^{(10)} =$	**0,894708237632265**	0,498889182342356	1,661158357851270	0,926261657188641
$y^{(11)} =$	**0,894708237632261**	0,498889182342352	1,661158357851290	0,926261657188647
$y^{(12)} =$	**0,894708237632261**	0,498889182342352	1,661158357851290	0,926261657188647
$y^{(13)} =$	**0,894708237632261**	0,498889182342352	1,661158357851290	0,926261657188647

Figure 2.2 – Example of an interactive solving of Eq. 2.3.

2.3 Results and Discussion

2.3.1 Fluorescence Lifetimes of py10-PC and of py6-PC in POPC Bilayers

Fluorescence lifetimes of py10-PC and py6-PC in POPC LUV were determined in the presence of oxygen, as was the case for all measurements. This option removes the uncertainty in the degassing procedures, and the oxygen quenching is treated as an additional photophysical process that lowers the fluorescence lifetimes. LUV were used in these time-resolved experiments to ensure a diminished light scattering, because while fluorescence lifetimes determined in MLV in the same conditions were found to be relatively indistinguishable from those obtained in LUV, the decays were of significant lesser quality.

We can see in Figure 2.3 the depiction of the best decays of py10-PC and py6-PC acquired at 25ºC. The decays were fitted using the software provided by the spectrofluorometer manufacturer, and were of monoexponential nature, although two-exponential fits had to be utilized due to a strong lamp profile caused by a lower photomultiplier resolution. The smaller lifetime refers to the adjustment made to fit the lamp distortion and was always in the 10^{-11}s range.

(a)

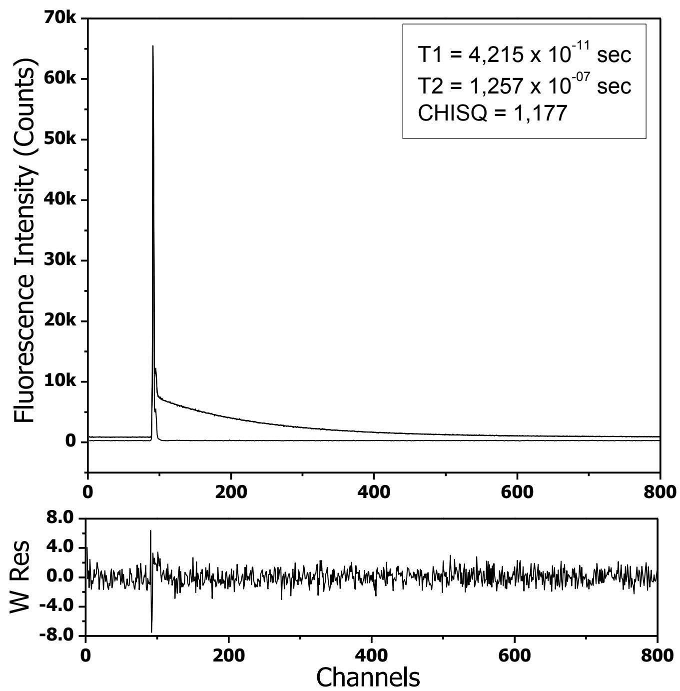

(b)

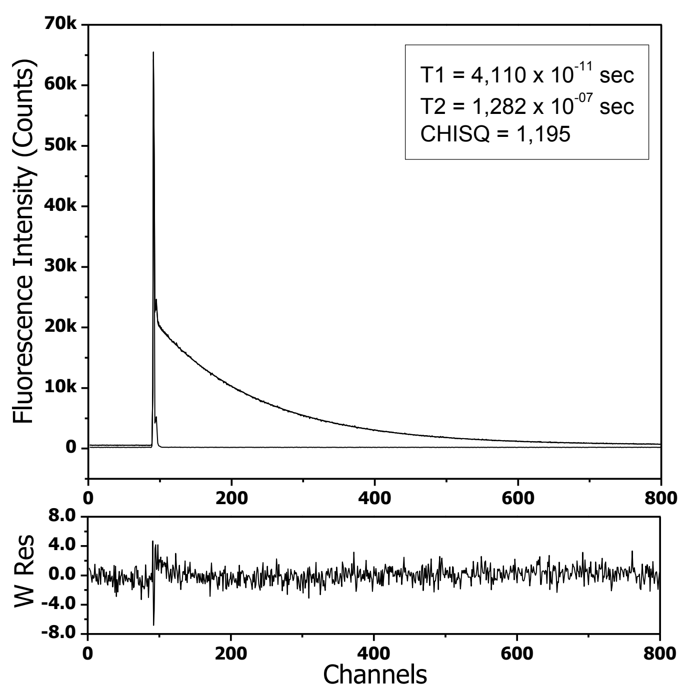

Figure 2.3 – Lamp prompt and fluorescence decay of the emission at 376 nm, in POPC LUV at 25ºC, with a probe to lipid ratio of 1:800 of: **(a)** py10-PC and **(b)** py6-PC. Weighted residuals (W Res) are a result of the two-exponential fitting applied.

Table 2.1 presents the average fluorescence lifetimes obtained (minimum of three independent experiments) for both probes at the three temperatures examined. The lifetimes obtained were very similar between the two pyrenyl probes and decreased with temperature as expected. Because these were recorded in the presence of oxygen the fluorescent lifetimes were obviously significantly lower than those obtained when a degassing procedure was adopted [Martins & Melo, 2001].

	τ (ns)	
Temperature (ºC)	**py10-PC**	**py6-PC**
25	125.4±0.3	128.3±0.1
35	114.8±2.6	113.4±2.8
45	102.4±2.2	101.5±0.3

Table 2.1 – Results of fluorescence lifetimes of the py10-PC and py6-PC probes determined in POPC LUV at various temperatures

These lifetimes fulfill the condition described in the methods section that the mean lifetime of unquenched fluorophore should be around the 10^{-7}s range for the formalism used.

2.3.2 Fluorescence Quenching of py10-PC by 10-DOXYL-PC in POPC Bilayers

We began by looking at the py10-PC/10-DOXYL-PC system, and it should be noted that both py10-PC and 10-DOXYL-PC may interact between opposing leaflets due to their length being bigger than half of the POPC bilayer in the fluid phase [Martins *et al.*, 1996; Repáková *et al.* 2006]. A representation of this is shown in Figure 2.4, and the 2D concentration of 10-DOXYL-PC was calculated taking this fact into account.

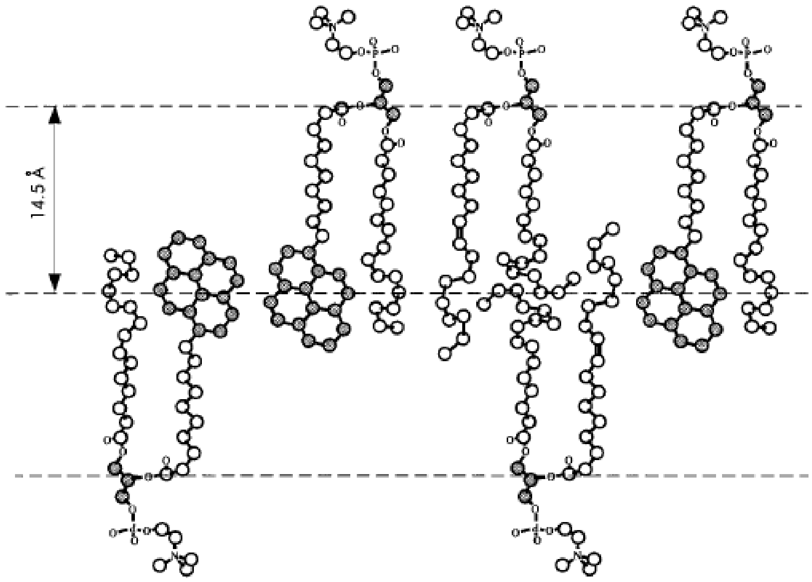

Figure 2.4 – Representation of a portion of a bilayer of POPC with py10-PC probes in the two leaflets showing that both pyrene pertaining to the same leaflet and to opposite layers can interact. From Martins *et al.*, 1996.

In Figure 2.5 we compare the experimental ratios between the fluorescence intensities of py10-PC in the absence of quencher, and in the presence of the several concentrations of 10-DOXYL-PC used, with the theoretical points that were calculated by the procedures described before, employing all the terms previously defined, including the lifetimes we determined in this work.

(a)

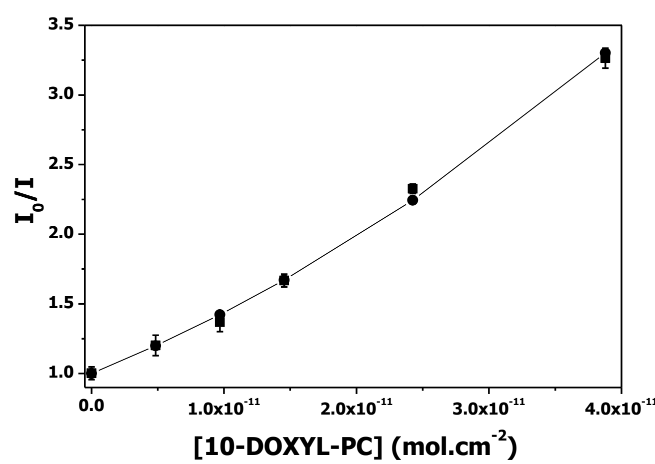

(b)

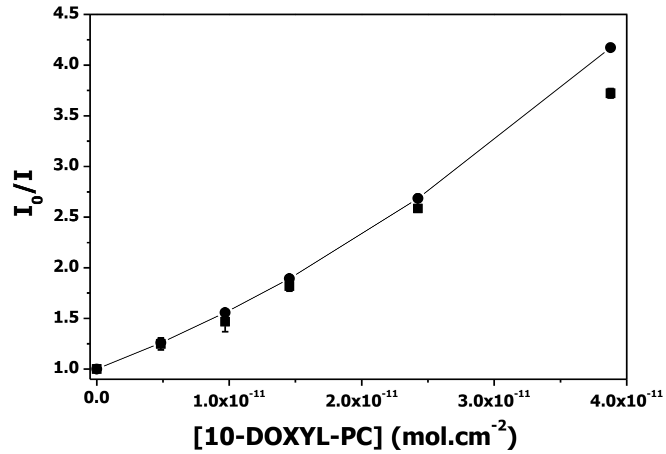

(c)

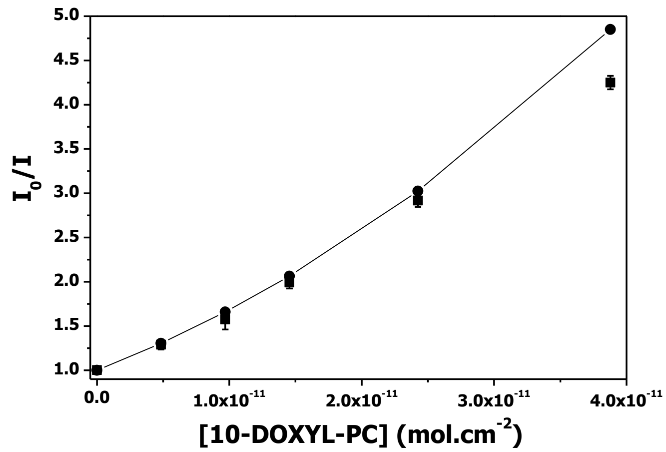

Figure 2.5 – Reason of steady-state fluorescence intensities of py10-PC in the absence (I_0) and presence (I) of quencher, plotted against the 2D concentration of 10-DOXYL-PC in POPC MLV at: **(a)** 25ºC, **(b)** 35ºC, and **(c)** 45ºC. The squares (■) are the experimental results, while the circles (●) are the theoretical predictions.

We observe the expected upward curve along with an increase in quenching with the introduction of DOXYL content, and also an increase of quenching with the higher temperatures. The system appears to be an ideal diffusion controlled reaction, as the results show an unequivocal agreement between the experimental and the theoretical values for all three temperatures. This demonstrates that there is no need to invoke the simultaneous occurrence of static and dynamic mechanisms for fluorescence quenching processes taking place within lipid bilayers [Lakowitz, 2006; Lúcio et al., 2009]. Instead, the use of a correct/necessary kinetic formalism is sufficient.

A small downwards deviation is noticeable at 8% of 10-DOXYL-PC quencher at 35ºC and 45ºC, it is possible that there a slightly diminished diffusion by the probe. It is also possible that the presence of the DOXYL group may cause an increased stiffness of the phospholipid chain, leading to a very small decrease in membrane fluidity with that amount of probe content, something that molecular simulations have shown to occur with py-10-PC probe [Repáková *et al.*, 2006].

2.3.3 Fluorescence Quenching of py6-PC by 5-DOXYL-PC in POPC Bilayers

In order to analyze the quenching of py6-PC by 5-DOXYL-PC, we had to estimate the diffusion coefficients of both probes, since no available data exists for these specific. We assumed that py6-PC has a slightly higher diffusion than its counterpart py10-PC, and attributed values of $4.0 \times 10^{-8}\,\mathrm{cm^2/s}$ at 25ºC, $6.5 \times 10^{-8}\,\mathrm{cm^2/s}$ at 35ºC and $1.0 \times 10^{-7}\,\mathrm{cm^2/s}$ at 45ºC, respectively. For 5-DOXYL-PC we presumed, as with 10-DOXYL-PC, that its diffusion coefficients should be compared to the diffusion of POPC [Vaz *et al.*, 1985].

In Figure 2.6, we compare the experimental ratios between the fluorescence intensities of py6-PC in the absence of quencher, and in the presence of the several concentrations of 5-DOXYL-PC used, with the two series of theoretical points that were calculated by the procedures described before, one with $R_\mathrm{C} = 6.7$ Å, that is significantly and systematically lower than what we found experimentally, and another with $R_\mathrm{C} = 11$ Å, that fits the results obtained very closely.

(a)

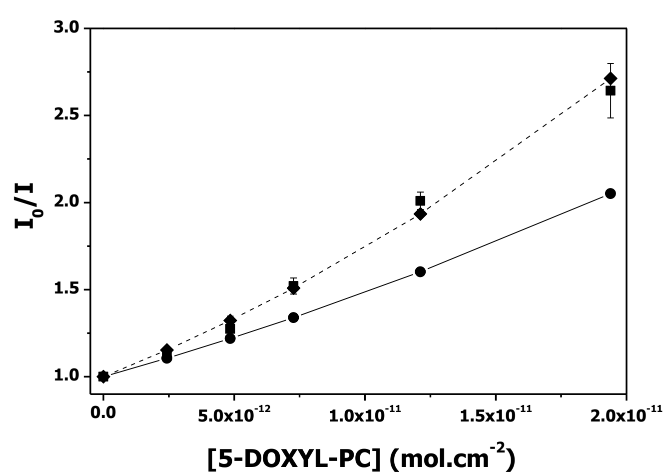

(b)

(c)

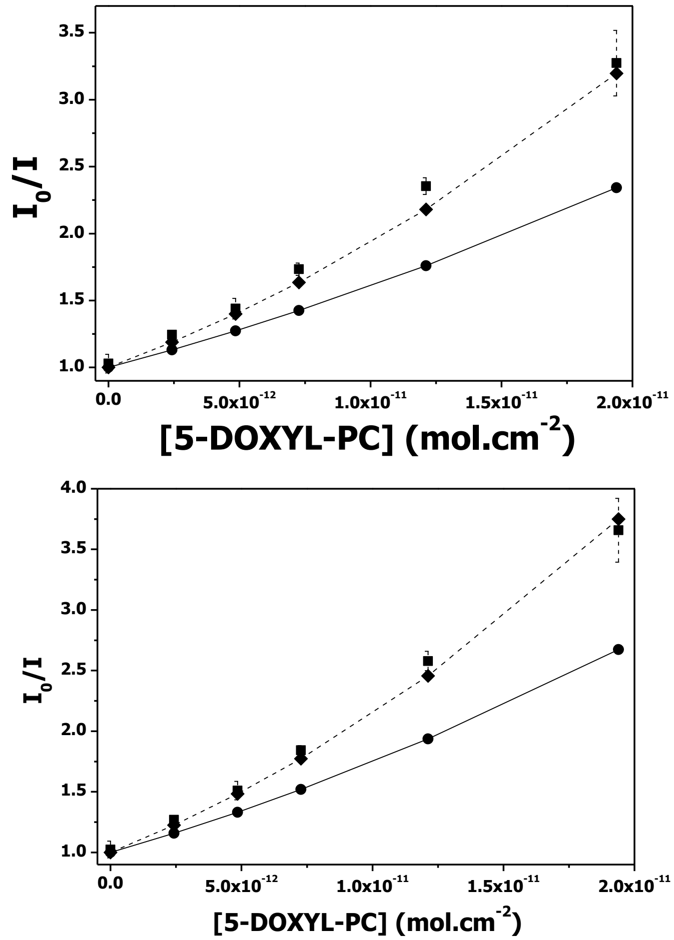

Figure 2.6 – Reason of steady-state fluorescence intensities of py6-PC in the absence (I_0) and presence (I) of quencher, plotted against the 2D concentration of 5-DOXYL-PC in POPC MLV at: **(a)** 25ºC, **(b)** 35ºC, and **(c)** 45ºC. The squares (■) are the experimental results, while the circles (●) are the theoretical predictions, with the straight line representing $R = 6.7$ Å and the dotted line $R = 11$ Å.

Figure 2.6 shows an unexpected result as the obtained experimental values of $\mathrm{I_0/I}$ are significantly higher than it was predicted by the kinetic formalism used here, indicating that fluorescence quenching was occurring at a level above what was expected for the values of terms as defined previously with $R_\mathrm{C} = 6.7$ Å. This also occurs at all three temperatures studied.

We considered three possible explanations that, at a first approximation, could be the cause of this outcome. The more obvious possible effects affecting the deviation observed are the following:

i) Variation in the lateral diffusion coefficients of both the fluorescent probe and the quenching phospholipid would appear to be the most straightforward justification. However, the deviation observed would require more than doubling the values of both diffusion coefficients in order for the theoretical I_0/I values to compare to the experimental averages. This is untenable from the physical point of view, since it would imply a significant augment of free-volume in the bilayer, and there is not a single evidence for the presumed increasing in the free-volume [Vaz *et al.*, 1985];

ii) Variation in the 2D concentration values (which in turn, will affect the steady-state rate constant calculations), since the relatively bulky spin group of the 5-DOXYL-PC probes are locating (the volume of the DOXYL ring is about 143 $Å^3$ [Zhao *et al.*, 2003]) in the more ordered portion of POPC bilayers. When increasing the probe proportion in the bilayers, the molecular area of POPC bilayers (that is assumed as invariant, for the calculation of the 2D concentration of spin-probes) would be varying, as the molecular structure of 5-DOXYL-PC would be imposing a larger molecular area in lipid bilayers. However, we have evaluated this influence as negligible to explain the deviations, as this effect would produce a very minor difference. Moreover, this is not happening in the py10-PC/10-DOXYL-PC system, since in this case, the spin-probe will be located at the level of the *cis* double bond of the oleoyl chain, which allows to accommodate the DOXYL group (within the limits of the concentration range under analysis), maintaining the molecular area of the lipid POPC matrix essentially unaffected;

iii) Increased fluorescence quenching efficiency, simply by augmenting the collisional distance from 6.7 Å, to about 11 Å (Fig. 2.6), gives an excellent accordance between the experimental and theoretical outcomes. This non-conventional explanation would be based in several arguments, mainly underpinned in structural features of lipid bilayers. The quenching kinetics is commonly treated as identical both for py10-PC/10-doxyl-PC and py6-PC/5-doxyl-PC systems, as in experiments to monitor depth-dependent quenching of fluorophores in membranes [Lakowicz, 2006]. However, it is crucial to realize that a lipid bilayer is not just a thin slab of a low dielectric hydrocarbon medium surrounded by an aqueous solvent, but is really a highly stratified structure with a definite trans-bilayer molecular profile originated on the distinct chemical groups (ionic or polar head-groups, the interface glycerol and carbonyls, the ordered and disordered segments of methylenic chains) and different intermolecular interactions, that manifest in the so-called polarity and fluidity gradients [Gennis, 1989]. Additionally, the distribution profile of lateral pressure [Marsh, 1996; Cantor, 1997] can also potentially affect the collisions between probes located in the more ordered section of the bilayer. Furthermore, recent electron spin resonance (EPR) studies of bimolecular encounters of DOXYL and TEMPO probes in a series of alkanes [Vandenberg *et al.*, 2012] and ethanol [Kurban, 2011] make visible the cage effect in collisions of nitroxides probes. On the absence of any other evidence, this cage effect based on lateral pressure would likely render the bimolecular quenching process more effective in the more ordered section of lipid bilayers (were an interplay between the head-group repulsion and the interfacial tension a location of nearly zero lateral pressure); on the other hand, in the more disorganized center of lipid bilayers, the lateral pressure is positive (as in an alkane solvent), and the calculation of the collisional distance is dealt with as if a small probe being immersed in a "homogeneous fluid solvent"). Also deviations to the hydrodynamic lateral diffusion physical requirements are not fulfilled in the more ordered section of lipid bilayers, but these very same requirements are somehow mimicked in the more disorder hydrophobic core of bilayers [Hynes *et al*., 1979]. One must likewise consider that from a conformational freedom point of view there is a significant difference between the two bilayers depths in study here. At the 5-DOXYL-PC depth, the dynamic assumption of the small probe being immersed in a "homogeneous fluid solvent" may not necessarily be a totally appropriate approximation considering that the DOXYL group is severely constricted and is sensing a molecular environment (ordered portion of POPC molecules oriented in bilayers) whose typical dimensions are far bigger than DOXYL itself. In this sense, it is unequivocally questionable the consideration of an equivalent situation for DOXYL in the ordered and disordered sections. Another factor that cannot be excluded is the extended formation of hydrogen bonds between the spin probes and water [Kurban, 2011], something that is especially relevant because the quantity of water present at the depth of the 5-DOXYL-PC probe is significantly higher [Marsh, 2002] in relation to 10-DOXYL-PC.

2.4 Conclusions

The goal of the results presented here was to demonstrate that the use of a directed 2D kinetic model for the analysis of bimolecular reactions in phospholipid bilayers is in fact appropriate and of crucial importance to correctly interpret experimental outcomes, while maintaining present the complex nature of lipid membranes.

We have demonstrated that the formalism introduced by Razi Naqvi in 1974 is sufficient to execute a complete and self-consistent analysis of the kinetics of quenching of py10-PC by 10-DOXYL-PC in POPC bilayers, in the range of temperatures studied, using steady-state and lifetime fluorescence measurements. All the parameters were pre-determined, including the fluorescence lifetime we determined in this work, and we found an excellent agreement between the experimental values and the theoretical prediction. One must say that this is due to the fact of this particular experimental system does not exhibit unacceptable experimental or molecular deviations to the theoretical requirements, which is something we cannot exclude from our analysis of the quenching of py6-PC by 5-DOXYL-PC. In this system we found a surprisingly increased quenching efficiency when compared to the theory, that although we tried to justify this behavior, we unfortunately cannot state for certain what causes this deviation. We believe however that the different settings of the bilayer at the depth of the py6-PC/5-DOXYL-PC, and how those settings vary from the depth of the py10-PC/10-DOXYL-PC, several factors in terms of bilayer lateral pressure, water membrane penetration and the characteristics of nitroxide probes' reactions, are unquestionably influences that have to be considered.

2.5 References

Almeida, P.F.F., Vaz, W.L.C., Lateral diffusion in membranes, in: R. Lipowsky, E. Sackmann (Eds.), Handbook of Biological Physics, Elsevier, Amsterdam, 1995.

Axelrod, D., Lateral motion of membrane proteins and biological fuction, J. Memb. Biol. 75, 1-10 (1983).

Bieri, V.G., Wallach, D.F.H., Fluorescence quenching in lecithin and lecithin/cholesterol liposomes by paramagnetic lipid analogues. Introduction of a new probe approach, Biochim. Biophys. Acta 389 (3), 413–427 (1975).

Blackwell, M.F., Gounaris, K., Zara, S.J., Barber, J., A method for estimating lateral diffusion coefficients in membranes from steady-state fluorescence quenching studies, Biophys. J. 51, 735-744 (1987).

Cantor, R.S., The lateral pressure profile in membranes: A physical mechanism of general anesthesia, Biochemistry 36(9), 2339-2344 (1997).

Chance, B., Erecinska, M., Radda, G.K., 12-(9-Anthroyl)stearic acid, a fluorescent probe for ubiquinone region of mitochondrial membrane, Eur. J. Biochem. 54, 521–529 (1975).

Chen, Y., Lagerholm, B.C., Yang, B., Jacobson, K., Methods to measure the lateral diffusion of membrane lipids and proteins, Methods 39, 147–153 (2006).

Clegg, R.M., Vaz, W.L.C., Translational diffusion of proteins and lipids in artificial lipid bilayer membranes. A comparison of experiment with theory, in: Progress in Protein–Lipid Interactions, Vol. 1, eds A. Watts and J.J.H.H.M. De Pont, Elsevier, Amsterdam, 1985.

Edward, J.T., Molecular volumes and the Stokes-Einstein equation, J. Chem. Ed. 47, 261-270 (1970).

Elson, E.L., Fluorescence correlation spectroscopy: past, present, future, Biophys. J. 101, 2855–2870 (2011).

Gennis, R.B., Biomembranes, Molecular Structure and Function, Springer-Verlag, New York, 1989.

Kalay, Z., Fujiwara, T.K., Kusumi, A., Confining Domains Lead to Reaction Bursts: Reaction Kinetics in the Plasma Membrane, PLoS ONE 7 (3), e32948 (2012).

Kalay, Z., Reaction kinetics in the plasma membrane, Biotechnol. J. 7, 745-752 (2012).

Kučerka, N., Tristam-Nagle, S., Nagle, J.F.,. Structure of fully hydrated lipid bilayers with monounsaturated chains. J. Membr. Biol. 208, 193–202 (2005).

Kurban, M.K., A study of the relation between translational and rotational diffusion through measurement of molecular recollision, J. Phys. Chem. 134, 034503 (2011).

Lakowicz, J.R, Principles of Fluorescence Spectrocopy 3rd Ed., Springer Science, 2006.

London, E., Feigenson, G.W., Fluorescence quenching in model membranes: 1. Characterization of quenching caused by a spin-labeled phospholipid, Biochemistry 20, 1932–1938 (1981).

Lúcio, M., Nunes, C., Gaspar, D., Gołębska, K., Wisniewski, M., Lima, J.L.F.C., Brezesinski, G., Reis S., Effect of anti-inflammatory drugs in phosphatidylcholine membranes: A fluorescence and calorimetric study, Chem. Phys. Letters 471, 300–309 (2009).

MacDonald, R.C., MacDonald, R.I., Menco, B.P., Takeshita, K., Subbarao, N.K., Hu, L.R., Small volume extrusion apparatus for preparation of large, unilamellar vesicles, Biochim. Biophys. Acta 1061, 297–303 (1993).

Manuel, M., Martins, J., Partitioning of 1-pyrenesulfonate into zwitterionic and mixed zwitterionic/anionic fluid phospholipid bilayers, Chem. Phys. Lipids 154, 79-86 (2008).

Marsh, D., CRC Handbook of Lipid Bilayers. CRC Press, Boca Raton, 1990.

Marsh, D., Lateral pressure in membranes, Biochim. Biophys. Acta 1286, 183-223 (1996).

Marsh, D., Membrane water-penetration profiles from spin labels, Eur. Biophys. J. 31 (2002) 559–562.

Martins, J., Vaz, W.L.C., Melo, E., Long-Range Diffusion Coefficients in Two-Dimensional Fluid Media Measured by the Pyrene Excimer Reaction, J. Phys. Chem. 100, 1889-1895 (1996).

Martins, J., Melo, E., Molecular Mechanism of Lateral Diffusion of py10-PC and Free Pyrene in Fluid DMPC Bilayers, Biophys. J. 80, 832-840 (2001).

Medhage, B., Almgren, M., Diffusion-influenced fluorescence quenching dynamics in one to three dimensions, J. Fluoresc. 2, 2–21 (1992).

Melo, E., Martins, J., Kinetics of bimolecular reactions in model bilayers and biological membranes. A critical review, Biophys. Chem. 123, 77–94 (2006).

Owen, C.S., Two dimensional diffusion theory: cylindrical diffusion model applied to fluorescence quenching, J. Chem. Phys. 62, 3204-3207 (1975).

Razi Naqvi, K., Diffusion-controlled reactions in two-dimensional fluids: discussion of measurements of lateral diffusion of lipids in biological membranes, Chem. Phys. Lett. 28 280–284 (1974).

Razi Naqvi, K., Martins, J., Melo, E., Recipes for Analyzing Diffusion-Controlled Reactions in Two Dimensions: Time-Resolved and Steady-State Measurements, J. Phys. Chem. B, 104, 12035-12038 (2000).

Repáková, J., Holopainen, J.M., Karttunen, M., Vattulainen, I., Influence of Pyrene-Labeling on Fluid Lipid Membranes, J. Phys. Chem. B 110, 15403-15410 (2006).

Saxton, M.J., Lateral diffusion of lipids and proteins, Current Topics in Membranes, 48, 229-282 (1999).

Saxton, M.J., Wanted: A Positive Control for Anomalous Subdiffusion, Biophys. J. 103 (12), 2411–2422 (2012).

Szabo, A., Theory of Diffusion- Influenced Fluorescence Quenching, J. Phys. Chem. 93, 6929-6939 (1989).

Szoka Jr., F., Papahadjopoulos, D., Comparative properties and methods of preparation of lipid vesicles (liposomes), Annu. Rev. Biophys. Bioeng. 9, 467-508 (1980).

Valeur, B., Molecular Fluorescence: Principles and Applications, Wiley-VCH, 2002.

Vandenberg, A.D., Bales, B.L., Salikhov, K.M., Peric, M., Bimolecular Encounters and Re-Encounters (Cage Effect) of a Spin-Labeled Analogue of Cholestane in a Series of n-Alkanes: Effect of Anisotropic Exchange Integral, J. Phys. Chem. A 116, 12460−12469 (2012).

Vaz, W.L.C., Clegg, R.M., Hallmann, D., Translational Diffusion of Lipids in Liquid Crystalline Phase Phosphatidylcholine Multibilayers. A Comparison of Experiment with Theory, Biochemistry 24 (3), 781-786 (1985).

Wieser, S., Schütz, G.J., Tracking single molecules in the live cell plasma membrane — Do's and Don’t’s, Methods 46:131–140 (2008).

Wiener, M.C., White, S.H., Structure of a fluid dioleoylphosphatidylcholine bilayer determined by joint refinement of x-ray and neutron diffraction data. III. Complete structure. Biophys J. 61 (2), 434-447 (1992).

White, S.H., Wiener, M.C., The liquid-crystallographic structure of fluid lipid bilayer membranes. In Membrane Structure and Dynamics (K.M. Merz & B. Roux, eds), Birkhäuser, Boston, 1996.

Zhao, Y.H., Abraham, M.H., Zissimos, A.M., Fast Calculation of van der Waals Volume as a Sum of Atomic and Bond Contributions and Its Application to Drug Compounds, J. Org. Chem. 68, 7368-7373 (2003).

Chapter 3

Excimer Formation in Fluid Lipid Bilayers at Higher Pyrenyl-Labeled Phospholipid Probes Concentration

3.1 Introduction

Since the early 80's it is well established that lateral diffusion of membrane components is essential to a variety of cellular reactions and processes occurring in the plane of plasma and organelle membranes [Axelrod, 1983; Clegg & Vaz, 1985]. That is to say that many biochemical reactions take place in membrane lipid bilayers, which can be idealized as a two-dimensional (2D) media [Melo & Martins, 2006]. Even though, the kinetics of cellular reactions under dimensional constraints (in 2D systems) have not received much attention, mostly from the experimental perspective, since biomembranes are very complex biological supramolecular assemblies, whose chemical composition, structure, organization and dynamics are very difficult to define under a rather complete experimental control within the framework of *in vivo* kinetic research. To circumvent these difficulties, model bilayers and model reactants have been widely used to study molecular encounters giving rise to a reaction in membranes. The most favorable situation to model 2D kinetics is the use of diffusion-controlled reactions, provided that this type of reaction has activation energy near zero, and the kinetics only relies on features that are geometric in nature: the mutual arrangement, accessibility and orientation of reactants, and the dimensionality of the reaction space [Melo & Martins, 2006]. Among the experimental methods used to study bimolecular encounters in lipid bilayers, the pyrene excimer formation has been the most popular method [Somerharju, 2002; Melo & Martins, 2006]. This is mainly due to the unusually long fluorescence lifetime (more than 100 ns in a variety of aerated solvents, micelles, and membrane systems) and concentration-dependent and/or viscosity-dependent excimer formation. Also, due to these distinctive features, both free pyrene and pyrene-labeled lipids have been used to probe diverse features (structure, organization, dynamics, solvation, lipid trafficking and metabolism) in varied membrane biophysics studies [Somerharju, 2002].

A consistent analysis of pyrene excimer formation in fluid homogeneous bilayers used the 2D variant of the Smoluchowski formalism for diffusion-controlled reactions [Martins *et al.*, 1996; Martins & Melo, 2001]. Smoluchowski's approach yields, in the case of 2D systems [Razi Naqvi, 1974], unwieldy expressions for the time-dependent rate-coefficient (used to solve the differential equations inherent to kinetic schemes), and for the corresponding concentration-dependent rate constant (which determines the rate of a diffusion-controlled reaction under stationary conditions) [Razi Naqvi *et al.*, 2000]. Still, most of the efforts [Martins *et al.*, 1996;

Martins & Melo., 2001] were devoted to the analysis of time-resolved fluorescence data, and it must be recognized that the analysis of photostationary results did not reach the level of getting rid of the wearisome mathematical difficulties in data analysis. Fortunately, Razi-Naqvi and collaborators (2000) make available a recipe, based on a mean-field approach presented by Szabo (1989), to analyze photostationary fluorescence quenching experiments, and verified that pyrene excimer formation studied through steady-state data can be successfully analyzed [Razi Naqvi *et al.*, 2000]. Yet, only a very limited range of self-quenching concentration range was tested (probe to lipid ratio varying from 0.5 to 1.33 mol%) [Martins *et al.*, 1996].

In the present study, we give attention to develop an unfailing and trustworthy analysis of diffusion-controlled self-quenching of pyrenyl-labeled phospholipids, through steady-state and lifetime fluorescence determinations, in fluid homogeneous POPC (1-palmitoyl-2-oleoyl-*sn*-glycero-3-phosphocholine) bilayers. This approach is precise for a wider range of quenching species (until the proportion 8 mol% of the pyrenyl-labeled phospholipids), and makes use of an intermediate level instrumentation, available in most of the fluorescence laboratories. When using the mean-field approach to analyze photostationary fluorescence data [Szabo, 1989; Razi Naqvi *et al.*, 2000] one must be aware of that the concentration-dependent rate constant alters the classical linear Förster-Kasper plot (the ratio of the excimer fluorescence quantum yield, divided by the corresponding pyrene monomer quantum yield, depends linearly on the pyrenyl probe concentration [Valeur, 2002]) with an upward curvature. Unfortunately, in the study presented by Martins *et al.* (1996) and analyzed by Razi-Naqvi *et al.* (2000) the concentration range scrutinized was much too limiting and the upward curvature could not be unequivocally perceived. However, the upward curvature was already noticed in spin quenching studies in model membranes involving small fluorophores [London & Feigenson, 1981] and membrane-spanning peptides [Caputo & London, 2003], but it was mainly attributed to the involvement of static quenching. In the present work, we make a thoughtful use of this recipe in the analysis of 2D fluorescence quenching data, showing that it is exact for specific experimental conditions and reveal some deviations from particular requirements inherent to the theoretical framework. We show that the fluorescence self-quenching of py10-PC (1-palmitoyl-2-(1-pyrenedecanoyl)-*sn*-glycero-3-phosphocholine) and py6-PC (1-palmitoyl-2-(1-pyrenehexanoyl)-*sn*-glycero-3-phosphocholine), in fluid POPC (1-palmitoyl-2-oleoyl-*sn*-glycero-3-phosphocholine) is within the experimental error, in complete accordance with the theoretical prediction, until the probe to lipid molar proportion of 2 and 4 mol %, respectively. All the analysis is based in independent values of lateral diffusion coefficients determined previously [Martins *et al.*, 1996], as well as for the experimental fluorescence lifetimes. The collisional distance was calculated from well-established molecular considerations [Edward, 1970; Zhao et al., 2003], and was taken as 7.1 Å, as in previous studies [Martins *et al.*, 1996; Martins & Melo., 2001]. Above 2 mol % for py10-PC and above 4 mol % for py6-PC until 8 mol %, the experimental results display a quenching efficiency lower than the theoretical predictions, for an analysis procedure considering that the lateral diffusion coefficients of the probes are unchanged at a fixed temperature. However, if one considers in the analysis that the lateral diffusion coefficient is lower for higher values of probe concentration, other things being equal, we obtain a precise accordance with theory. Molecular dynamics (MD) simulations of py10-PC in fluid lipid bilayers [Repáková *et al.*, 2006] have shown increased ordering and more tight packing of lipid acyl chains in the vicinity of the probe molecule and interdigitation of pyrene group into the apposed leaflet. This would account for the diminishing diffusion of both probes, with the py10-PC probe evidently causing a more noticed friction between the apposed monolayers [Merkel *et al.*, 1989].

3.2. Experimental Methods

3.2.1 Chemicals and Solvents

1-Palmitoyl-2-oleoyl-sn-glycero-3-phosphocholine (POPC), purity > 99.9%, was purchased from Avanti Polar Lipids (Alabaster, AL, USA). 1-Hexadecanoyl-2-(1-pyrenedecanoyl)-sn-glycero-3-phosphocholine (py10-HPC), 1-Hexadecanoyl-2-(1-pyrenehexanoyl)-sn-glycero-3-phosphocholine (py6-HPC), 1,2-bis-(1-pyrenedecanoyl)-sn-glycero-3-phosphocholine (Bis-py10-PC) and 1,2-bis-(1-pyrenebutanoyl)-sn-glycero-3-phosphocholine (Bis-py4-PC) were purchased from Molecular Probes (Eugene, Oregon, USA). MilliQ water was obtained using a Millipore Simplicity 185 system (electrical conductivity and pH are $5.4 \times 10^{-6}\,\mathrm{S}.m^{-1}$ and around 6.6–7, respectively, at room temperature). All organic solvents (highest purity) were from Merck (Darmstadt, Germany).

3.2.2 Stock Solutions

As referred in the previous chapter, lipids and probes obtained in the form of powder were diluted in a chloroform:methanol 2:1 (v/v) mixture to the desired concentrations. When acquired as a solution in chloroform instead of powder form, dilutions using the same mixture were made. The stock solutions were then kept at -20ºC.

3.2.3 Aqueous Liposome Suspensions

MLV were prepared according the protocol specified in the previous chapter, based on firmly established method [Szoka, Jr. and Papahadjopolous, 1980] as described before [Manuel & Martins, 2008]. Stock solutions of phospholipid and spin probe, dissolved in chloroform:methanol 2:1 (v/v), were mixed in settled proportions in a evaporating flask (volume of 20 cm^3) with a conical shape bottom, this increases the homogeneity of the dry lipid film. The organic solvents were then dried at 50ºC using a rotary evaporator Heidolph VV-micro (vacuum pump Büchi V-500, coupled to a Büchi V-800 digital control, isolated from the rotary evaporator by a liquid N_2 trap) with slow rotation, 15 min at 150 mBar until a homogeneous lipid film was formed, followed by 1 h at 5 mBar, to remove traces of organic solvents. The lipidic film was hydrated with MilliQ water during at least 1 h at 50ºC, well above the phase transition temperature (T_M) of POPC (T_M = -2.6ºC) [Marsh, 1990], vortexing regularly, forming multilamellar vesicles (MLV) as the lipid sheets detach during agitation and self-close.

Again, in order to minimize light scattering, fluorescence lifetimes of the excimers formed by the dipyrenil probes were determined using large unilamellar vesicles (LUV). These were prepared by the extrusion method [MacDonald et al., 1993], using an Avanti Mini-Extruder (Alabaster, AL, USA), forcing the MLV to pass 15 times at room temperature through a pair of Nucleopore polycarbonate filters (Wathman, USA), with pore size of 0.1 μm.

All the liposome aqueous suspensions were kept in the refrigerator and usually used within 24 h.

3.2.4 Time-resolved Fluorescence

In order to determine the excimer fluorescence lifetime, the dipyrenyl probes Bis-py10-PC and Bis-py4-PC were used, assuming that the excimer formed by intermolecular mechanism is identical to the intramolecular mechanism. Furthermore, in the absence of a dipyrenyl probe labeled with hexadecanoyl as in py6-PC probe, we used the probe Bis-py4-PC as an analogous compound for the py6-PC probe, and the experimental results reinforce the certitude of this option. Time-resolved fluorescence measurements were made in a Spex Fluoromax-4 spectrofluorimeter (Jobin Yvon–Horiba, France) equipped with a thermostated cell holder with magnetic stirring accessory, coupled to a refrigerated/heated circulator Julabo F12-ED (precision of 0.1 °C). The LUV suspensions were placed in 1 cm quartz cuvettes and were stirred continuously during the measurements. Excitation wavelength was 342 nm while emission wavelength was set to 480 nm, and slit width was 1 nm for both excitation and emission. Collections were made in 1024 channels and measurement range was 800 ns. A collection of the prompt for the lamp (at 342 nm) was made before the each collection of a corresponding sample. Collections were only stopped when counts reached at least 2×10^4. Total lipid concentration of LUV suspensions used was 0.1 mM, with probe molecular percentage set at 0.125% (1 probe per 800 phospholipids). Along with the low concentration and LUV utilization, a cut-off filter of 360 nm (Corion, WG360) was used to try to minimize light scattering. Decays were fitted with the manufacturer's software using two exponentials and no initial constrictions, and fluorescence lifetimes were determined by averaging the best decays obtained with χ^2 below 1.2, as well as judging the weighted residuals plot.

3.2.5 Steady-state Fluorescence

Fluorescence spectra were recorded in a similar way to Chapter 2, on a Spex Fluoromax-3 spectrofluorimeter (Jobin Yvon–Horiba, France) equipped with a thermostated cell holder with magnetic stirring accessory, coupled to a refrigerated/heated circulator Julabo F12-ED (precision of 0.1°C). Emission spectra were corrected for the wavelength dependent response of monochromators, collimating optics and detection using the correction file provided by the manufacturer.

The MLV suspensions, total lipid concentration of 1 mM, were placed in 1 cm quartz cuvettes and were stirred continuously during the measurements. Spectra were acquired between 360 and 600 nm, slit width of 1.5 nm, and wavelength sampling interval of 0.5 nm, at temperatures of 25, 35 and 45ºC. Samples with py10-PC and py6-PC molecular percentage of 1, 2, 4, 6 and 8% were studied. Values to quantify excimer formation were retrieved by comparing the area of the band of monomer emission (376 nm) between 371 and 381 nm and the area of the band of excimer emission (480 nm) between 475 and 485 nm (Figure 3.1), and at least four different experiments were averaged. This way, we ensured that the estimation of the monomer and excimer quantum yields is sufficiently robust and consistent, instead of using simply the intensity at a particular wavelength, which for this purpose was not very reliable.

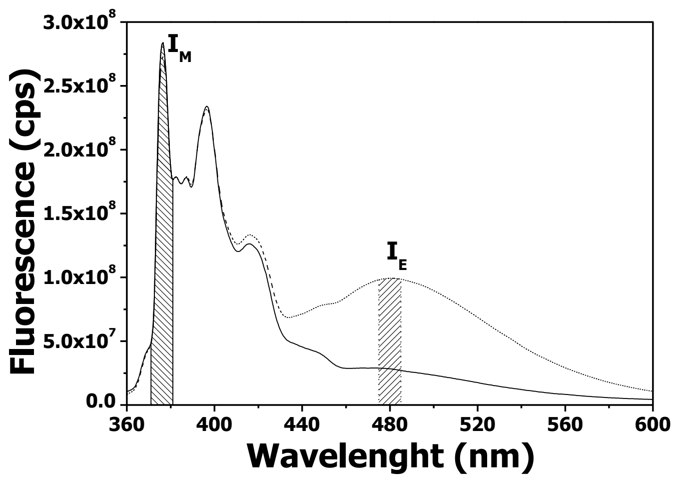

Figure 3.1 – Fluorescence emission spectra of py10-PC in POPC MLV (1 mol % straight line, 4 mol % dotted line), with the areas corresponding to the monomer (I_M) and of the excimer (I_E).

3.2.6 Two-dimensional Kinetic Analysis

Like it was mentioned in section 2.2.6, fluorescence quenching cases occurring in 2D dimensional media like a membrane bilayer an adapted 2D Stern-Volmer formalism should be used. In this particular case the py10-HPC and py6-HPC fluorescent probes self-quenching must be analyzed specifically accounting the excimer formation [Razi Naqvi et al., 2000]:

$$\frac{I_E}{I_M}=\frac{k_{FE}}{k_{FM}}.k_2.[Q]_2.\tau_E \qquad \textbf{(Eq. 3.1)}$$

I_E and I_M are the fluorescence intensities of the excimer and monomer, respectively, k_{FE} and k_{FM} are the rate constants for the excimer and monomer fluorescence and τ_E is the fluorescence lifetime. The k_{FE}/k_{FM} ratio is usually estimated to be around 2. The steady-state rate constant for quenching reactions occurring in 2D media is k_2, while the quencher 2D concentration is represented by $[Q]_2$. The calculation of k_2 was resolved using Eq. 2.3 iteratively in the same manner as described in section 2.2.6, the diffusion coefficients of py10-PC in phospholipid bilayers are known [Martins & Melo, 2001], we estimated slightly higher coefficients for the py6-PC probe, and with the monomer lifetime (τ_M) determined in Chapter 2 and τ_E determined in this chapter. Eq. 3.1 was then utilized to estimate theoretical I_E/I_M ratios.

3.3 Results and Discussion

3.3.1 Fluorescence Lifetimes of Bis-py10-PC and Bis-py4-PC Excimers in POPC Bilayers

Fluorescence lifetimes of Bis-py10-PC and Bis-py4-PC excimers in POPC LUV were determined in the presence of oxygen, as was the case for all measurements. LUV were again used in these time-resolved experiments to have a diminished light scattering, because while fluorescence lifetimes determined in MLV in the same conditions were found to be relatively indistinguishable from those obtained in LUV, the decays were of significant lesser quality. The dipyrenyl probes (structures in Figure 3.2) were used because of the easiness of determining the excimer lifetime using a small amount of probe, which wouldn't be the case of finding τ_E with a monopyrenyl probe. There was no commercial available dipyrenyl version of py6-PC, so we considered the lifetimes obtained with Bis-py4-PC sufficiently comparable.

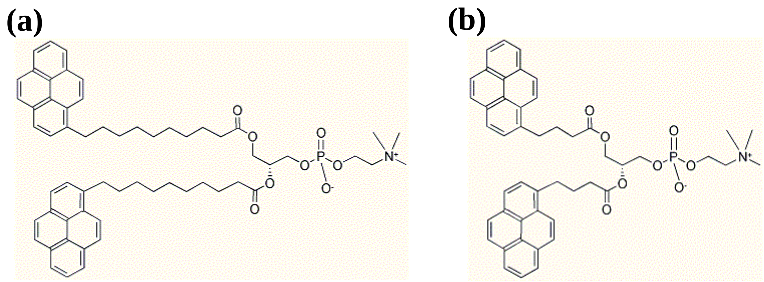

Figure 3.2 – Structures of **(a)** Bis-py10-PC, and **(b)** Bis-py4-PC.

We can see in Figure 3.3 the depiction of the best decays of Bis-py10-PC and Bis-py4-PC acquired at 25ºC. The decays were fitted using the software provided by the spectrofluorometer manufacturer, and were of biexponential nature, although three-exponential fits had to be utilized due to a strong lamp profile caused by a lesser optimal photomultiplier resolution. The smaller lifetime refers to the adjustment made to fit the lamp distortion and was always in the 10^{-9}s range. There were also always two lifetimes very close to each, although one was systematically a little lower, which we assumed was the monomer lifetime. The monomer lifetime is much lower than what we found in the monopyrenyl probes because of the close proximity of the two pyrene groups that allows the very quick formation of the excimer.

(a)

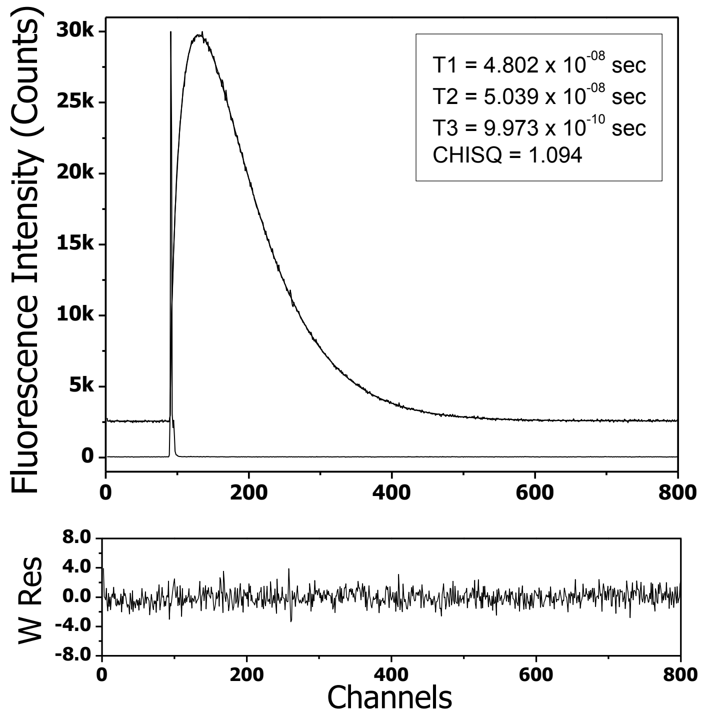

(b)

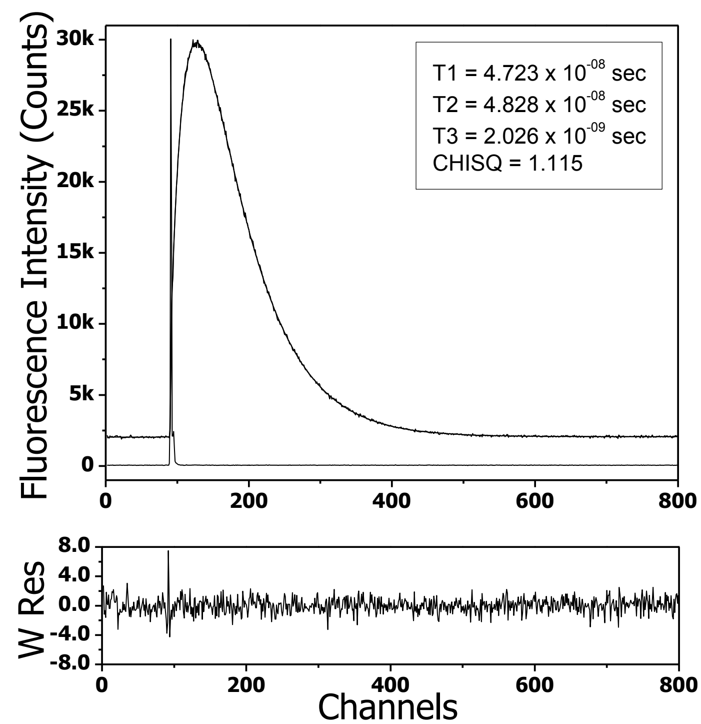

Figure 3.3 – Lamp prompt and fluorescence decay of the emission at 480 nm, in POPC LUV at 25ºC, with a probe to lipid ratio of 1:800 of: **(a)** Bis-py10-PC and **(b)** Bis-py4-PC. Weighted residuals (W Res) are a result of the three-exponential fitting applied.

Table 3.1 presents the average fluorescence lifetimes obtained (minimum of three independent experiments) for both probes at the three temperatures examined. The lifetimes obtained were very similar between the two pyrenyl probes and decreased with temperature as expected. Because these were recorded in the presence of oxygen the fluorescent lifetimes were obviously significantly lower than those obtained in in the absence of oxygen [Martins *et al.*, 1996].

	***τ* (ns)**	
Temperature (ºC)	**Bis-py10-PC**	**Bis-py4-PC**
25	51.0 ± 0.8	50.0 ± 3.0
35	48.8 ± 0.2	47.9 ± 2.6
45	42.5 ± 0.9	46.9 ± 0.2

Table 3.1 – Results of fluorescence lifetimes of the excimer of Bis-py10-PC and Bis-py4-PC probes determined in POPC LUV at various temperatures

3.3.2 Excimer Formation of py10-PC in POPC Bilayers

The excimer formation of py10-PC has been studied through steady-state fluorescence before, but it has been done at lower and narrower range of probe content of what we used in this work [Martins *et al.*, 1996].

The calculation of the 2D concentration of py10-PC was made taking into account that it interacts between opposing leaflets due to its length being bigger than half of the POPC bilayer in the fluid phase [Martins *et al.*, 1996; Repáková *et al.*, 2006].

In Figure 3.4 we compare the experimental I_E/I_M ratios of increasing concentrations of py10-PC with the theoretical points that were calculated by the procedures described before, employing all the terms previously defined, including the lifetimes we determined in this work, at the three temperatures studied.

(a) (b) (c)

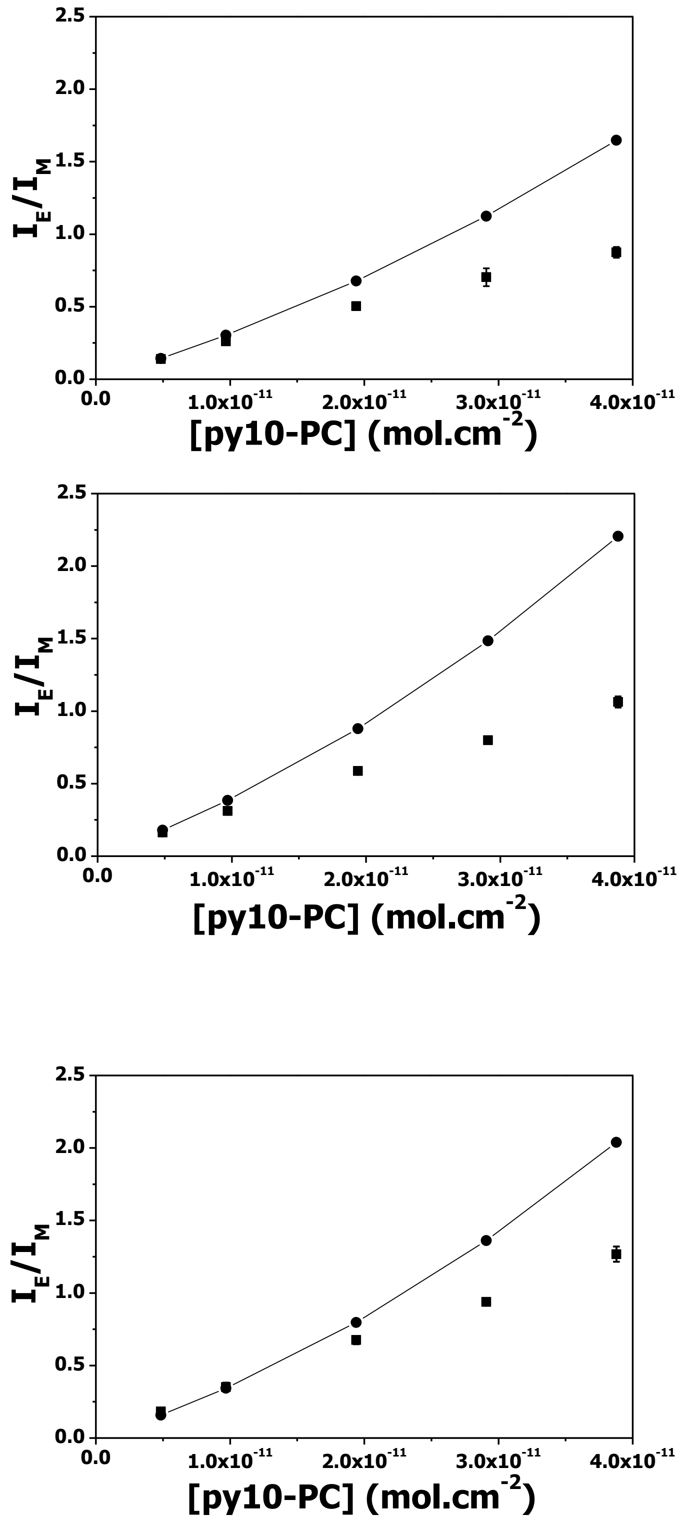

Figure 3.4 – Reason of steady-state fluorescence intensities between the excimer (I_E) and monomer (I_M) emissions of py10-PC, plotted against its 2D concentration in POPC MLV: **(a)** 25ºC, **(b)** 35ºC, and **(c)** 45ºC. The squares (■) are the experimental results, while the circles (●) are the theoretical predictions.

Results using LUV were also found to be reproducible and within the same experimental error of MLV samples, even after 48 h.

We observe the expected upward curve with the increase in excimer formation along with the adding of content of pyrenyl probe, and also a rise of excimer formation with the higher temperatures as expected, however it is clear that at 4 mol % and above the formation of excimer no longer keeps up with theoretical predictions. We are forced to assume that the lateral diffusion dynamics is being hindered, and if we change the diffusion coefficient at the divergent points to a lower value, other things being equal, we can obtain a very good agreement of experiment with theory. Furthermore, even if it would be the fluorescence lifetime changing, the small variations that the lifetime might exhibit could not explain solely the observed larger deviations.

Within the view introduced qualitatively by Hresko *et al.* (1986) and quantitatively through kinetics and structural considerations by Martins *et al.* (1996), for py10-PC probes in lipid bilayers, there is in fact interaction between pyrenyls groups located in apposed monolayers. This way, the excimer is formed from probe molecules pertaining either to the same monolayer and located is apposed leaflets. This aspect has been corroborated and reinforced by molecular dynamics (MD) simulations of this probe in fluid lipid bilayers (Figure 3.5) [Repáková *et al.*, 2006] and by excimer formation of 1-pyrenyl labeled fatty acids (increasing from nonanoic, through decanoic and dodecanoic, and being maximum for hexadecanoic) inserted in lipid bilayers [Mazor *et al.*, 2012; Martins *et al.*, 2012].

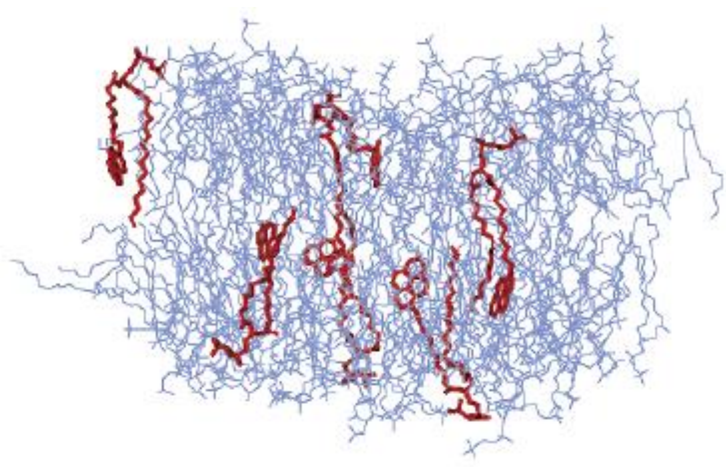

Figure 3.5 – Snapshot of a simulated bilayer configuration at 4.9 mol % of py10-PC showing an example of substantial penetration (interdigitation) to the opposing leaflet. Water has been omitted to clarify the presentation. Adapted from Repáková *et al.*, 2006.

From the MD studies, a distinctive aspect appears: the pyrenyl group in the end of the decanoyl in position *sn*1 in the pyrenyl phospholipid probe causes ordering of the neighboring lipidic acyl chains, which would be part of the disorganized section of the POPC bilayers hydrophobic core. These perturbations are said to influence the adjacent region up to a distance of about 1.0-1.5 nm, which corresponds to about 2-3 molecular diameters and about 15 lipid molecules in the neighborhood of the probe. When considering higher concentrations of probe (like 8 mol %), if one envisions a proposed lipid regular distribution in membranes [Chong & Sugár, 2002], we have to consider that the entire bilayer might be under this effect. Repáková *et al.* (2006) also used concentration of 0.8, 3.2 and 4.9 mol %, and for increasing amounts of py10-PC, found a slight increase in the interdigitation of pyrene into the apposed leaflets. This way, the increasing ordering of methylenic chain terminal sections is likely decreasing the lateral diffusion of these probes. This reasoning is based on the measurements of the coefficient of viscous friction between apposed fluid monolayers and comparing with gel/fluid system by Merkel *et al.* (1989). They found that the viscous friction is much lower in the former system, since it increases with the degree of interdigitation between the hydrocarbon chains, which is in turn determined by the ordering conformations of acyl chains in the gel phase. This finding has been substantiated by recent MD studies [den Otter & Shkulipa, 2007].

3.3.3 Excimer Formation of py6-PC in POPC Bilayers

In order to analyze the excimer formation of the py6-PC probe, we had to estimate the diffusion coefficients because no available data exists for this specific. We assumed that py6-PC has a slightly higher diffusion than its counterpart py10-PC [Martins & Melo, 2001], and attributed values of $4.0 \times 10^{-8}\,\mathrm{cm}^2/\mathrm{s}$ at 25ºC, $6.5 \times 10^{-8}\,\mathrm{cm}^2/\mathrm{s}$ at 35ºC and $1.0 \times 10^{-7}\,\mathrm{cm}^2/\mathrm{s}$ at 45ºC, respectively. This reasoning is simply based on the lower molecular mass of the py6-PC probe, when comparing with the py10-PC probe.

In Figure 3.6 we compare the experimental $\mathrm{I_E}/\mathrm{I_M}$ ratios of increasing concentrations of py6-PC with the theoretical points that were calculated by the procedures described before, employing all the terms previously defined, including the lifetimes we determined in this work, at the three temperatures studied.

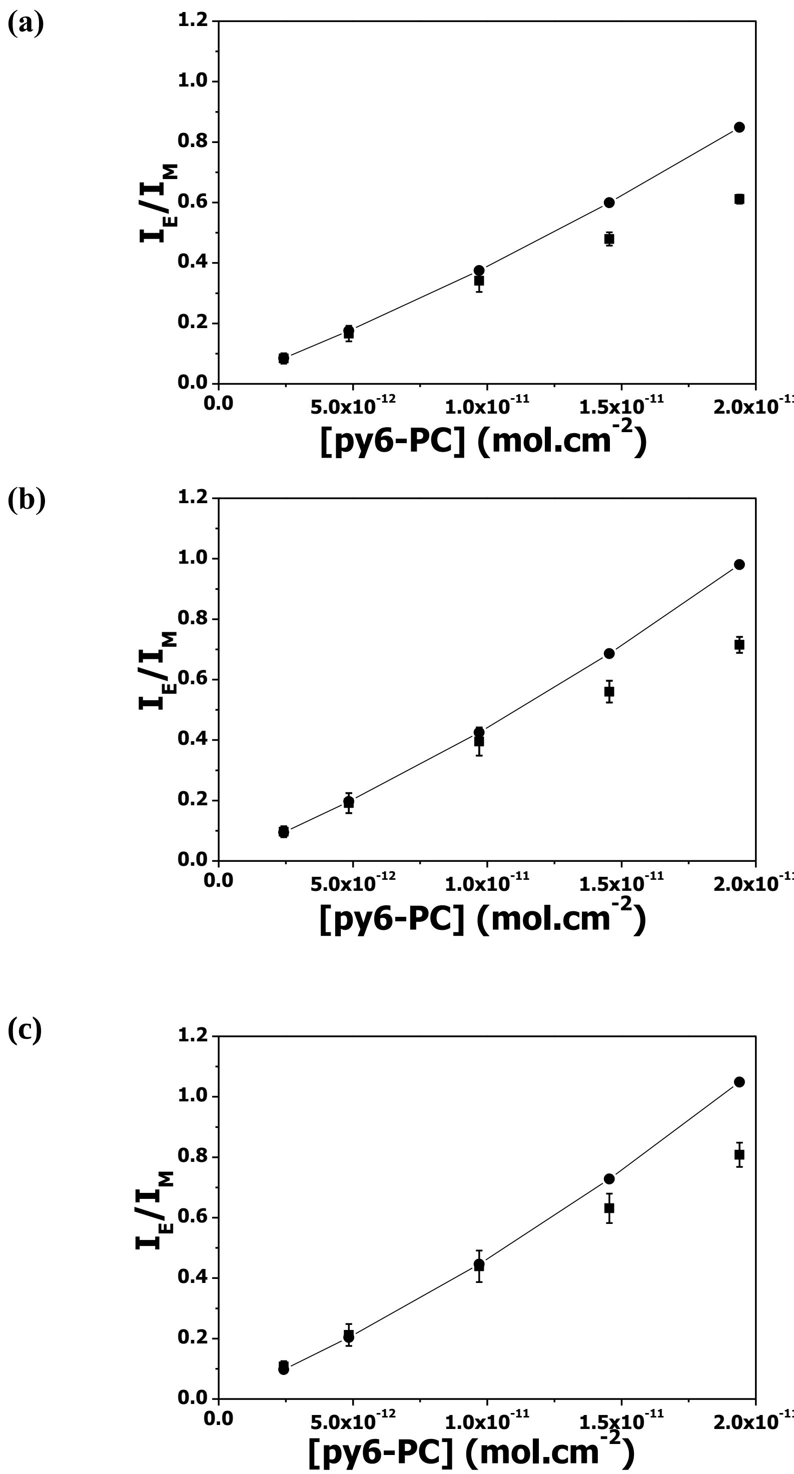

Figure 3.6 – Reason of steady-state fluorescence intensities between the excimer (I_E) and monomer (I_M) emissions of py6-PC, plotted against its 2D concentration in POPC MLV: **(a)** 25ºC, **(b)** 35ºC, and **(c)** 45ºC. The squares (■) are the experimental results, while the circles (●) are the theoretical predictions.

What is observed in figure 3.6 for the excimer formation of py6-PC is quite similar to the behavior shown of py10-PC, however there is significantly less downwards deviation and the 4 mol % point is still in accordance with the theoretical prediction. We infer that while the lateral diffusion of py6-PC is also hindered, it is not to the degree of py10-PC. We assume that, like py10-PC [Repáková *et al.*, 2006], py6-PC experiences the same increased ordering and more tight packing of lipid acyl chains in the vicinity of the probe molecule. Conversely, py6-PC likely does not interdigitates as prominently as py10-PC (there is no excimer formation between molecules on apposed monolayers) and therefore the friction between the monolayers is reasoned as being not as intense as the friction cause by py10-PC's bilayer presence.

It is also a noteworthy to consider that, while there is most certainty a diminishing diffusion coefficient of py6-PC with the increase of probe content, this is different than what was encountered when analyzing the quenching of py6-PC by 5-DOXYL-PC (Chapter 2). This system showed a higher than predicted quenching efficiency, but the absence of such observations for the py6-PC excimer formation would seem to indicate that the DOXYL spin probe is the part of the system responsible for the discrepancy found.

3.4 Conclusions

We have established that use of a directed 2D kinetic model for the analysis of bimolecular reactions in phospholipid bilayers introduced by Razi Naqvi in 1974 is appropriate to execute a complete and self-consistent analysis of the kinetics of excimer formation of py10-PC and of py6-PC in POPC bilayers, using steady-state and lifetime fluorescence measurements. All the parameters were pre-determined, including the fluorescence lifetime of the excimers that we determined in this work. We found a good agreement between the experimental values and the theoretical prediction up until 2 mol % for py10-PC and 4 mol % for py6-PC. However, above these molar concentrations, we conclude that the lateral diffusion dynamics of both probes is being hindered by an increased ordering in the lipids in the probes' proximity. This ordering in caused by the presence of the pyrenyl groups and is even more significant for the py10-PC case because of significant interdigitation and the additional friction between apposed monolayers that is triggered.

3.5 References

Axelrod, D., Lateral motion of membrane proteins and biological fuction, J. Memb. Biol. 75, 1-10 (1983).

Caputo, G.A., London, E., Using a novel dual fluorescence quenching assay for measurement of tryptophan depth within lipid bilayers to determine hydrophobic alpha-helix locations within membranes, Biochemistry 42 (11), 3265-3274 (2003).

Chong, P.L.-G., Sugár, I.P., Fluorescence studies of lipid regular distribution in membranes, Chem. Phys. Lipids 116, 153-175 (2002).

Clegg, R.M., Vaz, W.L.C., Translational diffusion of proteins and lipids in artificial lipid bilayer membranes. A comparison of experiment with theory, in: Progress in Protein–Lipid Interactions, Vol. 1, eds A. Watts and J.J.H.H.M. De Pont, Elsevier, Amsterdam, 1985.

den Otter, W.K., Shkulipa, S.A., Intermonolayer Friction and Surface Shear Viscosity of Lipid Bilayer Membranes, Biophys J. 93 (2), 423–433 (2007).

Edward, J.T., Molecular volumes and the Stokes-Einstein equation, J. Chem. Ed. 47, 261-270 (1970).

Hresko, R.C., Sugár, I.P., Barenholz, Y., Thompson, T.E., Lateral distribution of a pyrene-labeled phosphatidylcholine in phosphatidylcholine bilayers: fluorescence phase and modulation study, Biochemistry 25 (13), 3813–3823 (1986).

London, E., Feigenson, G.W., Fluorescence quenching in model membranes: 1. Characterization of quenching caused by a spin-labeled phospholipid, Biochemistry 20, 1932–1938 (1981).

MacDonald, R.C., MacDonald, R.I., Menco, B.P., Takeshita, K., Subbarao, N.K., Hu, L.R., Small volume extrusion apparatus for preparation of large, unilamellar vesicles, Biochim. Biophys. Acta 1061, 297–303 (1993).

Manuel, M., Martins, J., Partitioning of 1-pyrenesulfonate into zwitterionic and mixed zwitterionic/anionic fluid phospholipid bilayers, Chem. Phys. Lipids 154, 79-86 (2008).

Marsh, D., CRC Handbook of Lipid Bilayers. CRC Press, Boca Raton, 1990.

Marsh, D., Lateral pressure in membranes, Biochim. Biophys. Acta 1286, 183-223 (1996).

Martins, J., Vaz, W.L.C., Melo, E., Long-Range Diffusion Coefficients in Two-Dimensional Fluid Media Measured by the Pyrene Excimer Reaction, J. Phys. Chem. 100, 1889-1895 (1996).

Martins, J., Melo, E., Molecular Mechanism of Lateral Diffusion of py10-PC and Free Pyrene in Fluid DMPC Bilayers, Biophys. J. 80, 832-840 (2001).

Martins, J., Arrais, D., Manuel, M., Can pyrene be localized inside lipid bilayers by simultaneously measuring Py values, and fulfilling the excimer formation conditions?, Chem. Phys. Lipids 165, 866-869 (2012).

Mazor S., Vanounou, S., Fishov, I., Pyrene as a membrane depth gauge: Wavelength selective fluorescence approach to monitor pyrene localizations in the membrane, Chem. Phys. Lipids 165, 125-131 (2012).

Melo, E., Martins, J., Kinetics of bimolecular reactions in model bilayers and biological membranes. A critical review, Biophys. Chem. 123, 77–94 (2006).

Merkel, R., Sackmann, E., Evans, E., Molecular friction and epitactic coupling between monolayers in supported bilayers, J. Phys. France 50 (12), 1535-1555 (1989).

Razi Naqvi, K., Diffusion-controlled reactions in two-dimensional fluids: discussion of measurements of lateral diffusion of lipids in biological membranes, Chem. Phys. Lett. 28 280–284 (1974).

Razi Naqvi, K., Martins, J., Melo, E., Recipes for Analyzing Diffusion-Controlled Reactions in Two Dimensions: Time-Resolved and Steady-State Measurements, J. Phys. Chem. B, 104, 12035-12038 (2000).

Repáková, J., Holopainen, J.M., Karttunen, M., Vattulainen, I., Influence of Pyrene-Labeling on Fluid Lipid Membranes, J. Phys. Chem. B 110, 15403-15410 (2006).

Somerharju, P.J., Pyrene-labeled lipids as tools in membrane biophysics and cell biology, Chem. Phys. Lipids 116, 57–74 (2002).

Szabo, A., Theory of Diffusion- Influenced Fluorescence Quenching, J. Phys. Chem. 93, 6929-6939 (1989).

Szoka Jr., F., Papahadjopoulos, D., Comparative properties and methods of preparation of lipid vesicles (liposomes), Annu. Rev. Biophys. Bioeng. 9, 467-508 (1980).

Valeur, B., Molecular Fluorescence: Principles and Applications, Wiley-VCH, 2002.

Zhao, Y.H., Abraham, M.H., Zissimos, A.M., Fast Calculation of van der Waals Volume as a Sum of Atomic and Bond Contributions and Its Application to Drug Compounds, J. Org. Chem. 68, 7368-7373 (2003).

Chapter 4

Pyrene and 1-Pyrenesulfonate Fluorescence Quenching by 5-DOXYL-labeled Phospholipid Spin Probe in Fluid Lipid Bilayers

4.1 Introduction

Until the early 70's the main applications of photophysical techniques in biophysics were to reveal aspects such as interactions (molecular distances measured by FRET – Förster Resonance Energy Transfer) and rotational mobility of small and macromolecules (trough fluorescence and phosphorescence polarization), as well as estimating electrostatic properties of some biological microenvironments (by using solvent effects in fluorescence spectra) [Weber, 1972]. In 1972, Radda and Vanderkooi (1972) suggested that it would be possible to estimate the diffusion coefficient of small aromatic molecules inserted in model lipidic membranes, from the analysis of linear Stern-Volmer plots of fluorescence quenching [Lakowicz, 2006]. Later, London and Feigenson (1981) elaborated about the analysis of quenching for several small fluorophores (diphenylhexatriene – DPH, *p*-terphenyl, pyrene) by a spin-labeled phospholipid, and introduced a non-linear variation for the classical Stern-Volmer plot. Also, studies about the localization of fluorescent probes (free and/or linked to lipids, peptides and proteins) inside lipid bilayers, through depth-dependent quenching (by typical lipid quenchers, such as nitroxide-labeled phospholipids or fatty acids, and brominated phosphatidylcholines) were introduced [Abrams & London, 1992; London & Ladokhin, 2002] and used rather extensively. For example, the localization of fluorescent probes with charged groups inserted in lipid bilayers (both free and covalently linked to phospholipids and fatty acids), has been presented [Kachel *et al.*, 1998].

The pyrene excimer formation by free pyrene molecules in amphiphilic structures has been studied since the last 40 years. The first kinetic application of the pyrene excimer reaction can be assigned to Pownall and Smith (1973), who attempted to measure the viscosity of the hydrocarbon region of micelles, provided that they found that the excimer formation being linear with the viscosity of a homologous series of solvents. Contemporary, it was Galla and Sackmann (1974) and Vanderkooi and Callis (1974), that proposed the pyrene excimer formation to study lateral diffusion in lipid bilayers. By the end of the 90's, a necessary and sufficient analysis of pyrene excimer reaction in two-dimensional (2D) systems was presented in a series of papers [Martins *et al.*, 1996; Martins & Melo, 2001; Melo & Martins, 2006]. The formation of the 1-pyrenesulfonate (PSA) excimer formation has also been observed in neutral and anionic micelles [Turro&Kuo, 1987], but the counterpart in lipid bilayers has never been either observed or attempted. In this work, we are analyzing the fluorescence quenching of small free probes (pyrene and PSA), by the spin-probe 1-palmitoyl-2-stearoyl-(5-DOXYL)-*sn*-glycero-3-phosphocholine (5-DOXYL-PC), localized within fluid POPC (1-palmitoyl-2-oleoyl- *sn*-glycero-3-phosphocholine) model membranes. We use a steady-sate fluorescence quenching and lifetime analysis adequate for two-dimensional media [Razi Naqvi *et al.*, 2000], in order to shade some light upon the molecular details involved in the quenching mechanism.

The partition of PSA to model membranes from an aqueous solution, is ensured by the previous studies about the experimental conditions to fulfill its complete partition into fluid bilayers, $K_p = 6.9\times10^3$ at 25ºC [Manuel & Martins, 2008]. Additionally, localization of PSA has been estimated as being at the distance of about 17 Å from the center of a fluid DOPC (1,2-dioleoyl-*sn*-glycero-3-phosphocholine), e.g. at the level of carbonyls and below the phosphocholine group, in their description [Kachel *et al.*, 1998]. Also the complete partition of pyrene into bilayers is guaranteed by the following considerations: pyrene is essentially insoluble in water (solubility of about 6.5×10^{-7} M, at 25ºC [Pearlman *et al.*, 1984]) but fairly soluble in aliphatic hydrocarbons (e.g. solubility in dodecane 7.4×10^{-2} M, at room temperature [Almgren *et al.*, 1979]), one can estimate a very high value of about 10^5 for the partition constant into the hydrophobic interior of bilayers. The localization of free pyrene inside lipid bilayers has been established by direct methods such as NMR [Podo & Blasie, 1977; Hoff *et al.*, 2005] and molecular dynamics simulations [Hoff *et al.*, 2005; Čurdova *et al.*, 2007; Loura *et al.*, 2013], and indirectly, through a self-consistent kinetic analysis of pyrene excimer formation in 1,2-dimiristoyl-3-glycerophosphatidylcholine (DMPC) liposomes [Martins & Melo, 2001]. Pyrene appears inserted in the hydrophobic acyl chain region, close to the glycerol moiety and to the first methylenic groups of the ordered portion of the bilayer palisade structure (from C2 to C8 of the acyl methylenic chains of phospholipids), and significantly, displays a negligible displacement amplitude along the bilayer normal, when comparing with its dimensions and considering the thermal movements of the neighboring groups constituting the phospholipids [Loura *et al*., 2013]. Furthermore, even if the incorporation of molecular pyrene within bilayers is putatively not complete, the remaining free molecules in aqueous medium, besides being at very low concentration, have also a low down quantum yield in water [Birks, 1970], interfering this way insignificantly in the measurements of fluorescence intensity. Contrastingly, PSA is soluble in aqueous solutions and partitions extensively into bilayers (see [Manuel & Martins, 2008], for details), being fluorescent in both environments, rendering this probe suitable to study volume-surface processes (membrane chemoreception) by using fluorescence quenching approaches.

In this report, we aim to aid in the interpretation of experiments in which these fluorescent probes are used to examine membrane structure and dynamics, using their quenching by nitroxide-labeled phospholipids. In order to use the steady-state fluorescence and lifetime approach to 2D diffusion-controlled quenching of probes inside lipid bilayers, two conditions have to be satisfied: a previous knowledge of the lateral diffusion coefficients of both the fluorophores and quenchers, plus the fluorescence lifetime of fluorophores in the same experimental conditions of collecting the photostationary data. From the 2D analysis of pyrene quenching, it appears that as in the case of py$_6$-PC (Chapter 2.3.3), a consistent analysis demands that the collisional distance must be augmented from the sum of the van der Waals radii [Edward 1970; Zhao *et al.*, 2003] as 6.7 Å, to a value about 9.5 Å. We discuss the relevance of this finding, since it implies that for quenching processes involving the 5-DOXYL-PC probe, the observed quenching efficiency is higher than predicted by the direct application of a pure 2D diffusion-controlled formalism. For the PSA counterpart, we observe that the experimental quenching effectiveness is consistently much lower than expected. When trying to give a reliable interpretation to this finding, we must come to the conclusion that the PSA probe must be quite out of the influence of the quencher group, when comparing with the pyrene experiments. Hence, the study of quenching processes in the more ordered and hydrated section of lipid bilayers must be cautiously undertaken, either because of problems in the definition of the collisional distances or the accessibility of quenchers to fluorophores.

4.2 Experimental Methods

4.2.1 Chemicals and Solvents

1-Palmitoyl-2-oleoyl-sn-glycero-3-phosphocholine (POPC), purity > 99.9%, 1-Palmitoyl-2-stearoyl-(5-DOXYL)-*sn*-glycero-3-phosphocholine (5-DOXYL-PC) and 1-palmitoyl-2-stearoyl-(10-DOXYL)-*sn*-glycero-3-phosphocholine (10-DOXYL-PC) were purchased from Avanti Polar

Lipids (Alabaster, AL, USA).Pyrene (≥99%, for fluorescence grade) and PSA(1-pyrenesulfonic acid sodium salt, for fluorescence grade) were from Fluka (Buchs, Switzerland).MilliQ water was obtained using a Millipore Simplicity 185 system (electrical conductivity and pH are $5.4 \times 10^{-6}\ \mathrm{S}.m^{-1}$ and around 6.6–7, respectively, at room temperature). All organic solvents (highest purity) were from Merck (Darmstadt, Germany).

4.2.2 Stock Solutions

As referred in the previous chapters, lipids and lipidic probes obtained in the form of powder were diluted in a chloroform:methanol 2:1 (v/v) mixture to the desired concentrations. When acquired as a solution in chloroform instead of powder form, dilutions using the same mixture were made. These stock solutions were then kept at -20ºC. Pyrene stock solution was prepared in ethanol and PSA stock solution was prepared in MilliQ water, both were stored at 6 °C.

4.2.3 Aqueous Liposome Suspensions

MLV were prepared according the protocol specified in the previous chapter, based on firmly established method [Szoka, Jr. & Papahadjopolous, 1980] as described before [Manuel & Martins, 2008]. Stock solutions of phospholipid and spin probe, dissolved in chloroform:methanol 2:1 (v/v), were mixed in settled proportions in a evaporating flask (volume of 20 cm^3) with a conical shape bottom, this increases the homogeneity of the dry lipid film. When producing the pyrene containing samples, the necessary proportion of pyrene stock solution in ethanol was mixed in at this point. The organic solvents were then dried at 50ºC using a rotary evaporator Heidolph VV-micro (vacuum pump Büchi V-500, coupled to a Büchi V-800 digital control, isolated from the rotary evaporator by a liquid N_2 trap) with slow rotation, 15 min at 150 mBar until a homogeneous lipid film was formed, followed by 1 h at 5 mBar, to remove traces of organic solvents. The lipidic film was hydrated with MilliQ water for pyrene containing samples or with a PSA 0.1μM solution, during at least 1 h at 50ºC, well above the

phase transition temperature (T_m) of POPC (T_m = -2.6ºC) [Marsh, 1990], vortexing regularly, forming multilamellar vesicles (MLV) as the lipid sheets detach during agitation and self-close.
Again, in order to minimize light scattering, fluorescence lifetimes of both probes were determined using large unilamellar vesicles (LUV). These were prepared by the extrusion method [MacDonald *et al.*, 1993], using an Avanti Mini-Extruder (Alabaster, AL, USA), forcing the MLV to pass 15 times at room temperature through a pair of Nucleopore polycarbonate filters (Wathman, USA), with pore size of 0.1 μm.
All the liposome aqueous suspensions were kept in the refrigerator and usually used within 24 h.

4.2.4 Time-resolved Fluorescence

Time-resolved fluorescence measurements were made in a Spex Fluoromax-4 spectrofluorimeter (JobinYvon–Horiba, France) equipped with a thermostated cell holder with magnetic stirring accessory, coupled to a refrigerated/heated circulator Julabo F12-ED (precision of 0.1 °C). The LUV suspensions were placed in 1 cm quartz cuvettes and were stirred continuously during the measurements. Excitation wavelength was 342 nm while emission wavelength was set to 383 nm for pyrene and 374 nm for PSA, and slit width was 1 nm for both excitation and emission. Collections were made in 1024 channels and measurement range was 800 ns. A collection of the prompt for the lamp (at 342 nm) was made before the each collection of a corresponding sample. Collections were only stopped when counts reached at least around 10^4 at the beginning of the decay. Total lipid concentration of LUV suspensions used was 0.1 mM, with probe concentration set to 0.125μM (1 probe per 800 phospholipids). Along with the low concentration and LUV utilization, a cut-off filter of 360 nm (Corion, WG360) was used to try to minimize light scattering. Decays were fitted with the manufacturer's software using two exponentials and no initial constrictions, and fluorescence lifetimes were determined by averaging the best decays obtained with χ^2 below 1.2, as well as judging the weighted residuals plot.

4.2.5 Steady-state Fluorescence

Fluorescence spectra were recorded on a Spex Fluoromax-3 spectrofluorimeter (JobinYvon–Horiba, France) equipped with a thermostated cell holder with magnetic stirring accessory, coupled to a refrigerated/heated circulator Julabo F12-ED (precision of 0.1°C). Emission spectra were corrected for the wavelength dependent response of monochromators, collimating optics and detection using the correction file provided by the manufacturer.

The MLV suspensions, total lipid concentration of 1 mM, were placed in 1 cm quartz cuvettes and were stirred continuously during the measurements. Spectra were acquired between 360 and 600 nm, slit width of 1 nm, and wavelength sampling interval of 0.5 nm, at temperatures of 25, 35 and 45ºC. Samples with spin probe molecular percentage of 1, 2, 3, 5 and 8% were studied, while fluorescent probe concentration was kept at 1 μM. Values to quantify quenching were retrieved at the peak of maximum emission at 383 nm for pyrene (corresponds to a band of an allowed transitionwhich is practically insensitive to polarity [Kalyanasundaram&Thomas, 1977] and 374 nm for PSA, and at least four different experiments were averaged.

4.2.6 Two-dimensional Kinetic Analysis

Like it was mentioned in section 2.2.6, fluorescence quenching cases occurring in 2D dimensional media like a membrane bilayer an adapted 2D Stern-Volmer formalism should be used:

$$\frac{\mathrm{I}_0}{\mathrm{I}}=1+k_2.[\mathrm{Q}]_2.\tau \qquad \textbf{(Eq. 4.1)}$$

I_0 and I are the fluorescence intensities in absence and presence of the quencher, respectively, and τ is the unquenched fluorescence lifetime. The steady-state rate constant for quenching reactions occurring in 2D media is k_2, while the quencher 2D concentration is represented by $[Q]_2$. The calculation of k_2 was resolved using Eq. 2.3 iteratively in the same manner as described in section 2.2.6. We take on the values published for the lateral diffusion of pyrene in DMPC bilayers [Martins &Melo, 2001] for both pyrene and PSA, and assume that the lateral diffusion of 5-DOXYL-PC is analogous to POPC [Vaz *et al.*, 1985]. The independent measurements of lifetimes for pyrene and PSA have been all completed. Eq. 4.1 was then utilized to estimate theoretical I_E/I_M ratios.

4.3 Results and Discussion

4.3.1 Fluorescence Lifetimes of Pyrene and PSA in POPC Bilayers

Fluorescence lifetimes of pyrene and PSA in POPC LUV were determined in the presence of oxygen, as was the case for all measurements. This option removes the uncertainty in the degassing procedures, and the oxygen quenching is treated as an additional photophysical process that lowers the fluorescence lifetimes. LUV were used in these time-resolved experiments to ensure a diminished light scattering, because while fluorescence lifetimes determined in MLV in the same conditions were found to be relatively indistinguishable from those obtained in LUV, the decays were of significant lesser quality.

Table 4.1 presents the average fluorescence lifetimes obtained (minimum of three independent experiments) for both probes at the three temperatures examined. Because these were recorded in the presence of oxygen the pyrene fluorescent lifetimes were obviously significantly lower than those obtained when a degassing procedure was adopted [Martins&Melo, 2001]. PSA lifetimes were comparable to those obtained in aqueous solutions [Bohne *et al.*, 1990].

	τ (ns)	
Temperature (ºC)	**Pyrene**	**PSA**
25	150.7±0.6	59.3±0.2
35	127.5±4.0	57.5±0.1
45	110.9±1.5	55.8±0.1

Table 4.1 – Results of fluorescence lifetimes of the pyrene and PSA probes determined in POPC LUV at various temperatures

These lifetimes fulfill the condition described in the methods section that the mean lifetime of unquenched fluorophore should be around the 10^{-7}s range for the formalism used, although the PSA lifetime might be considered a little low.

4.3.2 Fluorescence Quenching of Pyrene by 5-DOXYL-PC in POPC Bilayers

Pyrene diffusion coefficients have been determined in DMPC bilayers (1,2-dimyristoyl-*sn*-glycero-3-phosphocholine) for all three temperatures in use in this study [Martins & Melo, 2001], while 5-DOXYL-PC continues to be assumed to have a diffusion very similar to POPC [Vaz *et al.*, 1985].

In Figure 4.1 we compare the experimental ratios between the fluorescence intensities of pyrene in the absence of quencher, and in the presence of the several concentrations of 5-DOXYL-PC used, with the two series of theoretical points that were calculated by the procedures described before, one with $R_C = 6.7$ Å, that is significantly and systematically lower than what we found experimentally, and another with $R_C = 9.5$ Å, that fits the results obtained very closely.

(a)

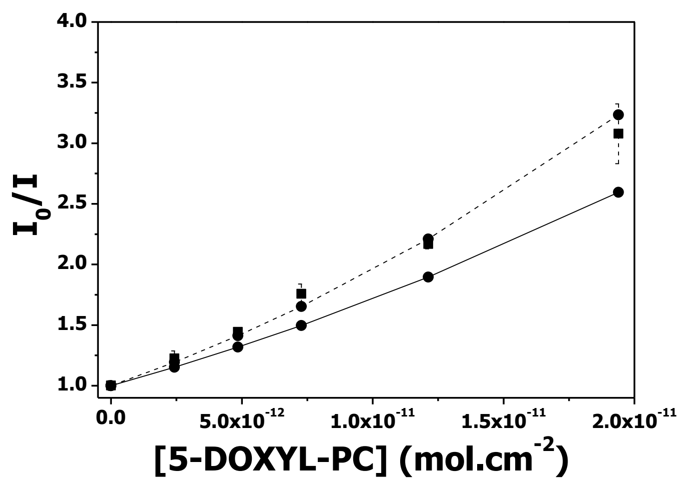

(b)

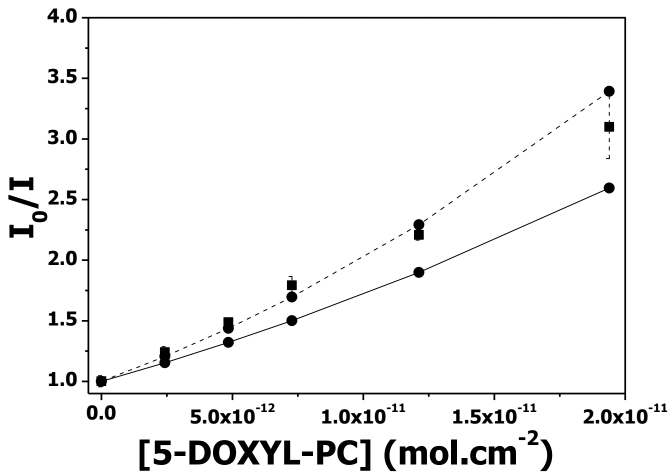

(c)

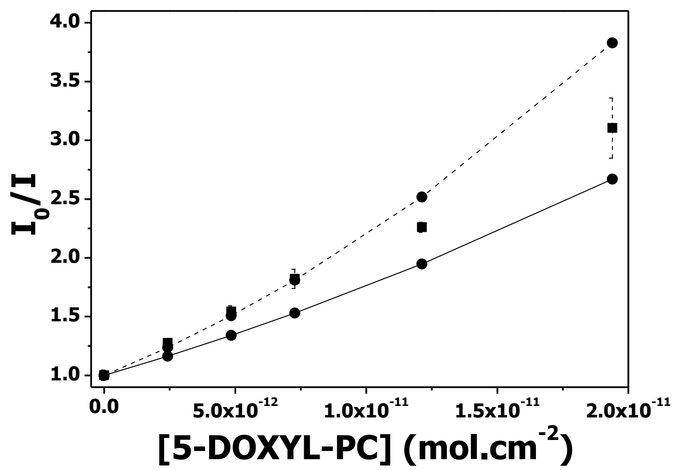

Figure 4.1– Reason of steady-state fluorescence intensities of pyrene in the absence (I_0) and presence (I) of quencher, plotted against the 2D concentration of 5-DOXYL-PC in POPC MLV at: **(a)** 25ºC, **(b)** 35ºC, and **(c)** 45ºC. The squares (■) are the experimental results, while the circles (●) are the theoretical predictions, with the straight line representing $R = 6.7$ Å and the dotted line $R = 9.5$ Å.

We observe the expected upward curve along with an increase in quenching with the introduction of 5-DOXYL-PC content, however Figure 4.1 shows an unexpected result as the obtained experimental values of I_0/I are significantly higher than it was predicted by the kinetic formalism used here. This indicates that fluorescence quenching was occurring at a level above what was expected for the values of terms as defined previously with $R_C = 6.7$ Å. This also occurs at all three temperatures studied.

In the absence of a better explanation, and provided that the analysis of the free pyrene and py6-PC excimer formation did not implied additional considerations in the interpretation of the self-quenching process [Martins & Melo, 2001; Chapter 3.3.3], one must come to the conclusion that the particular localization of the nitroxide quencher in the bilayer should be playing a role in the observed results like we discussed in Chapter 2.3.3.

Reviewing the possible explanations considered, we believe that both variation in the lateral diffusion coefficients (the deviation observed would require doubling the values of both diffusion coefficients, which seems untenable from the physical point of view), and variation in the 2D concentration values (this effect would produce a very minor difference) would not adequately elucidate the experimental deviations observed. However, increased fluorescence quenching efficiency, simply by augmenting the collisional distance from 6.7 Å, to about 9.5 Å (Fig. 4.1), gives a very good accordance between the experimental and theoretical outcomes. This non-conventional explanation would be based in several arguments, mainly underpinned in structural features of lipid bilayers. The quenching kinetics is commonly treated as identical both across the bilayer, as in experiments to monitor depth-dependent quenching of fluorophores in membranes [Lakowicz, 2006]. Nevertheless, it is crucial to realize that a lipid bilayer is not just a thin slab of a low dielectric hydrocarbon medium surrounded by an aqueous solvent, but is really a highly stratified structure with a definite trans-bilayer molecular profile originated on the distinct chemical groups [Gennis, 1989]. Additionally, the distribution profile of lateral pressure [Marsh, 1996; Cantor, 1997] can also potentially affect the collisions between probes located in the more ordered section of the bilayer. Furthermore, recent electron spin resonance (EPR) studies of bimolecular encounters of DOXYL and TEMPO probes in a series of alkanes [Vandenberg *et al.*, 2012] and ethanol [Kurban, 2011] make visible the cage effect in collisions of nitroxides probes based on lateral pressure, that would likely render the bimolecular quenching process more effective in the more ordered section of lipid bilayers. Another factor that cannot be excluded is the extended formation of hydrogen bonds between the spin probes and water [Kurban, 2011], something that is especially relevant because the quantity of water present at the depth of the 5-DOXYL-PC probe is significantly higher [Marsh, 2002] than at lower bilayer depths.

4.3.3 Fluorescence Quenching of PSA by 5-DOXYL-PC in POPC Bilayers

In order to analyze the quenching of PSA by 5-DOXYL-PC, we had to estimate the diffusion coefficients of both probes, since no available data exists for these specific. We assumed that PSA has roughly the same diffusion coefficients as pyrene [Martins&Melo, 2001]. For 5-DOXYL-PC we continued to presume that its diffusion coefficients should be compared to the diffusion of POPC [Vaz *et al.*, 1985].

In Figure 4.2, we compare the experimental ratios between the fluorescence intensities of PSA in the absence of quencher, and in the presence of the several concentrations of 5-DOXYL-PC used, with the theoretical points that were calculated by the procedures described before, employing all the terms previously defined, including the lifetime we determined in this work.

(a)

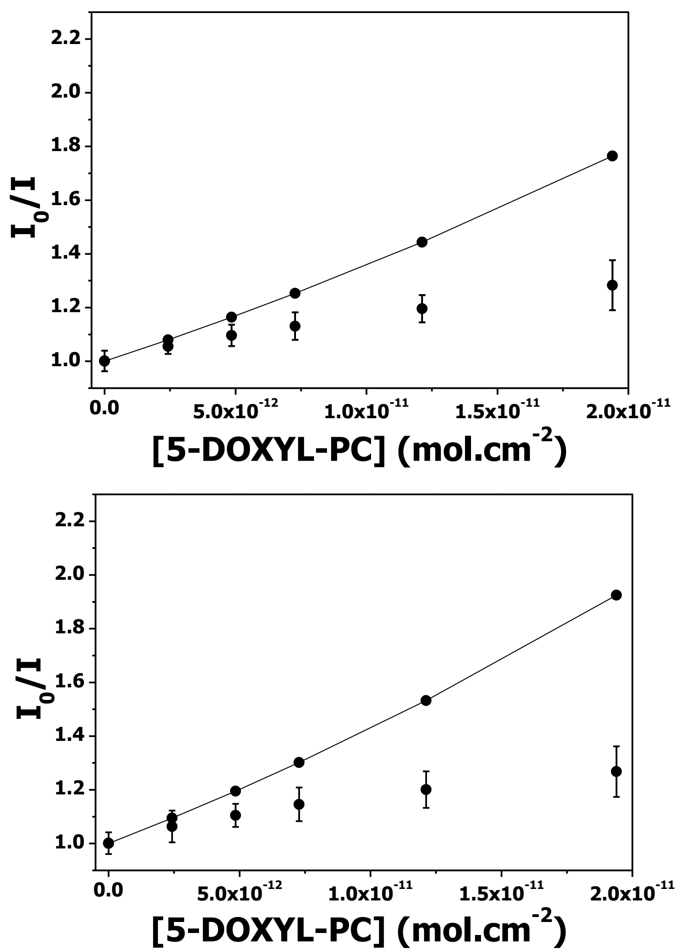

(b)

(c)

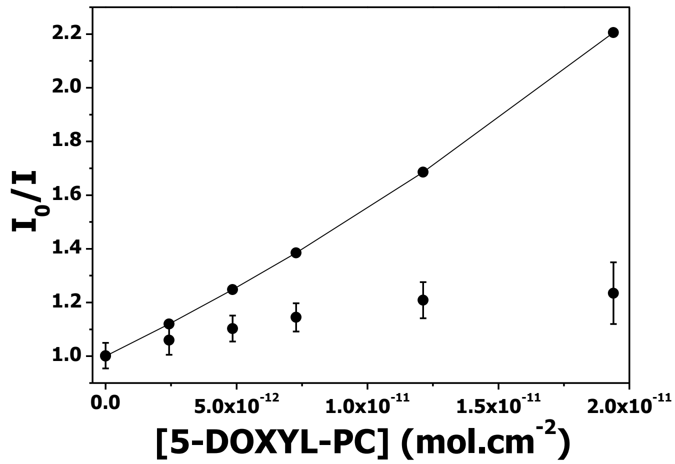

Figure 4.2 – Reason of steady-state fluorescence intensities of PSA in the absence (I_0) and presence (I) of quencher, plotted against the 2D concentration of 5-DOXYL-PC in POPC MLV at: **(a)** 25ºC, **(b)** 35ºC, and **(c)** 45ºC. The squares (■) are the experimental results, while the circles (●) are the theoretical predictions.

Figure 4.2 shows that quenching of PSA fluorescence does not increase very significantly with increasing DOXYL concentration. The partition of PSA to model membranes from an aqueous solution, is ensured at the probe to lipid ratio here utilized [Manuel&Martins, 2008], but PSA, being an anionic molecule, must be located in bilayers above the localization of pyrene. Consequently we must recognize that, even though PSA should be located around position 1 of the acyl chains [Kachel *et al.*, 1998], PSA's average location is not close enough to the DOXYL group's average location to allow a fully 2D diffusion controlled reaction.

We have also attempted to study the accessibility of a head-group labeled phospholipid, 1-palmitoyl-2-oleoyl-*sn*-glycero-3-phospho(TEMPO)choline, to PSA. The results show even less fluorescence quenching occurring, revealing that PSA is as well out of the quenching scope this spin probe in bilayers. Therefore we must concede that neither of these two systems of PSA with either spin probe may be adequate to analyze using the kinetic 2D formalism we intended in this work.

4.4 Conclusions

We attempted to use the same Razi Naqvi 2D kinetic formalism used for membrane-bound pyrenyl probes before [Chapter 2], to study the quenching of two free pyrene fluorescent probes by a DOXYL-labeled lipid.

The quenching of pyrene by 5-DOXYL-PC showed the same characteristics we observed for the quenching of py6-PC of the same spin probe. We discussed how the different settings of the bilayer at the depth of the pyrene /5-DOXYL-PC and several factors in terms of bilayer lateral pressure, water penetration into bilayers and the characteristics of nitroxide probes' reactions, should unquestionably be considered. We feel that these influences, while definitely being a factor in justifying the increased quenching efficiency found when compared to the theory, we alas cannot state for certain to be the full causes of this deviation.

For the PSA fluorescence, the experimental quenching effectiveness was consistently much lower than expected. We concluded that the PSA probe must be quite out of the influence of the quencher group, when comparing with the pyrene experiments, thus the formalism used does not sufficiently apply to the systems involving PSA examined.

These results demonstrate that the definition of the collisional distances or the accessibility of quenchers to fluorophores are complications that should be taken into account when studying of quenching processes in the more ordered and hydrated section of lipid bilayers.

4.5 References

Abrams, F.S., London, E., Calibration of the parallax fluorescence quenching method for determination of membrane penetration depth: refinement and comparison of quenching by spin-labeled and brominated lipids, Biochemistry 31, 5312-5322 (1992).

Almgren, M., Grieser, F., Thomas, J.K., Dynamic and static aspects of solubilization of neutral arenes in ionic micellar solutions, J. Am. Chem.Soc. 101, 279–291 (1979).

Birks, J.B., Photophysics of Aromatic Molecules, Wiley-Interscience,London, 1970.

Bohne, C., Abuin, E.B., Scaiano, J.C., Characterization of the triplet-triplet annihilation process of pyrene and several derivatives under laser excitation, J. Am. Chem. Soc. 112, 4226-4231 (1990).

Cantor, R.S., The lateral pressure profile in membranes: A physical mechanism of general anesthesia, Biochemistry 36(9), 2339-2344 (1997).

Čurdova, J., Čapková, P., Plášek, J., Repáková, J., Vattulainen, I., Free pyrene probes in gel and fluid membranes: perspective through atomistic simulations, J. Phys. Chem. B 111, 3640–3650 (2007).

Edward, J.T., Molecular volumes and the Stokes-Einstein equation, J. Chem. Ed. 47, 261-270 (1970).

Galla, H.-J., Sackmann, E., Lateral diffusion in the hydrophobic region of membranes: use of pyrene excimers as optical probes, Biochim.Biophys.Acta.339(1), 103-115 (1974).

Gennis,R.B., Biomembranes. Molecular Structure and Function, Springer-Verlag, New York, 1989.

Hoff, B., Strandberg, E., Ulrich, A.S., Tieleman, D.P., Posten, C., ^{2}H-NMR study and molecular dynamics simulation of the location, alignment,and mobility of pyrene in POPC bilayers, Biophys. J. 88, 1818–1827 (2005).

Kachel, K., Asuncion-Punzalan,E., London, E., The location of fluorescence probes with charged groups in model membranes, Biochim. Biophys. Acta 1374, 63-76 (1998).

Kalyanasundaram, K., Thomas, J.K., The environmental effects on vibronic band intensities in pyrene monomer fluorescence and their application instudies of micellar systems, J. Am. Chem. Soc. 99, 2039–2044 (1977).

Kurban, M.K., A study of the relation between translational and rotational diffusionthrough measurement of molecular recollision, J. Phys. Chem. 134, 034503 (2011).

Lakowicz, J.R, Principles of Fluorescence Spectrocopy, 3rd Ed., Springer Science, 2006.

London, E., Feigenson, G.W., Fluorescence quenching in model membranes: 1. Characterization of quenching caused by a spin-labeled phospholipid, Biochemistry 20, 1932–1938 (1981).

London, E., Ladokhin, A.S., Measuring the depth of amino acid residues in membrane-inserted peptides by fluorescence quenching, Curr. Top. Membr. 52, 89–115 (2002).

Loura, L.M.S., Martins do Canto, A.M.T., Martins, J., Sensing hydration and behavior of pyrene in POPC and POPC/cholesterol bilayers: A molecular dynamics study, Biochim. Biophys. Acta 1828, 1094–1101 (2013).

Marsh, D., CRC Handbook of Lipid Bilayers. CRC Press, Boca Raton, 1990.

Marsh, D., Lateral pressure in membranes, Biochim. Biophys. Acta 1286, 183-223 (1996).

Marsh, D., Membrane water-penetration profiles from spin labels, Eur. Biophys. J. 31, 559–562 (2002).

Manuel, M., Martins, J., Partitioning of 1-pyrenesulfonate into zwitterionic and mixed zwitterionic/anionic fluid phospholipid bilayers, Chem. Phys. Lipids 154, 79-86 (2008).

Martins, J., Vaz, W.L.C., Melo, E., Long-Range Diffusion Coefficients in Two-Dimensional Fluid Media Measured by the Pyrene Excimer Reaction, J. Phys. Chem. 100, 1889-1895 (1996).

Martins, J., Melo, E., Molecular mechanism of lateral diffusion of py_{10}-PC and free pyrene in fluid DMPC bilayers, Biophys. J. 80, 832-840 (2001).

Melo, E., Martins, J., Kinetics of bimolecular reactions in model bilayers and biological membranes. A critical review, Biophys. Chem. 123, 77–94 (2006).

Pearlman, R.S., Yalkowsky, S.H., Banerjee, S., Water solubilities of polynuclear aromatic and heteroaromatic compounds, J. Phys. Chem. Ref. Data 13, 555–562 (1984).

Podo, F., Blasie, J.K., Nuclear magnetic resonance studies of lecithin bimolecular leaflets with incorporated fluorescent probes, Proc. Natl.Acad. Sci. USA 74, 1032–1036 (1977).

Pownall, H.J., Smith, L.C., Viscosity of the hydrocarbon region of micelles. Measurement by excimer fluorescence, J. Am. Chem. Soc. 95 (10), 3136–3140 (1973).

Radda, G.K., Vanderkooi, J.M., Can fluorescent probes tell us anything about membranes?, Biochim. Biophys. Acta 265 (4), 509–549 (1972).

Razi Naqvi, K., Martins, J., Melo, E., Recipes for analyzing diffusion-controlled reactions in two dimensions: time-resolved and steady-state measurements, J. Phys. Chem. B 104, 12035-12038 (2000).

Szoka Jr., F., Papahadjopoulos, D., Comparative properties and methods of preparation of lipid vesicles (liposomes), Annu. Rev. Biophys. Bioeng. 9, 467-508 (1980).

Turro, N.J., Kuo, P.-L., Excimer formation of a water soluble fluorescence probein anionic micelles and nonionic polymer aggregates. Langmuir 3, 773–777 (1987).

Vandenberg, A.D., Bales, B.L., Salikhov, K.M., Peric,M., Bimolecular encounters and re-encounters (cage effect) of a spin-labeled analogue of cholestane in a series of n‑alkanes: effect of anisotropic exchange integral, J. Phys. Chem. A 116, 12460−12469 (2012).

Vanderkooi, J.M., Callis, J.B., Pyrene - Probe of lateral diffusion in the hydrophobic region of membranes, Biochemistry 13, 4000–4006 (1974).

Vaz, W.L.C., Clegg, R.M., Hallmann, D., Translational diffusion of lipids in liquid crystalline phase of phosphatidylcholines multibilayers. A comparison of experiment with theory, Biochemistry 24, 781-786 (1985).

Weber, G., Uses of fluorescence in biophysics: some recent developments, Annu. Rev. Biophys. Bioeng. 1, 553-570 (1972).

Zhao, Y.H., Abraham, M.H., Zissimos, A.M., Fast calculation of van der Waals volume as a sum of atomic and bond contributions and its application to drug compounds, J. Org. Chem. 68, 7368-7373 (2003).

Chapter 5

Excimer Formation of Pyrenyl Probes in POPC:Cholesterol Mixed Bilayers

The work presented in this chapter was realized
in part by undergraduate student Mónica Faria and
Miguel Manuel under supervision of Jorge Martins

5.1 Introduction

Fluorescence quenching has been used extensively to improve the knowledge about the lipid bilayers structure and dynamcis, particularly on cholesterol containing lipidic mixtures forming model membrane [London, 2002]. Cholesterol is the single most abundant lipid species in mammalian cell membranes and roughly 90% of all cellular cholesterol resides in the plasma membrane, where it composes between 25 and 50% of the lipids, depending on the cell type [Bloch, 1991]. Binary mixtures of cholesterol and phospholipids in bilayers are non-ideal, displaying single or phase coexistence, depending on chemical composition and on other thermodynamic parameters, e.g., temperature or pressure [McConnell & Vrljic, 2003]. Cholesterol has been shown to be of crucial importance to the formation of lipid rafts [Simons & Vaz, 2004], and fluorescence quenching has been used to elucidate on the underlying features [Wang *et al.*, 2000; Wang & Silvius, 2001], specifically pyrenyl probes excimer formation [Koivusalo *et al.*, 2004].

A consistent analysis of pyrene excimer formation in fluid homogeneous bilayers used the 2D variant of the Smoluchowski formalism for diffusion-controlled reactions [Martins *et al.*, 1996; Martins & Melo, 2001]. Smoluchowski's approach yields, in the case of 2D systems [Razi Naqvi, 1974], unwieldy expressions for the time-dependent rate-coefficient (used to solve the differential equations inherent to kinetic schemes), and for the corresponding concentration-dependent rate constant (which determines the rate of a diffusion-controlled reaction under stationary conditions) [Razi Naqvi *et al.*, 2000]. Razi-Naqvi and collaborators (2000) made available a recipe, based on a mean-field approach presented by Szabo (1989), to analyze photostationary fluorescence quenching experiments, and verified that pyrene excimer formation studied through steady-state data can be successfully analyzed.

In this work, we attempt to add some information to the lateral diffusion conditions in POPC:Chol mixed bilayers by using fluorescence self-quenching of membrane-bound pyrenyl probes py10-PC (1-palmitoyl-2-(1-pyrenedecanoyl)-*sn*-glycero-3-phosphocholine) and py6-PC (1-palmitoyl-2-(1-pyrenehexanoyl)-*sn*-glycero-3-phosphocholine). We found that high cholesterol content severely hinders the diffusion dynamics of both probes, although the deviations appear smaller with increasing temperature. This decrease in lateral diffusion seems to result from the organization introduced by the cholesterol presence [Ferreira *et al.*, 2013], since we have previously studied rather completely in Chapter 3, the equivalent processes in fluid and homogeneous POPC bilayers.

5.2 Experimental Methods

5.2.1 Chemicals and Solvents

1-Palmitoyl-2-oleoyl-sn-glycero-3-phosphocholine (POPC), purity > 99.9%, was purchased from Avanti Polar Lipids (Alabaster, AL, USA). Cholesterol, purity > 99.9%, was obtained from Sigma-Aldrich. 1-Hexadecanoyl-2-(1-pyrenedecanoyl)-sn-glycero-3-phosphocholine (py10-HPC), 1-Hexadecanoyl-2-(1-pyrenehexanoyl)-sn-glycero-3-phosphocholine (py6-HPC), 1,2-bis-(1-pyrenedecanoyl)-sn-glycero-3-phosphocholine (Bis-py10-PC) and 1,2-bis-(1-pyrenebutanoyl)-sn-glycero-3-phosphocholine (Bis-py4-PC) were purchased from Molecular Probes (Eugene, Oregon, USA). MilliQ water was obtained using a Millipore Simplicity 185 system (electrical conductivity and pH are $5.4 \times 10^{-6}\ S.m^{-1}$ and around 6.6–7, respectively, at room temperature). All organic solvents (highest purity) were from Merck (Darmstadt, Germany).

5.2.2 Stock Solutions

As referred in the previous chapters, lipids and probes obtained in the form of powder were diluted in a chloroform:methanol 2:1 (v/v) mixture to the desired concentrations. When acquired as a solution in chloroform instead of powder form, dilutions using the same mixture were made. The stock solutions were then kept at -20ºC.

5.2.3 Aqueous Liposome Suspensions

MLV were prepared according the protocol specified before, based on firmly established method [Szoka, Jr. & Papahadjopolous, 1980] as described before [Manuel & Martins, 2008]. Stock solutions of lipid and spin probe, dissolved in chloroform:methanol 2:1 (v/v), were mixed in settled proportions in a evaporating flask (volume of 20 cm^3) with a conical shape bottom, this increases the homogeneity of the dry lipid film. The organic solvents were then dried at 50ºC using a rotary evaporator Heidolph VV-micro (vacuum pump Büchi V-500, coupled to a Büchi V-800 digital control, isolated from the rotary evaporator by a liquid N_2 trap) with slow rotation, 15 min at 150 mBar until a homogeneous lipid film was formed, followed by 1 h at 5 mBar, to remove traces of organic solvents. The lipidic film was hydrated with MilliQ water during at least 1 h at 50ºC, vortexing regularly, forming multilamellar vesicles (MLV) as the lipid sheets detach during agitation and self-close. LUV for fluorescence lifetime determinations, were produced by extrusion through 1µm Nucleopore polycarbonate filters (Wathman, USA), using an Avanti Mini-Extruder.

All the liposome aqueous suspensions were kept in the refrigerator and usually used within 24 h.

5.2.4 Time-resolved Fluorescence

We determined monomer fluorescence lifetimes of both py10-PC and of py6-PC in LUV containing POPC:Chol mixtures (95:05, 80:20 mol %) and in MLV for POPC:Chol (60:40, molar ratio). In order to determine excimer fluorescence lifetime in the same mixtures, the dipyrenil probes Bis-py10-PC and Bis-py4-PC were used. Time-resolved fluorescence measurements were made in a Spex Fluoromax-4 spectrofluorimeter (Jobin Yvon–Horiba, France) equipped with a thermostated cell holder with magnetic stirring accessory, coupled to a refrigerated/heated circulator Julabo F12-ED (precision of 0.1 °C). The LUV suspensions were placed in 1 cm quartz cuvettes and were stirred continuously during the measurements. Excitation wavelength was 342 nm while emission wavelength was set to 376 nm and 480 nm, for the monomer and for the excimer, respectively, and slit width was 1 nm for both excitation and emission. Collections were made in 1024 channels and measurement range was 800 ns. A collection of the prompt for the lamp (at 342 nm) was made before the each collection of a corresponding sample. Collections were only stopped when counts reached at least around 10^4 at the beginning of the decay for the monomer lifetimes, while for the excimer collections were only stopped when counts reached at least 2×10^4. Total lipid concentration of LUV or MLV suspensions used was 0.1 mM, with probe molecular percentage set at 0.125 mol % (1 probe per 800 phospholipids). A cut-off filter of 360 nm (Corion, WG360) was used to try to minimize light scattering. Decays were fitted with the manufacturer's software using two exponentials or three exponentials and no initial constrictions, and fluorescence lifetimes were determined by averaging the best decays obtained with χ^2 below 1.2, as well as judging the weighted residuals plot.

5.2.5 Steady-state Fluorescence

Fluorescence spectra were recorded in a similar way to Chapter 2, on a Spex Fluoromax-3 spectrofluorimeter (Jobin Yvon–Horiba, France) equipped with a thermostated cell holder with magnetic stirring accessory, coupled to a refrigerated/heated circulator Julabo F12-ED (precision of 0.1°C). Emission spectra were corrected for the wavelength dependent response of monochromators, collimating optics and detection using the correction file provided by the manufacturer.

The MLV suspensions, total lipid concentration of 1 mM, were placed in 1 cm quartz cuvettes and were stirred continuously during the measurements. Spectra were acquired between 360 and 600 nm, slit width of 1.5 nm, and wavelength sampling interval of 0.5 nm, at temperatures of 25, 35 and 45ºC. Samples with py10-HPC and py6-HPC molecular percentage of 1 and 4% were studied in MLV containing POPC:Chol mixtures with the following ratios: 95:05, 80:20, 65:35, 60:40, and 55:45 mol %. Values to quantify excimer formation were retrieved by comparing the area of the band of monomer emission (376 nm) between 371 and 381 nm and the area of the band of excimer emission (480 nm) between 475 and 485 nm (Figure 3.1), and at least four different experiments were averaged.

5.2.6 Two-dimensional Kinetic Analysis

Like it was mentioned before [Chapter 3], fluorescence quenching cases occurring in 2D dimensional media like a membrane bilayer an adapted 2D Stern-Volmer formalism should be used. In this particular case the py10-HPC and py6-HPC fluorescent probes self-quenching must be analyzed specifically accounting the excimer formation [Razi Naqvi *et al.*, 2000]:

$$\frac{\mathrm{I_E}}{\mathrm{I_M}}=\frac{k_{FE}}{k_{FM}}.k_2.[\mathrm{Q}]_2.\tau_{\mathrm{E}} \qquad \textbf{(Eq. 5.1)}$$

$\mathrm{I_E}$ and $\mathrm{I_M}$ are the fluorescence intensities of the excimer and monomer, respectively, k_{FE} and k_{FM} are the rate constants for the excimer and monomer fluorescence and τ_{E} is the fluorescence lifetime. The k_{FE}/k_{FM} ratio is usually estimated to be around 2. The steady-state rate constant for quenching reactions occurring in 2D media is k_2, while the quencher 2D concentration is represented by $[\mathrm{Q}]_2$, and was calculated taking the lower cholesterol area [Greenwood *et al.*, 2006; Gallová *et al.*, 2010] at the appropriate ratios. The calculation of k_2 was resolved using Eq. 2.3 iteratively in the same manner as described in section 2.2.6, and with the monomer lifetime (τ_{M}) and τ_{E} that were determined specifically for bilayers containing the defined POPC/cholesterol mixtures. The diffusion coefficients of py10-PC in phospholipid bilayers [Martins & Melo, 2001] were used to compare with the results we observe here with the presence of cholesterol, and we also used the slightly higher coefficients for the py6-PC probe that utilized in Chapters 2 and 3. Eq. 5.1 was then utilized to estimate theoretical $\mathrm{I_E}/\mathrm{I_M}$ ratios.

5.3 Results and Discussion

5.3.1 Flourescence Lifetimes of py10-PC and py6-PC Monomers and of Bis-py10-PC and of Bis-py4-PC Excimers in POPC:Chol Bilayers

Fluorescence lifetimes of both the monomer and the excimer in POPC:Chol mixtures were determined in the presence of oxygen, as was the case for all measurements. The dipyrenyl probes (structures in Figure 3.2) were used because of the easiness of determining the excimer lifetime using a small amount of probe, which wouldn't be the case of finding τ_{E} with a monopyrenyl probe. There was no commercial available dipyrenyl version of py6-PC, so we considered the lifetimes obtained with Bis-py4-PC sufficiently comparable.

Table 5.1 presents the average fluorescence lifetimes obtained (minimum of three independent experiments) for all four probes at the three temperatures examined.

The lifetimes of the monomer and of excimer obtained were very similar between the two pyrenyl probes and usually decreased with temperature as expected. The most noticeable discrepancy is the monomer lifetime of py6-PC in POPC:Chol (60:40 mol %) that was higher than observed in the other mixtures. There was also an increase of the excimer lifetime of both dipyrenyl probes at 25ºC in the Chol containing mixtures, this may be due to a lesser conformational freedom of the acyl chains, forcing the pyrene groups to be closer to each other and therefore facilitating excimer formation and length of time in the excited state.

These lifetimes fulfill the condition described in the methods section that the mean lifetime of unquenched fluorophore should be around the 10^{-7}s range for the formalism used.

		τ (ns)			
MLV	**Temperature (ºC)**	**py10-PC**	**py6-PC**	**Bis-py10-PC**	**Bis-py4-PC**
POPC	25	125.4 ± 0.3	128.3 ± 0.1	51.0 ± 0.8	50.0 ± 3.0
	35	114.8 ± 2.6	113.4 ± 2.8	48.8 ± 0.2	47.9 ± 2.6
	45	102.4 ± 2.2	101.5 ± 0.3	42.5 ± 0.9	46.9 ± 0.2
POPC:Chol (95:05 mol %)	25	119.7 ± 3.0	125.0 ± 1.6	56.4 ± 0.8	48.9 ± 0.3
	35	103.9 ± 1.5	106.2 ± 0.1	47.5 ± 0.2	50.1 ± 1.7
	45	91.4 ± 1.9	100.7 ± 0.7	44.1 ± 1.3	46.2 ± 1.0
POPC:Chol (80:20 mol %)	25	120.2 ± 4.1	126.3 ± 2.3	55.5 ± 1.5	58.4 ± 1.7
	35	105.7 ± 7.3	113.7 ± 5.5	48.1 ± 1.1	53.5 ± 0.1
	45	89.7 ± 3.8	98.8 ± 0.7	42.9 ± 0.7	48.1 ± 0.2
POPC:Chol (60:40 mol %)	25	127.6 ± 1.8	140.3 ± 2.4	57.8 ± 0.7	58.6 ± 4.0
	35	113.4 ± 1.2	125.0 ± 2.4	51.9 ± 1.0	55.7 ± 0.4
	45	102.3 ± 2.0	116.9 ± 1.8	46.5 ± 0.7	48.2 ± 2.0

Table 5.1 – Results of fluorescence lifetimes of the py10-PC and py6-PC monomers, and of Bis-py10-Pc and Bis-py4-PC excimers determined in POPC:Chol mixtures at various temperatures.

5.3.2 Excimer Formation of py10-PC and of py6-PC in POPC:Chol Bilayers

In Figure 5.1 we compare the experimental I_E/I_M ratios of py10-PC and of py6-PC in POPC:Chol mixed bilayers, with the theoretical points that were calculated by the procedures described before, employing all the terms previously defined, at the three temperatures studied. The calculation of the 2D concentration was made considering the area of POPC and of cholesterol at their respective ratios, and the calculation for py10-PC was made taking into account that it interacts between opposing leaflets due to its length being bigger than half of the POPC bilayer in the fluid phase [Martins *et al.*, 1996; Repáková *et al.*, 2006]. The lifetimes were the determined in this work, with the lifetimes obtained in the POPC:Chol (60:40 mol %) mixture being used for the POPC:Chol (65:35 mol %) and POPC:Chol (55:45 mol %).

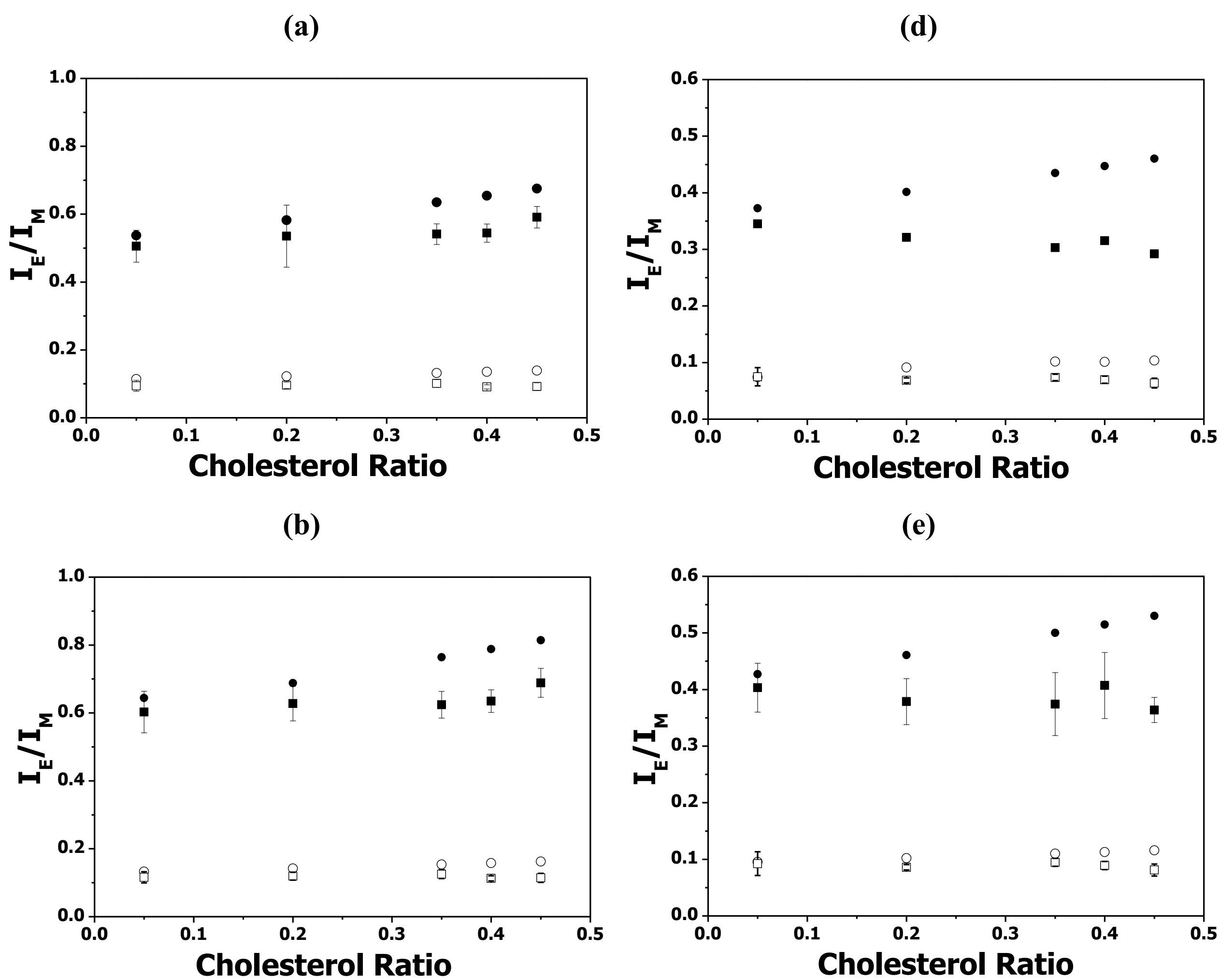

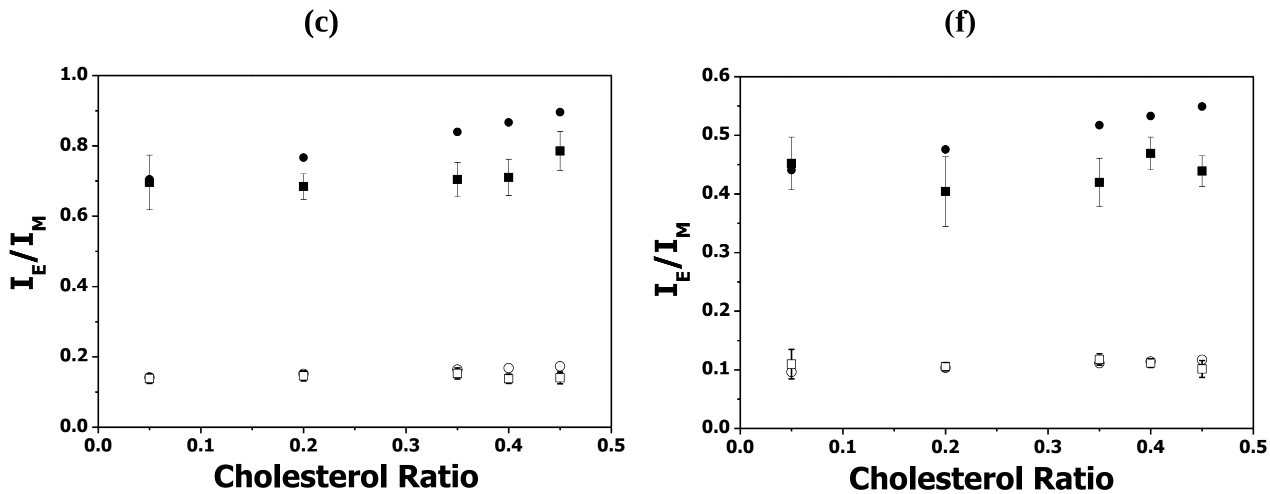

Figure 5.1 – Ratio of steady-state fluorescence intensities between the excimer (I_E) and monomer (I_M) emissions plotted against cholesterol content ratio in POPC:Chol bilayers: py10-PC at **(a)** 25ºC, **(b)** 35ºC, and **(c)** 45ºC, and py6-PC at **(d)** 25ºC, **(e)** 35ºC, and **(f)** 45ºC. The squares (□,■) are the experimental results, while the circles (○,●) are the theoretical predictions. The hollow points (□,○) represent 1 mol % of probe content, while the full points (■,●) represent 4 mol % of probe content.

We observe that the excimer formation does not increase with cholesterol concentration, as it is predicted theoretically due the smaller area of cholesterol when compared to POPC. In fact excimer formation levels remain relatively equal with increasing cholesterol content, and in the case of py6-PC at 25ºC and at 35ºC, it even appears to diminish. The deviations seem however smaller when increasing temperature to 45ºC.

Cholesterol has been shown to decrease POPC diffusion in POPC:Chol bilayers by NMR studies performed by Filippov *et al.* (2003), as such we assume that the lateral diffusion dynamics is being hindered, and if we change the diffusion coefficient at the divergent points to a lower value, other things being equal, we can obtain a very good agreement of experiment with theory.

It has also been demonstrated the cholesterol presence augments the organization of the POPC:Chol bilayer [Ferreira *et al.*, 2013] and this seems to be reason for the diminishing lateral diffusion. In particular, excimer formation of py6-PC did not show, even at 4 mol %, any deviation from the 2D kinetic model in pure POPC bilayers [Chapter 3], however here we observed a significant downwards deviation. At this probe ratio in the MLV, only py10-PC showed lower diffusion dynamics due to in the interdigitation of pyrene group into the apposed leaflets and the friction between apposed fluid monolayers that this entails.

The increase in temperature would allow a significant disorganization of the bilayer and therefore permit the closer matching of experimental results to the theoretical predictions, which is observed principally at 1 mol % fluorescent probe content.

5.4 Conclusions

We applied the same Razi Naqvi 2D kinetic formalism used before for excimer formation of membrane-bound pyrenyl probes in POPC MLV [Chapter 3], to study POPC:Chol mixed bilayers.

The results show that cholesterol slowed down diffusion of both py10-PC and py6-PC, which is probably due to the amount of organization that cholesterol introduces into the bilayer. The deviations that py6-PC in particular demonstrated show the significance of the decrease of diffusion dynamics caused by cholesterol, when compared to what was observed to be triggered by the ordering that the pyrene group of these pyrenyl probes. Temperature increase to 45ºC was found to somewhat reverse this effect, especially for lower the probe content.

5.5 References

Bloch, K., Cholesterol: evolution of structure and function, in: D.E. Vance, J.E. Vance (Eds.), Biochemistry of Lipids, Lipoproteins and Membranes, Elsevier, Amsterdam, 1991.

Ferreira, T.M., Coreta-Gomes, F., Ollila, O.H., Moreno, M.J., Vaz, W.L.C., Topgaard, D., Cholesterol and POPC segmental order parameters in lipid membranes: solid state ^{1}H–^{13}C NMR and MD simulation studies, Phys. Chem. Chem. Phys. 15, 1976- 1989 (2013).

Filippov, A., Orädd, G., Lindblom, G., The effect of cholesterol on the lateral diffusion of phospholipids in oriented bilayers, Biophys J. 84 (5), 3079-3086 (2003).

Gallová, J., Uhríková, D., Kučerkaa, N., Teixeira, J., Balgavy, P., Partial area of cholesterol in monounsaturated diacylphosphatidylcholine bilayers, Chem. Phys. Lipids 163, 765–770 (2010).

Greenwood, A.I., Tristram-Nagle, S., Nagle, J.F., Partial molecular volumes of lipids and cholesterol, Chem. Phys. Lipids 143, 1–10 (2006).

Koivusalo, M., Alvesalo, J., Virtanen, J.A., Somerharju, P., Partitioning of pyrene-labeled phospho- and sphingolipids between ordered and disordered bilayer domains, Biophys. J. 86, 923–935 (2004).

London, E., Insights into lipid raft structure and formation from experiments in model membranes, Curr. Opin. Struct. Biol. 12(4), 480-486 (2002).

Manuel, M., Martins, J., Partitioning of 1-pyrenesulfonate into zwitterionic and mixed zwitterionic/anionic fluid phospholipid bilayers, Chem. Phys. Lipids 154, 79-86 (2008).

Martins, J., Vaz, W.L.C., Melo, E., Long-range diffusion coefficients in two-dimensional fluid media measured by the pyrene excimer reaction, J. Phys. Chem. 100, 1889-1895 (1996).

Martins, J., Melo, E., Molecular mechanism of lateral diffusion of py_{10}-PC and free pyrene in fluid DMPC bilayers, Biophys. J. 80, 832-840 (2001).

McConnell, H.M., Vrljic, M., Liquid–liquid immiscibility in membranes, Annu. Rev. Biophys. Biomol. Struct. 32, 469–492 (2003).

Razi Naqvi, K., Diffusion-controlled reactions in two-dimensional fluids: discussion of measurements of lateral diffusion of lipids in biological membranes, Chem. Phys. Lett. 28 280–284 (1974).

Razi Naqvi, K., Martins, J., Melo, E., Recipes for analyzing diffusion-controlled reactions in two dimensions: time-resolved and steady-state measurements, J. Phys. Chem. B, 104, 12035-12038 (2000).

Repáková, J., Holopainen, J.M., Karttunen, M., Vattulainen, I., Influence of pyrene-labeling on fluid lipid membranes, J. Phys. Chem. B 110, 15403-15410 (2006).

Simons, K., Vaz, W.L.C., Model systems, lipid rafts and cell membranes, Annu. Rev. Biophys. Biomol. Struct. 33, 269–295 (2004).

Szabo, A., Theory of diffusion-influenced fluorescence quenching, J. Phys. Chem. 93, 6929-6939 (1989).

Szoka Jr., F., Papahadjopoulos, D., Comparative properties and methods of preparation of lipid vesicles (liposomes), Annu. Rev. Biophys. Bioeng. 9, 467-508 (1980).

Wang, T.Y., Leventis, R., Silvius, J.R., Fluorescence-based evaluation of the partitioning of lipids and lipidated peptides into liquid-ordered lipid microdomains: a model for molecular partitioning into “lipid rafts”, Biophys. J. 79, 919–933 (2000).

Wang, T.Y., Silvius, J.R., Cholesterol does not induce segregation of liquid-ordered domains in bilayers modeling the inner leaflet of the plasma membrane, Biophys. J. 81, 2762–2773 (2001).

<u>Chapter 6</u>

Concluding Remarks

6.1 General conclusions

The main objective of this work was to demonstrate that the use of a directed 2D kinetic model for the analysis of bimolecular reactions in phospholipid bilayers is in fact appropriate and of crucial importance to correctly interpret experimental outcomes, while maintaining present the complex nature of lipid membranes.

We proved that the formalism introduced by Razi Naqvi in 1974 was sufficient to execute a complete and self-consistent analysis of the kinetics of quenching of py10-PC by 10-DOXYL-PC in POPC bilayers, in the range of temperatures studied, using steady-state and lifetime fluorescence measurements. We determined the fluorescence lifetimes of both probe, and together with all the pre-determined parameters, found an excellent agreement between the experimental values and the theoretical prediction. However in the analysis of the quenching of py6-PC by 5-DOXYL-PC, we found a surprisingly increased quenching efficiency when compared to the theory, something that we cannot at the present moment fully explain. We believe however that the different settings of the bilayer at the depth of the py6-PC/5-DOXYL-PC, and how those settings vary from the depth of the py10-PC/10-DOXYL-PC, several factors in terms of bilayer lateral pressure, water membrane penetration and the characteristics of nitroxide probes' reactions, are unquestionably influences that have to be considered.

We also found a good agreement for the kinetics of excimer formation of py10-PC and of py6-PC in POPC bilayer between the experimental values and the theoretical prediction, with the excimer lifetimes that we obtained this work. This was though not case above 2 mol % for py10-PC and 4 mol % for py6-PC, and we conclude that the lateral diffusion dynamics of both probes is being hindered by an increased ordering in the lipids in the probes' proximity. This ordering in caused by the presence of the pyrenyl groups and is even more significant for the py10-PC case because of significant interdigitation and the additional friction between apposed monolayers that is triggered.

We then attempted to use the same Razi Naqvi 2D kinetic formalism to study the quenching of two free pyrene fluorescent probes by a DOXYL-labeled lipid. We determined the lifetimes of pyrene and of pyrenesulfonate in the conditions used. The results for the quenching of pyrene by 5-DOXYL-PC showed the same characteristics we observed for the quenching of py6-PC of the same spin probe. We discussed how the different settings of the bilayer at the depth of the pyrene

/5-DOXYL-PC and several factors in terms of bilayer lateral pressure, water penetration into bilayers and the characteristics of nitroxide probes' reactions, should unquestionably be considered. Conversely, the experimental quenching effectiveness of the PSA fluorescence was consistently much lower than expected. We concluded that the PSA probe does not sufficiently locate in the zone of the influence of the quencher group, when comparing with the pyrene experiments.

Finally we attempted a small application of this formalism presented to study excimer formation of membrane-bound pyrenyl probes in POPC:Chol mixed bilayers. Cholesterol apparently diminished diffusion of both py10-PC and py6-PC, which is probably due to the amount of organization that cholesterol introduces into the bilayer. The deviations that py6-PC in particular demonstrated show the significance of the decrease of diffusion dynamics caused by cholesterol, when compared to what was observed to be triggered by the ordering that the pyrene group of these pyrenyl probes.

The results overall presented are proof that it is possible to gain valuable knowledge of the lipid membrane by studying the kinetics of reactions in 2D with the adequate formalism while mainly using steady-state fluorescence. The results also demonstrate that the characteristics and properties of the probes used, the precise definition of the collisional distances and the accessibility of quenchers to fluorophores are complications that should be taken into account when studying of quenching processes in the more ordered and hydrated section of lipid bilayers.

6.2 Perspectives

The quality of the results obtained with medium class spectrofluorimeters established that a great deal of scientific knowledge can be produced in the field of reaction kinetics in biomembranes if proper attention is paid to the theoretical framework.

The specific outcomes of this work suggest some interesting experiments to envisage. Consequences of the use of higher probe concentration that so many works have employed are still to be properly evaluated. The unexpected effect of the use of 5-DOXYL has also leaved significant questions unanswered, that perhaps the use of other fluorescence quenchers may solve. Mixed compositions of lipids in the model membranes have not receive much attention using the Razi Naqvi formalism, so expanding the cholesterol experimentations and the introduction of charged lipids are undoubtedly appealing.